NTNU – Trondheim
Norwegian University of
Science and Technology

Flexible Pipe Stress and Fatigue Analysis

Henan Li

Marine Technology
Submission date: June 2012
Supervisor: Svein Sævik, IMT

Norwegian University of Science and Technology
Department of Marine Technology

THESIS WORK SPRING 2012

for

Stud. tech. Henan Li

Flexible Pipe Stress and Fatigue Analysis

Spennings- og utmatnings-analyse av fleksible stigerør

The flexible riser represents a vital part of many oil and gas production systems. During operation of such risers, several failure incidents may take place e.g. caused by fatigue and corrosion. In limit cases where inspections indicate damage, the decision making with regard to continue operation or replacing the riser may have large economic and environmental consequences. Hence, the decision must be based on accurate models to predict the residual strength of the pipe. In most applications, one or several steel layers are used to carry the hoop stress resulting from internal pressure. This is further combined with two layers of cross-wound armour tendons (typically 40-60 tendons in one layer installed with an angle of 35^{o} with the pipe's length axis) acting as the steel tensile armour to resist the tension and end cap wall force resulting from pressure. The riser fatigue performance may in many cases be governed by the dynamic stresses in the tensile armour. The existing lifetime models for such structures is primarily based on inherent assumptions with respect to the slip properties of the tensile armour. This thesis work focus on establishing a FEM based model for analysis of the tensile armour, so as to analyse the stress and slip behaviour when exposed to different load conditions. The thesis work is to be based on the project work performed and shall include the following steps:

1) Literature study, including flexible pipe technology, failure modes and design criteria, analytical methods for stress analysis of flexible pipes, non-linear finite element methods relevant for non-linear FEM codes such as the Marintek software Bflex2010. A detailed literature review on models for stress and slip behaviour of flexible pipes shall be included and presented.
2) Establish four FE models in Bflex2010 using element type hshear353 with associated contact and core elements: Assume one cross-section diameter consisting of a two layered tensile armour with lay angles 25, 35, 45 and 55 degrees for each case.
3) From relevant literature, establish analytical formulas for stresses due to axisymmetric loads and the stresses and slip due to bending.

4) Use the FE model to investigate the correlation between the numerical and analytical stresses for the axisymmetric case as a function of internal pressure and tension.
5) Use the FE model to study the motion and stresses of the armour tendon for different levels of pre-stress, friction coefficient and bending curvature. Compare with the analytical calculations.
6) Use the FE model to study cyclic effects with respect to the slip behaviour assuming non-zero static curvature. Perform sensitivity with respect to the stick-slip parameter and the two different assumption applied related to the layer interaction in hcont453. Which of the two limit curves gives a best fit with regard to the stress ranges between max and min curvature?
7) Conclusions and recommendations for further work

The work scope may prove to be larger than initially anticipated. Subject to approval from the supervisors, topics may be deleted from the list above or reduced in extent.

In the thesis the candidate shall present his personal contribution to the resolution of problems within the scope of the thesis work

Theories and conclusions should be based on mathematical derivations and/or logic reasoning identifying the various steps in the deduction.

The candidate should utilise the existing possibilities for obtaining relevant literature.

Thesis format

The thesis should be organised in a rational manner to give a clear exposition of results, assessments, and conclusions. The text should be brief and to the point, with a clear language. Telegraphic language should be avoided.

The thesis shall contain the following elements: A text defining the scope, preface, list of contents, summary, main body of thesis, conclusions with recommendations for further work, list of symbols and acronyms, references and (optional) appendices. All figures, tables and equations shall be numerated.

The supervisors may require that the candidate, in an early stage of the work, presents a written plan for the completion of the work.

The original contribution of the candidate and material taken from other sources shall be clearly defined. Work from other sources shall be properly referenced using an acknowledged referencing system.

The report shall be submitted in two copies:
- Signed by the candidate

- The text defining the scope included
- In bound volume(s)
- Drawings and/or computer prints which cannot be bound should be organised in a separate folder.

Ownership

NTNU has according to the present rules the ownership of the thesis. Any use of the thesis has to be approved by NTNU (or external partner when this applies). The department has the right to use the thesis as if the work was carried out by a NTNU employee, if nothing else has been agreed in advance.

Thesis supervisors

Prof. Svein Sævik, NTNU.

Deadline: June 15th, 2012

Trondheim, January 15th, 2012

Svein Sævik

Candidate's - date and signature:

Henan Li, January 15th, 2012

Table of content

Acknowledgements

This thesis has been carried out at Norwegian University of Science and Technology (NTNU), Department of Marine Technology under the supervision of Professor. Svein Sævik. His suggestion and instructions are gratefully acknowledged.

Sincere thanks also give to the Senior Scientist Naiquan Ye at MARINTEK. His patient assistance on both analytical and software study helps me perform better of the thesis.

Thanks are also given to my classmates at Marine Technology who give helpful discussion throughout the thesis study.

Nomenclature

Symbols	Explanation
b	Thickness of tendon cross section(mm).
C_σ	Yong's modulus of elasticity (Nm^{-2}).
C_τ	Shear modulus(Nm^{-2}).
C_n	Penalty stiffness parameter.
G	Determinant of metric tensor.
$\boldsymbol{G_I}$	Base vectors directed along the local curvilinear coordinate in undeformed configurations.
$\boldsymbol{I_I}$	Base vectors directed along curve principal torsion-flexure axes.
I_t	Cross section torsion constant (m^4).
I_3	Inertia moment about X^3 axis (m^4).
m_I	Distributed moment acting about the local coordinate axes (N).
M_I	Moment stress resultant acting about the local coordinate axes (Nm).
Q_I	Force stress resultants acting along the local coordinate axes (N).
q_I	Distributed loads acting along the local coordinate axes (Nm^{-1}).
q_t	Distributed tangential reaction.
R	Radius from pipe centre line to tendon centre line (m).
S_0, S	Surface of rod in undeformed, deformed configurations.

$\boldsymbol{u}, u_i$	Vector and component form of displacement field.
v, w	Surface coordinates.
W_i	Internal virtual work contribution from beam element.
X^I, x^i	Local curvilinear coordinates.
Z^I	Cartesian coordinates refers to a Cartesian coordinate system arbitrarily positioned along the pipe centre line.
α	Tendon lay angle.
ε_z	Global pipe axial strain.
ε_1	Axial strain of rod.
θ_i	Rotation about the local curvilinear axis.
κ	Principal curvature along curve (m^{-1}).
κ_1	Total accumulated torsion of tendon centre line (m^{-1}).
κ_2	Total accumulated transverse curvature of the tendon centre line (m^{-1}).
κ_3	Total accumulated normal curvature of tendon centre line (m^{-1}).
κ_r, κ_c	Principal curvatures of the supporting surface (m^{-1}).
κ_t	Pipe surface curvature in transverse tendon direction (along the X^3 axis) (m^{-1}).
ρ	Curvature radius of pipe surface at neutral axis (m).
σ, σ^{ij}	Tensor and component form of the Cauchy stress tensor in the local Cartesian coordinate system.

τ	Torsion along curve (m^{-1}).
ϕ	Spherical coordinate angle
ω	Angle between surface normal and curve normal.
ω_1	Torsion deformation, i.e., twist (m^{-1}).
ω_2	Transverse curvature deformation (m^{-1}).
ω_3	Normal curvature deformation (m^{-1}).
β, β_i	Relative displacement vector or component.
w_i	Components of beam rotation.
$\Delta\pi$	Incremental potential

Abstract

Fatigue is an important character for the flexible pipes as they are always exposed to dynamic loading. For nonbonded flexible pipes, fatigue and stress analysis can be performed based on different assumptions of slip behaviour. Different slip assumptions used in estimating the slip stress always play a determinative role in the prediction of fatigue damage. Thus, this thesis will focus on the study of the slip behaviour between tensile armour layers of nonbonded flexible pipes. The results can be used to support the basic assumptions for further fatigue analysis.

The main object of this thesis is to summarize the existing analytical methods for stress and slip analysis of nonbonded flexible pipe armouring layers and to verify that the improved finite element models can give adequate description of the flexible pipe slip behaviour.

In previous version of BFLEX, the transverse slip effect for nonbonded flexible pipes has been neglected. In this thesis, transverse slip regime has been activated in the updated BFLEX by developing a new type of beam element hshear353 and a new type of contact element hcont453. Finite element models use these two elements have been made and several case studies have been carried out.

For axisymmetric loading, two analytical solutions, one obtained from the equations by Witz&Tan[13], one from Sævik[2] have been compared with the result from numerical simulation. It has been found that Sævik's solution matches better with the BFLEX solution comparing to Witz&Tan's solution.

For flexible pipes exposed to bending, influences on slip behaviour from several pipe parameters, namely friction coefficient, axial strain and global pipe curvature, have been investigated. The numerical results are also compared with analytical solutions obtained from Sævik[2]. It has been found that the numerical solutions can give excellent agreement with analytical solutions. It is further concluded that the outer tensile armour layer do not influence much on the inner layer slip behaviour.

In addition, the cyclic bending effects on nonbonded flexible pipes have been investigated. It has been found that the tendon behaves differently from case to case. The inner and outer layers behave differently. Only a few cases have been studied for this problem due to time limitation.

The overall conclusion is that the developed BFLEX model is capable of describing the stresses and local displacements of flexible pipe for simple cases. The developed numerical model can further be used in the study of fatigue in flexible risers. However, more studies on influence from multi-tensile layers and cyclic bending are needed in the future.

List of tables

List of figures

Chapter1 Introduction

1.1Flexible pipe technology

Flexible pipes are widely used in offshore oil and gas industry as connections for both fixed and floating platforms. Examples are risers connecting seabed to the surface and well product flowlines. The presence of flexible pipe offers the permanent connection between floating structures and subsea installations under extreme dynamic conditions because it can suffer larger bending deformations. At the same time, it is easy to transport and install. The most important characters for flexible pipe are lower bending stiffness and higher volume stiffness.

1.1.1 Applications

Common applications for flexible pipes are listed below[1] :

- Riser used to connect subsea installations with above water production facilities during the production phase.
- Flowlines for in-field connection of wellheads, templates, loading terminals, etc.
- Jumper lines between fixed and floating platforms.
- Loading hoses for offshore loading terminals.
- Small-diameter service lines, such as kill and choke lines, umbilicals, etc.

The present thesis will only focus on the response of flexible pipes used in fully dynamic riser systems connecting offshore production and offshore systems. Thus, only details on riser systems are discussed.

Key parameters for a riser system are the number, sizes, pressure, rating and internal coating requirements related to transfer function

According to [1], the requirements for the riser system support depend on

- Water depth
- Support vessel motions
- Current and wave loading

Key parameters for external loadings are:

- Tension
- Curvature

- Torsion
- Contact with other structures(interference)
- Compression

Common used riser configurations are given in Fig. 1.1 [3].

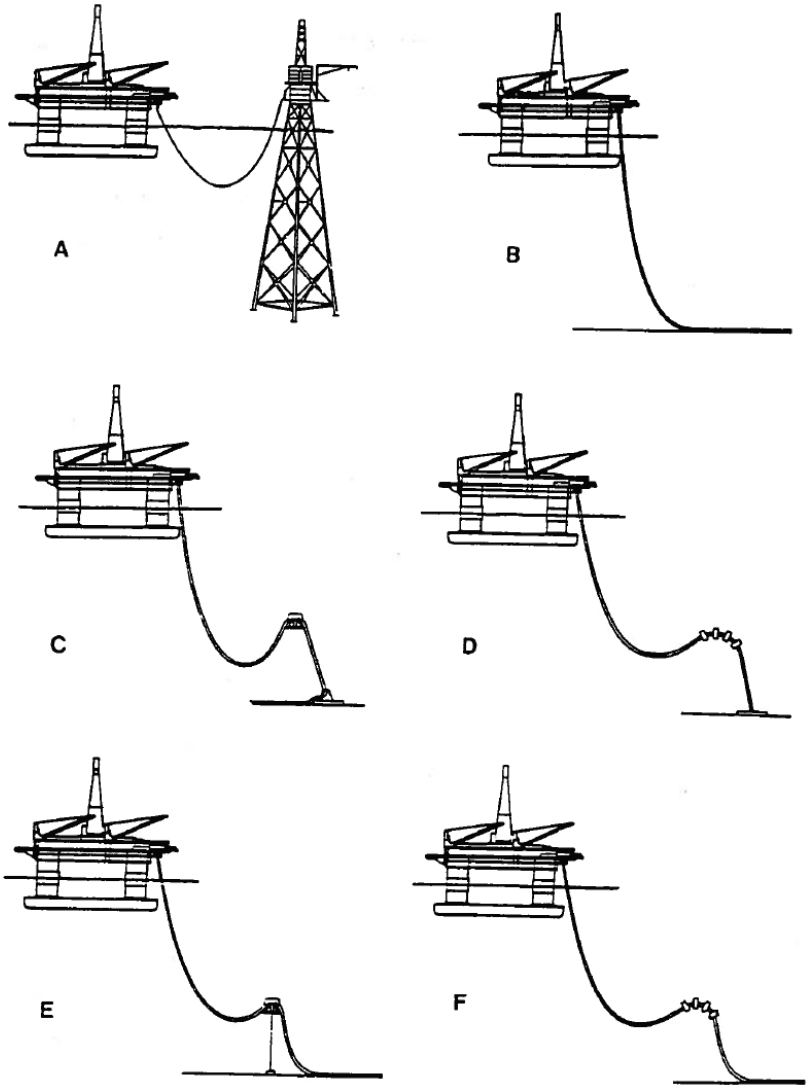

Figure 1-1 Flexible riser configurations[2]

- A: General configuration
- B. Free hanging catenary

  This is the simplest and cheapest configuration. This type of riser has poor dynamic

properties and severe response at the touch down area where the riser is connected to the vessel. It is reported that this type of configuration is likely to have compression buckling under large vessel motions[3] and large top tension when applied in deep water.

- C: Steep S

  For this shape of pipe, a buoy, either fixed or floating, is used to connect to the pipe to create the S-shape. The buoy can absorb the tension variation from the platform, and such the touch down point (TDP) has only small variation in tension. The S configuration is costly and only used for complex installation procedure. The steep S has larger curvature than lazy S.

- D: Steep wave

  In this configuration, buoyancy elements which is made by synthetic foam, is mounted on a longer length of the riser. A negative submerged weight is created by the buoyancy elements and a wave shape is made. This will decouple the vessel motion from the TDP. The steep wave configuration also needs a subsea base and a subsea bending stiffener. This type of configuration is commonly used in cases where the internal fluid density changes during life time. One problem of wave configuration is the buoyance elements tend to lose volume under high pressure and thus results an increased submerged weight. The wave configuration has to be designed to have up to 10% loss of buoyancy.

- E: Lazy S

  Lazy S configuration is similar with steep S configuration but with smaller curvature.

- F: Lazy wave

  The lazy wave configuration has similar principle as for steep wave configuration but with smaller curvature. The main difference is that the lazy wave does not require a subsea base and bend stiffener. Lazy wave is lower cost and more often preferred.

1.1.2 Classification on cross section properties[4]

Flexible pipe can be divided into bonded and nonbonded pipes based on cross section properties, i.e., the different principles of providing flexibility.

Layers for nonbonded flexible pipe are not fixed and free to move against each other. The flexibility of nonbonded pipe is provided by the relative slip of armouring tendons. Nonbonded pipes are often used as risers and be constructed in length up to several kilometers.

The relative slip is not available for bonded pipe since its layers are bonded with each other. The principle for bonded pipe is that the rubber has a relatively low shear modulus which will control and restrict the stresses induced by bending and hence provide flexibility. Bonded flexible pipe is mostly used when short length is required, due to the limitation of length per segment.

Typical cross sections for bonded and nonbonded pipe are given in the figure below[4].

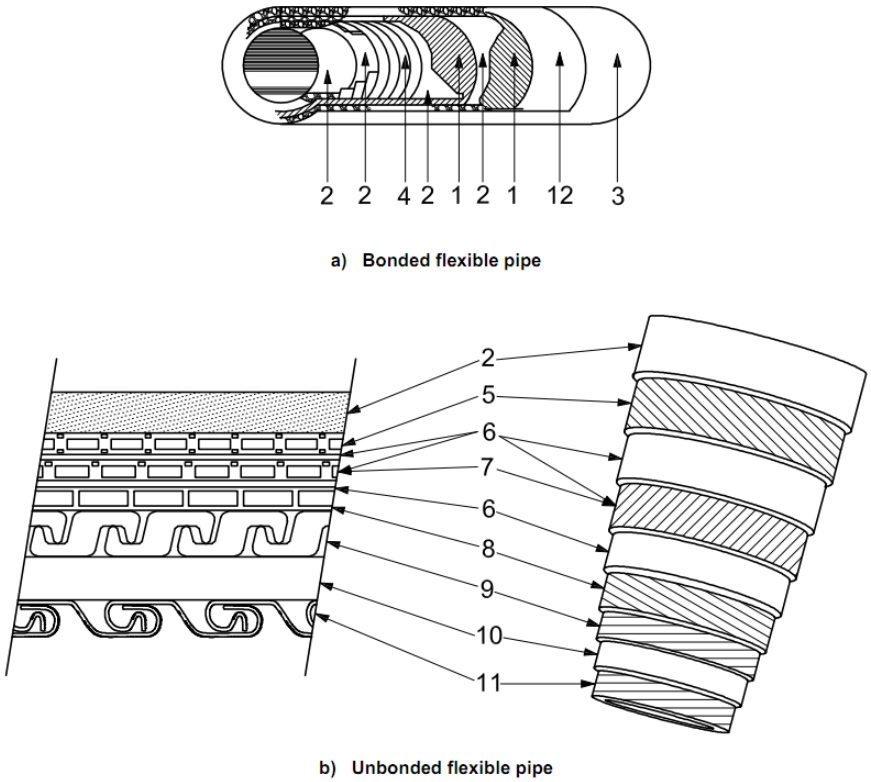

Figure 1-2 Flexible pipe cross section [4]

Namely:

1. Tensile layer
2. Anti-friction layer
3. Outer sheath
4. Hoop stress layer
5. Outer layer of tensile armour
6. Anti-wear layer
7. Inner layer of tensile armour
8. Back-up pressure armour
9. Interlocked pressure armour
10. Internal pressure sheath
11. Carcass
12. Anti-bird-cage layer

1.1.3 Cross section properties for nonbonded pipes

Today's dominating type of flexible pipe is the nonbonded pipe, which will be the main focus of this thesis work. A brief function description of main layers for nonbonded pipe is given below:

- Carcass

  Carcass is often the innermost layer of the nonbonded pipe. The function of inter locked stainless steel carcass is to provide resistance to the external hydrodynamic pressure and prevent collapse of the internal pressure sheath. Since the carcass will contact the inner fluid directly, its material is chosen due to anti-corrosion consideration. It is made of a stainless steel flat strip that is formed into an interlocking profile, which is shown in figure 1-3.

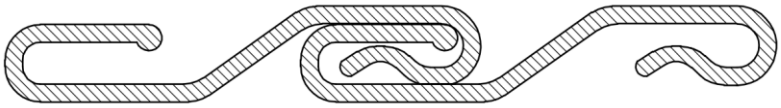

Figure 1-3 typical profile of the carcass[4]

- Internal pressure sheath
  Internal pressure sheath is used as sealing component provides internal fluid integrity. Usually, it is made from a thermoplastic by extrusion over the carcass.
- Pressure armour (Zeta spiral for example)
  Pressure armour consists of an interlocking profile, typically like the Zeta profile shown in the figure below, but other designs are known in use. Zeta spiral is made of Z-shaped interlocking wires. The pressure armour is used to provide capacity of loading in hoop direction caused by internal and external pressure. The pressure armour is typical made of low-alloyed carbon steel grades, with typical high yield strength.

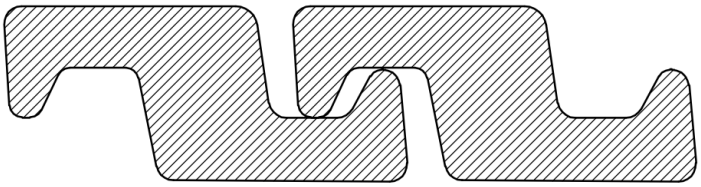

Figure 1-4 cross section of Zeta- shaped pressure armour[4]

- Double helically wound armours.

  The wound armours usually consists several tendons helically laid at around 30° - 55° to the longitudinal axis along the flexible riser. The main function of wound armour is to sustain axial and torsional loading. In addition, the flexibility of nonbonded pipe is ensured by the slip between the tendon and the inner support structures.

  In this thesis, we focus on the slip behaviour of the tendons and the stress analysis of non-bonded flexible pipe.

- Thermoplastic sheath.

  This layer also called outer sheath which people could see from the outside of the flexible riser. It separates other structures from sea water and provides protection against corrosion.

1.1.2 Typical failure modes

According to the FPS2000 report[1], the two typical failure mode shapes of a flexible pipe structure are leakage and reduction of internal cross section; it is further illustrated in the following figure:

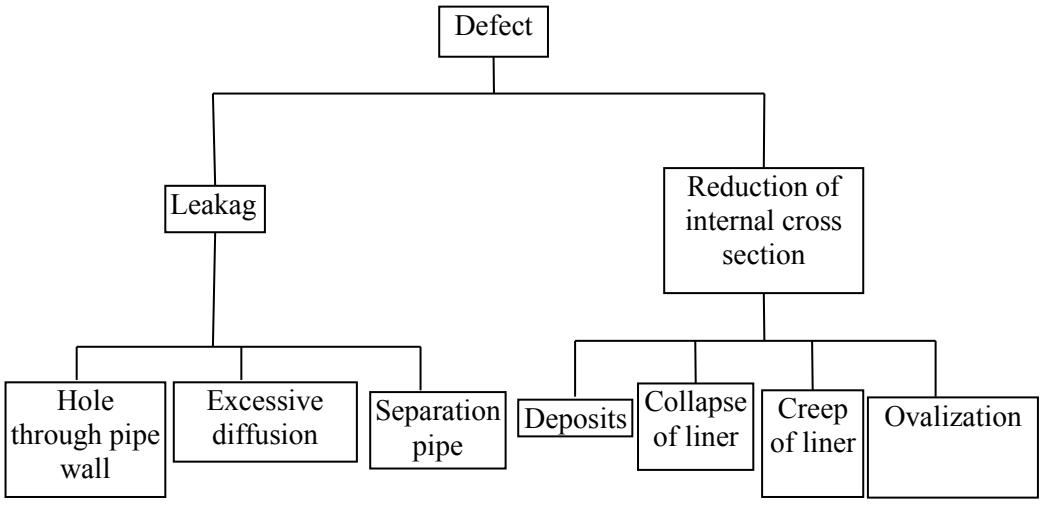

Figure 1-5 Typical failure modes[1]

One commonly used standard to design failure modes is American Petroleum Institute (API) standard 17B[4].

Since this thesis will mainly focus on the behaviour of non-bonded pipe armours , only the related failure modes are introduced. Details regarding other failure modes, please refer to API, 'Recommended Practice for Flexible Pipe 17B'.

Failures in armours can be caused by over load tension, compression, bending, torsion as well as fatigue. Also, the erosion of armour because of contacting sea water or diffused fluid should be taken into account if applicable. A short summery of API standard 17B[4] regarding failure mode of armours is given in the table below.

Table 1-1 Global failure modes[4]

Pipe global failure mode to design against	Potential failure mechanisms caused by armours	Design solution or variables
Tensile failure	Rupture of tensile armours due to excess tension	1)Increase tendon thickness or select higher strength material if feasible 2)Modity comfiguration designs to reduce loads 3)Add two more armour layers 4)Bury pipe
Compressive failure	Bird-caging of tensile-armour tendons	1)Avoid riser configurations that cause excessive pipe compression 2)Provide additional support/restraint for tensile armours, such as tape and/additional or thicker outer sheath
Overbending	Collapse of pressure armour	Modify configuration designs to reduce loads

Torsional failure	1)Failure of tensile armour tendon 2)Bird-caging of tensile-armour wires	1)Modify material selection 2)Modify cross-section design(e.g. change lay angle of tendons, add extra layer outside armour tendons, ets.) to increase torsional capacity
Fatigue failure	1)Tensile-armour-tendon fatigue 2)Pressure-armour-tendon fatigue	1)Increase tendon thickness or select alternative material, so that fatigue streeses are compatible with service-life requirements. 2)Modify design to reduce fatigue loads.

1.1.3 Design criteria

This chapter is based on the design criterion given by the API standard: Recommended Practice for Flexible Pipe 17B[4].

The design criteria for flexible pipes can generally be given in terms of the following design parameters:

- Strain (polymer sheath, unbonded pipe)
- Creep (internal pressure sheath, unbonded pipe)
- Stress (metallic layers and end fitting)
- Hydrostatic collapse (buckling load)
- Mechanical collapse(stress introduced from armour layers)
- Torsion
- Crushing collapse and ovalization (during installation)
- Compression (axial and effective)
- Service-life factor

In this thesis, we focus on the design criteria regarding armours. The degradation modes of the pressure and tensile armours include corrosion, disorganization or locking of armouring wires as well as fatigue and wear. The recommended criteria concluded from API 17B[4] is showed in the following table.

Table 1-2 Design criteria for pressure and tensile armours[4]

Component	Degradation mode	Design solution or variables
Pressure and tensile armours	Corrosion	Only general corrosion accepted, no crack initiation acceptable.
	Disorganization or locking of armouring wires	No disorganization of armouring wires when bending to minimum bend radius.
	Fatigue and wear	It is necessary to give consideration in the design of flexible pipe to service life or replacement of components/ancillary equipment as part of an overall service-life policy. Details in chapter 8.2.4

1.2 Scope of work

As mentioned above, this thesis will focus on the stress analysis and the slip behaviour of nonbonded flexible pipe.

Existing research on nonbonded flexible pipe states: when friction force is taken into account, the slip in transverse direction will become very small. Thus, in some software, e.g. previous BFLEX2010, transverse slip has been neglected in order to reduce the number of degrees of freedom.

In this thesis, the modified version of BFLEX2010 with a new beam element hshear353 and a new contact element hcont453 which can be used to describe transverse slip behaviour are used. Two BFLEX models with different pipe parameters are studied and compared to the analytical solution.

In chapter 2, existing analytical model valid for thin curved rods sliding on a curved circular surface are studied. Both axisymmetric and bending behaviour are discussed. Finite element implementation procedure is described.

In chapter 3, an introduction of BFLEX2010 is given. The finite element models used in this thesis together with formulations of the new element types are described.

In chapter 4, numerical simulations using the bflex models introduced in Chapter 3 are carried out.The numerical results are compared with analytical solutions in order to verify whether the modified BFLEX version can provide enough accuracy when describing the tendon's kinematic. Cases regarding to multi-layer influence and cyclic bending effects on local stress and slip behaviour are also carried out.

In chapter 5, a summary of the thesis and suggestions for future work are given.

Chapter2 Analytical description for nonbonded pipes

2.1 Introduction

In this chapter, the mechanical properties for flexible pipe under axisymmetric loading/bending are addressed. In addition, existing analytical model of a thin curved rod sliding on a curved circular surface is reviewed. This model can be used to describe slip behaviour of flexible pipe under axisymmetric loading as well as bending. In addition, strain and stress relationship and finite element implementation procedure are introduced. The theoretical result will be used to compare with the finite element result in Chapter 4.

2.2 Mechanical description

The physical behaviour of flexible pipe under tension, torsion and bending depends on the cross section properties. In order to simplify the problem, we assume that the bending and axial loads applied on helically wound armours could be uncoupled. This is illustrated in the figure below:

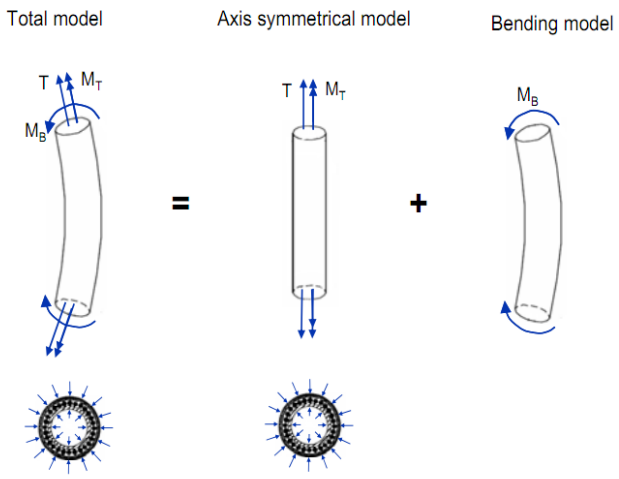

Figure 2-1 Models for cross-sectional analysis[5]

2.2.1 Axisymmetric behaviour

For flexible pipe, it is the tensile armour layers that carry most of the axial loads. When exposed to tension and torsion, the nonbonded pipes respond linearly within the relevant range, as shown in the figure 2.2[2]. The linear behaviour also applies to bonded pipes under any kinds of these loadings in a relative range.

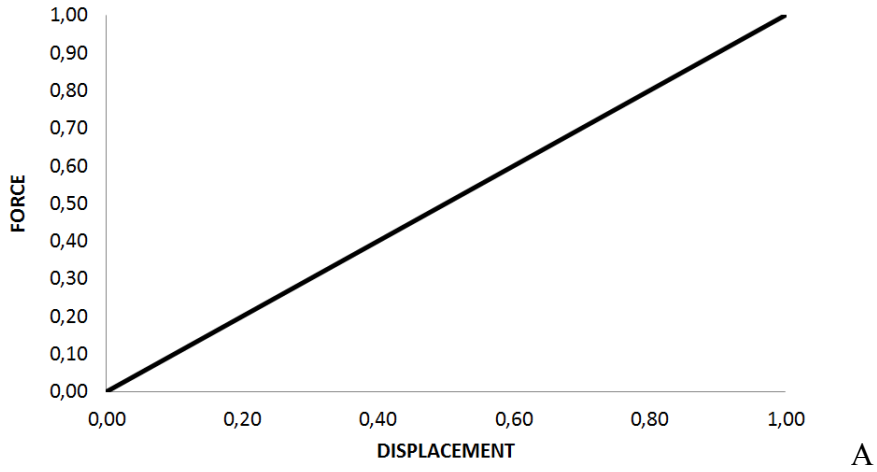

Figure 2-2 Axisymmetric loading behaviour[2]

2.2.2 Bending behaviour

Bending is one of the most important properties of flexible pipe comparing to ordinary steel risers. For a nonbonded pipe, this property is ensured by the slip between the armour tendons and the supporting structure. The nonbonded flexible pipe has a non-linear moment-curvature relationship as illustrated in the figure below.

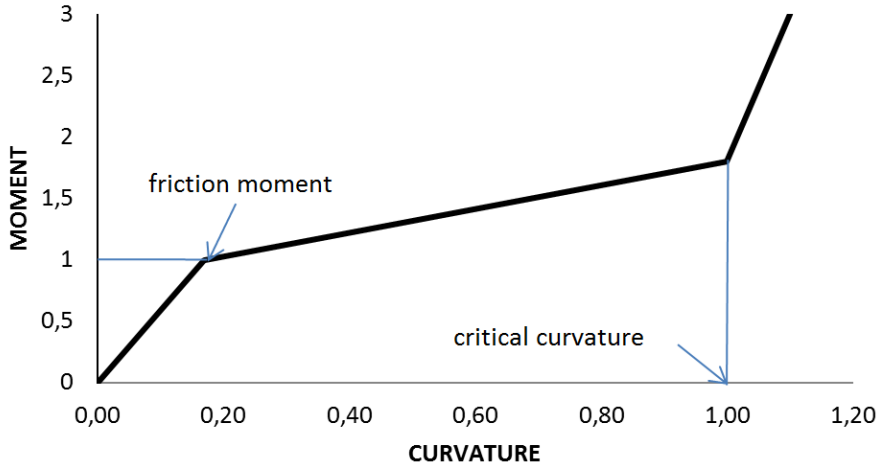

Figure 2-3 Bending behaviour[2]

It can be divided into three steps:

Step1, Ordinary beam- bending phase, small curvature

In this step, the cross-section of the tendon remains plane. This shows that no slip exists between tendon and supporting structure. The pipe will bend with a similar stiffness as a steel pipe with same cross section.

Step2, Low bending stiffness phase, intermedium curvature

As the moment applied on flexible pipe increases, slip will occur when the bending moment overcomes friction moment of the pipe, due to the development of shear stress in armour layer and the supporting structure. The bending stiffness in this step drops significantly. We define the bending stiffness at this step 'sliding bending stiffness' and it is govern by the stiffness of the plastic tubules and strain energy in each armour tendon.

Step3, Increasing bending stiffness, critical curvature

This phase begins at when the gap between each tendon is closed. In this phase, no sliding is allowed anymore. This is termed as critical radius and should be avoid in any operation.

In the following, this thesis pays its attention to step2 when studying the slip behaviour under bending. Basic assumptions are[4]:

1, The bending stiffness induced by local tendon behaviour at end restraints is at least one order of magnitude less than the effect of the total cross section bending stiffness and hence can be neglected. This is considered to be a reasonable assumption along the bending stiffener.

2, Each tendon behaves independently for the curvature range considered. This assumption is considered reasonable as long as the curvature is smaller than the critical curvature.

2.3 Analytical description for axisymmetric behaviour

In this part, an existing analytical model of a tube layer with an individual tendon sliding on it is reviewed. The model can be used to describe the armour tendon's behaviour under either axisymmetric loading or bending. Axisymmetric behaviour is discussed in this sub-chapter, and bending behaviour will be discussed in Chapter 2.4.

Since axisymmetric loading, i.e., tension, torsion and pressure does not change the shape of the pipe cross section. Therefore, axisymmetric behaviour can be assumed and relatively simple relations can be obtained.

2.3.1 Coordinate system

In order to describe a point on the surface of a circular cylinder with a constant radius ρ, a fixed Cartesian coordinate system with axes $\boldsymbol{Z^I}$ and unit vectors $\boldsymbol{E_I}$ is used. Supporting surface is represented by the radius R and surface coordinates w and v. See figure below.

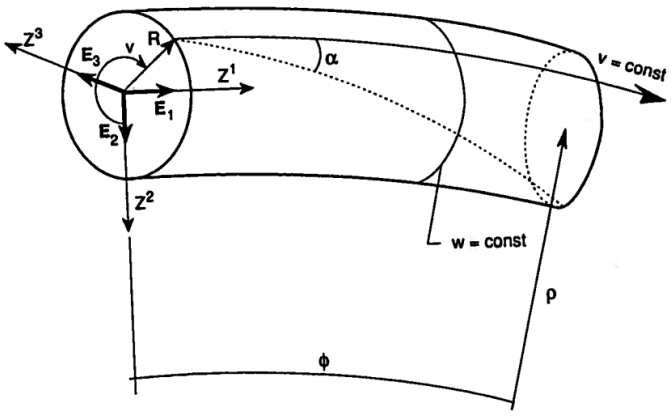

Figure 2-4 Definition of pipe center line system and basic quantities[2]

The Cartesian coordinates of an arbitrary point on the circular surface is hence expressed by Eq.(2.1)-(2.3):

$$Z^1 = (\rho - Rcosv)sin\varphi \tag{2.1}$$

$$Z^2 = \rho - (\rho - Rcosv)cos\varphi \tag{2.2}$$

$$Z^3 = Rsinv \tag{2.3}$$

When the pipe is exposed to high tensile stress, it is reasonable to assume that the rod cross section principal axes are fixed to the surface normal. In addition, a local orthonormal axes constructed at an arbitrary point with unit base vector $\boldsymbol{I_I}$ is developed in order to describe the principal torsion-flexure axes along the curve. See figure 2-5.

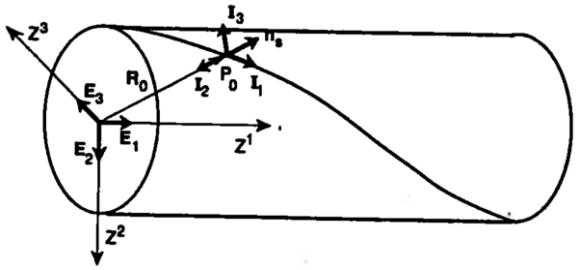

Figure 2-5 The $\boldsymbol{I_I}$ system[2]

The rotation of the local unit triad along an infinitesimal distance is given by the Seret-Frenet[6] differential formula, where X^1 represents for the arc length coordinate:

$$\begin{bmatrix} \frac{d\boldsymbol{I}_1}{dX^1} \\ \frac{d\boldsymbol{I}_2}{dX^1} \\ \frac{d\boldsymbol{I}_3}{dX^1} \end{bmatrix} = \begin{bmatrix} 0 & \kappa & 0 \\ -\kappa & 0 & \tau \\ 0 & -\tau & 0 \end{bmatrix} \begin{bmatrix} \boldsymbol{I}_1 \\ \boldsymbol{I}_2 \\ \boldsymbol{I}_3 \end{bmatrix} \tag{2.4}$$

Then, the torsion τ and principal curvature κ can be determined directly:

$$\tau = \boldsymbol{I}_3 \cdot \frac{d\boldsymbol{I}_2}{dX^1} \tag{2.5}$$

$$\kappa = \boldsymbol{I}_2 \cdot \frac{d\boldsymbol{I}_1}{dX^1} \tag{2.6}$$

Which for a rod being wound onto a circular helix gives:

$$\tau = \frac{sin\alpha cos\alpha}{R} \tag{2.7}$$

$$\kappa = \frac{sin^2\alpha}{R} \tag{2.8}$$

In addition, base vectors $\boldsymbol{G_I}$ directed along the local curvilinear coordinate axes $\boldsymbol{X^I}$ is introduced. $\boldsymbol{G}_1$is directed parallel to $\boldsymbol{I}_1$, $\boldsymbol{G}_2$ is oriented along the inwards surface normal and fixed to the cross section principal axes, $\boldsymbol{G}_3$is defined by the orthonormality condition. The angle between $\boldsymbol{I_I}$ and $\boldsymbol{G_I}$ is defined as ω, which represents for the relative rotation from cross section principal axes to the torsion-flexure axes as shown in the figure below.

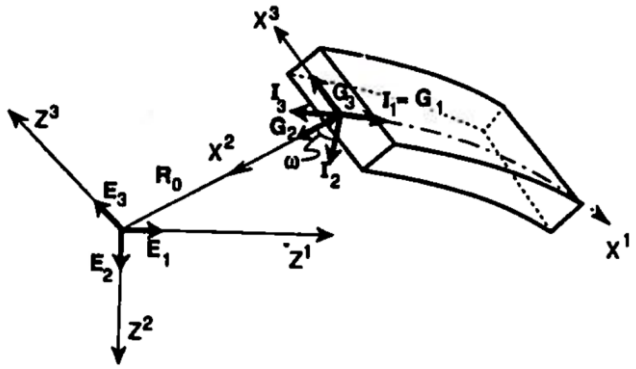

Figure 2-6 $\boldsymbol{G_I}$ system relative orientation to $\boldsymbol{I_I}$ system[2]

A generalized Seret-Frenet formula is obtained as:

$$\begin{bmatrix} \frac{d\boldsymbol{G}_1}{dX^1} \\ \frac{d\boldsymbol{G}_2}{dX^1} \\ \frac{d\boldsymbol{G}_3}{dX^1} \end{bmatrix} = \begin{bmatrix} 0 & \kappa_3 & -\kappa_2 \\ -\kappa_3 & 0 & \kappa_1 \\ \kappa_2 & -\kappa_1 & 0 \end{bmatrix} \begin{bmatrix} \boldsymbol{G}_1 \\ \boldsymbol{G}_2 \\ \boldsymbol{G}_3 \end{bmatrix} \tag{2.9}$$

Where:

$$\kappa_1 = \tau + \frac{d\omega}{dX^1} \tag{2.10}$$

$$\kappa_2 = \kappa \sin\omega \tag{2.11}$$

$$\kappa_3 = \kappa \cos\omega \tag{2.12}$$

κ_1 is the total accumulated torsion of the rod center line, where τ represents the geometric torsion of the rod center line, $\frac{d\omega}{dX^1}$ denotes the torsion of the cross section induced by the rotation of cross section relative to the torsion-flexure axes. κ_2 and κ_3 represent the components of the principal curvature κ in the (X^1, X^3) and (X^1, X^2) planes respectively.

From Eq.(2.9), the torsion and curvature components can be found directly:

$$\kappa_1 = \boldsymbol{G}_3 \cdot \frac{d\boldsymbol{G}_2}{dX^1} \tag{2.13}$$

$$\kappa_2 = -\boldsymbol{G}_3 \cdot \frac{d\boldsymbol{G}_1}{dX^1} \tag{2.14}$$

$$\kappa_3 = \boldsymbol{G}_2 \cdot \frac{d\boldsymbol{G}_1}{dX^1} \tag{2.15}$$

The transverse curvature will only occur when ω differs from zero, i.e., the surface normal dose not coincide with curve normal. Eq. (2.13)-(2.15) are used to find out the curvature increments in sub chapter 2.4.2.

2.3.3 Kinematic restraint

It is assumed that the tendon is forced to slide along the curvilinear axes X^1 and X^3only, thus the full three dimensional description can be eliminated.

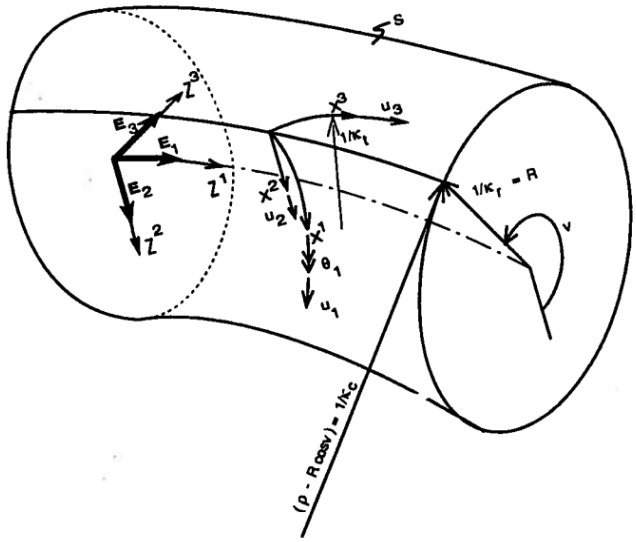

Figure 2-7 Restraint of the curvilinear plane[2]

Thus, a restraint on the rotation θ_1 of the rod about the X^1 axis is introduced:

$$\theta_1 = -\kappa_t u_3 + \kappa_1 u_1 \tag{2.16}$$

Where u_1 and $u_3$represent for the tendon's longitudinal and transverse displacement along the local curvilinear axes respectively.

κ_t is the pipe surface transverse curvature along X^3 direction and could be expressed by the following equation:

Similarly,

$$\kappa_t = \cos^2\alpha\, \kappa_r + sin^2\alpha\, \kappa_c \tag{2.17}$$

Where κ_r and κ_c represent the principal curvatures in the circumferential and longitudinal directions of the surface, where

$$\kappa_r = \frac{1}{R} \tag{2.18}$$

$$\kappa_c = \frac{1}{\rho - Rcosv} \tag{2.19}$$

2.3.4 Equilibrium equation

Figure 2-8 shows the forces and moments on an infinitesimal element of the curved rod.

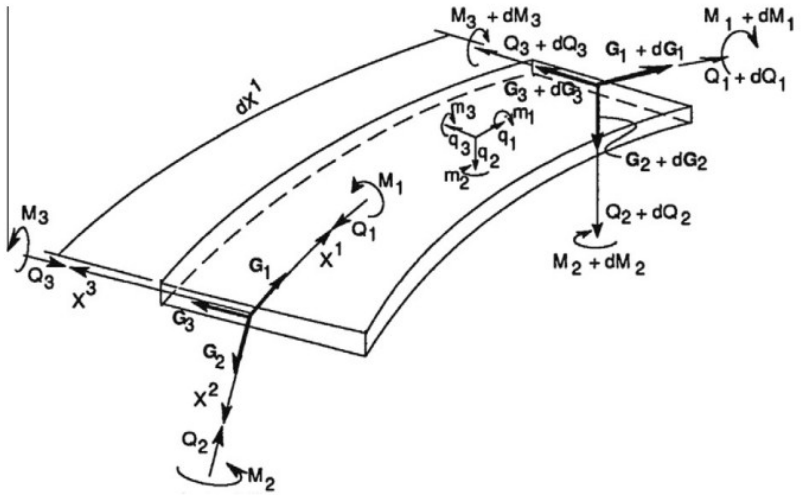

Figure 2-8 Curved infinitesimal beam element[2]

At the first end, there is a local coordinate system with axes $\boldsymbol{X^I}$ and base vector $\boldsymbol{G_I}$ together with stress resultants $\boldsymbol{Q_I}$ and $\boldsymbol{M_I}$. The axes are fixed to the rod cross section principal axes. At the second end, the axes change to $\boldsymbol{G_I + dG_I}$ and the stress change to $\boldsymbol{Q_I + dQ_I}$ and $\boldsymbol{M_I + dM_I}$. Consider force and moment equilibrium and introduce the generalized Seret-Frenet formula from Eq.(2.9), we can obtain the following six coupled

equilibrium equations:

$$\frac{dQ_1}{dX^1} - \kappa_3 Q_2 + \kappa_2 Q_3 + q_1 = 0 \tag{2.20}$$

$$\frac{dQ_2}{dX^1} + \kappa_3 Q_1 - \kappa_1 Q_3 + q_2 = 0 \tag{2.21}$$

$$\frac{dQ_3}{dX^1} - \kappa_2 Q_1 + \kappa_1 Q_2 + q_3 = 0 \tag{2.22}$$

$$\frac{dM_1}{dX^1} - \kappa_3 M_2 + \kappa_2 M_3 + m_1 = 0 \tag{2.23}$$

$$\frac{dM_2}{dX^1} + \kappa_3 M_1 - \kappa_1 M_3 - Q_3 + m_2 = 0 \tag{2.24}$$

$$\frac{dM_3}{dX^1} - \kappa_2 M_1 + \kappa_1 M_2 + Q_2 + m_3 = 0 \tag{2.25}$$

2.3.5 Local forces and moments caused by axisymmetric loading

It is easily to demonstrate that there is no transverse curvature for a helix been wound to a straight pipe[2], i.e., $\kappa_2 = 0$. When the pipe is exposed to axisymmetric loads, the tendon will still describe a helix, the transverse curvature κ_2 and all differentials will therefore vanish.

Furthermore, the equilibrium equations discussed in Chapter 2.3.4 for an infinitesimal element of the curved rod can be simplified and written as[2]:

$$\kappa_3 Q_1 - \kappa_1 Q_3 + q_2 = 0 \tag{2.26}$$

$$\kappa_3 M_1 - \kappa_1 M_3 - Q_3 = 0 \tag{2.27}$$

Where $Q_1$and M_1 are axial force and moment, Q_3 and M_3 are transverse force and moment respectively, q_2 represents for the distributed contact line load.

Eq. (2.26) represents the force equilibrium equation in the radial direction, Eq.(2.27) represents the moment equilibrium equation about the surface normal. When knowing the expression of Q_1, M_1, M_3 in terms of twist and curvature induced by axisymmetric loading, the unknown contact pressure q_2 and shear force Q_3 can be eliminated. In this part, analytical solution from Sævik.S[2] considering all the terms discussed above is introduced.

- Axial force

The axial force Q_1 can be found by using the axial strain ε_1 of the tendon centre line as a function of pipe global axial strain, local radial displacements and global twist given as:

$$\varepsilon_1 = \varepsilon_z cos^2\alpha - \frac{u_2}{R} sin^2\alpha + R\theta_{,z} sin\alpha cos\alpha \tag{2.28}$$

Where ε_z is the global axial strain caused by tension; u_2 is the radial displacement of the pipe induced by pressure; $\theta_{,z}$ is the global twist which represents torque. They are defined in the figure below:

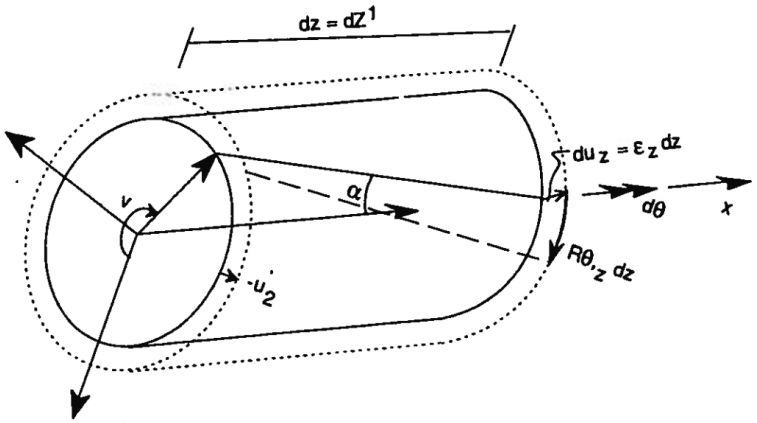

Figure 2-9 Geometric relation[2]

The axial force is found by:

$$Q_1 = C_\sigma A \varepsilon_1 \tag{2.29}$$

Where C_σ is the Young's modulus of elasticity (Nm^{-2}), A is the rod cross section area (m^2).

- Moments

The twist and normal curvature increments can be calculated by moving the rod from stress free state to the deformed equilibrium state. By using the coordinate system introduced in Chapter 2.3.1, it is found:

$$\Delta\kappa_1 = \kappa_1 u_{1,1} + (\kappa_3 - \kappa_t)u_{3,1} + \kappa_1\kappa_3 u_2 \tag{2.30}$$

$$\Delta\kappa_3 = -2\kappa_1 u_{3,1} - (\kappa_1)^2 u_2 + \kappa_3 u_{1,1} \tag{2.31}$$

$\Delta\kappa_1$ and $\Delta\kappa_3$ represent the twist and normal curvature increments. $u_{1,1}$ and $u_{3,1}$ are the derivatives of u_1 and u_3.

By decomposing the global displacements along the local coordinate axes shown in figure 2-10, the displacement differentials are obtained:

$$u_{1,1} = \varepsilon_z cos^2\alpha + R\theta_{,Z}\, sin\,\alpha cos\alpha \tag{2.32}$$

$$u_{3,1} = \varepsilon_z sin\,\alpha cos\alpha - R\theta_{,Z} cos^2\alpha \tag{2.33}$$

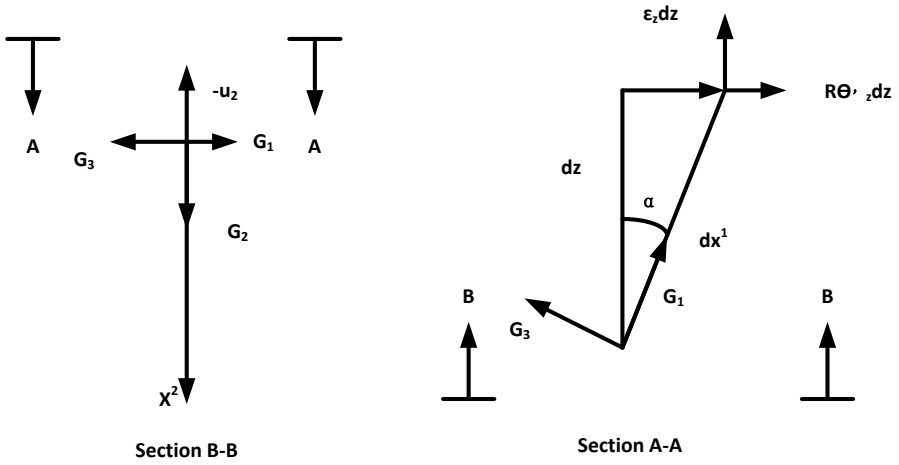

Figure 2-10 Components of deformation in local system[2]

By inserting Eqs.(2.32)-(2.33), Eqs. (2.7)-(2.8) and Eq.(2.17) into Eqs.(2.30)-(2.31), the following results are obtained:

$$\Delta\kappa_1 = \frac{sin\,\alpha cos\alpha}{R}\left(\varepsilon_z sin^2\alpha + R\Theta_{,Z}\frac{cos^3\alpha}{sin\alpha} + sin^2\alpha\frac{u_2}{R}\right) \tag{2.34}$$

$$\Delta\kappa_3 = \frac{sin^2\alpha}{R}(-\varepsilon_z cos^2\alpha + R\Theta_{,Z}\left(2\frac{cos^2\alpha}{tan\alpha} + sin\alpha cos\alpha\right) - cos^2\alpha\frac{u_2}{R}) \quad (2.35)$$

Thus, the moments M_1 and M_3 can be found by:

$$M_1 = C_\tau I_t \Delta\kappa_1 \quad (2.36)$$

$$M_3 = C_\sigma I_3 \Delta\kappa_3 \quad (2.37)$$

Where C_τ represents shear modulus (Nm^{-2}), and I_t represents the cross section torsion constant (m^4), I_3 is the inertia moment about X^3 axis (m^4).

2.4 Analytical description for bending

In this sub-chapter, an analytical solution describing bending problem by using the thin curved rod model developed in Chpater2.3 is performed.

2.4.1 Two limited curves

Given definitions of two limited curves regarding the movement of tendon when subjected to bending:

Geodesic curve: Geodesic curve is defined as the minimum curve between two sufficiently close points on the surface and has no transverse curvature. For two sufficiently close points, only one such curve exists. The curve normal vector is parallel to the surface normal vector on this curve.

Loxodromic curve: Loxodromic curve is defined as that the tendon is glued to the supporting core under infinite friction condition. The tendon along the loxodromic curve hence has neither longitudinal nor transverse slip. However, when a pipe is bent, no matter of the friction coefficient, the axial strain from the compression side to the tension side is too large and needs to be eliminated by a longitudinal slip along the loxodromic curve path.

In reference[7], it has been demonstrated that the helix along a straight cylinder follows the geodesic solution. When the pipe is bent, the tendon will have transverse curvature if the transverse slip relative to the core is prevented by friction. The tendon in this case follows a loxodromic path. If we assume zero friction, a certain transverse slip will occur in order to eliminate transverse curvature and the tendon will again follow the geodesic solution. A longitudinal slip always occurs from the compressive side to the tension side.

A figure illustrates the relative slips is given below:

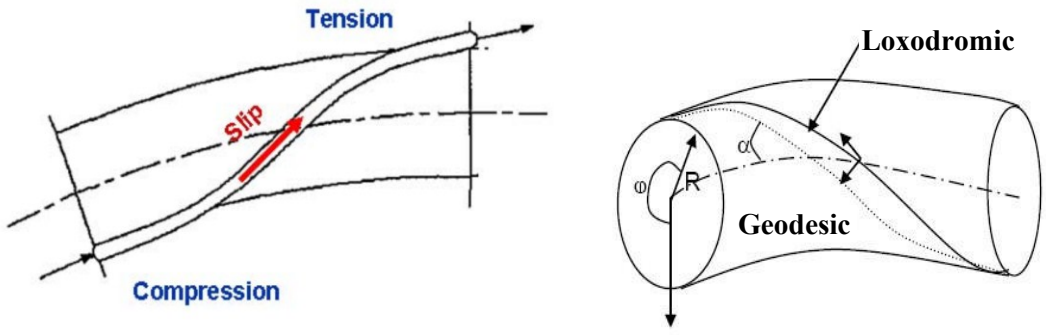

a. b.

Figure 2-11 a. Slip from compression side to the tensile side[5] b. The two limited curves[14]

- Geodesic solution

When the pipe is subjected to bending, the displacement and curvature increments in order to follow the geodesic solution, i.e., assuming no friction, are given below[2].

$$u_1 = \frac{R^2}{\rho}\frac{cos^2\alpha}{sin\alpha}sinv \tag{2.38}$$

$$u_3 = \frac{R^2}{\rho tan\alpha}\left(2sin\alpha + \frac{cos^2\alpha}{sin\alpha}\right)sinv \tag{2.39}$$

$$\Delta\kappa_1 = \frac{-sin\alpha cos\alpha}{\rho}\left(\frac{1}{sin^2\alpha} - 3\right)cosv \tag{2.40}$$

$$\Delta\kappa_3 = -\frac{3cos^2\alpha}{\rho}cosv \tag{2.41}$$

u_1 and $u_3$represent for the longitudinal and transverse displacement respectively, $\Delta\kappa_1$ and $\Delta\kappa_3$ represent for the twist and normal curvature increments.

- Loxodromic solution

The basic idea used to find out the loxodromic solution is first assuming that the center line of the tendon is directed along the loxodromic curve, and then calculates the corresponding curvature increments and cross section forces. Finally, a longitudinal

displacement along the loxodromic path from compressive side to the tensile side is introduced in order to eliminate the axial strain. However, an additional transverse movement is needed to reach geodesic.

All mathematical functions entering the theory are piecewise continuous in space and time. *Lagrangian* description with particle P and time t as independent variables is used.

Strains can be expressed by Green Strain tensor in the local curvilinear system and then transfers to a Cartesian strain tensor.

It is assumed no significant change of volume or area during deformation since the strains considered are assumed small.

The displacements, i.e., the curvature increments applying loxodromic assumption, before introducing the longitudinal displacement are given below:

$$\Delta\kappa_1 = \frac{sin\alpha cos\alpha}{\rho} cos^2\alpha cosv \tag{2.42}$$

$$\Delta\kappa_2 = -\frac{cos\alpha}{\rho}(1 + sin^2\alpha)sinv \tag{2.43}$$

$$\Delta\kappa_3 = -\frac{cos^2\alpha}{\rho} cos^2\alpha cosv \tag{2.44}$$

The longitudinal slip needed from the compression side to tension side is the same as Eq.(2.38). No transverse slip occurs for loxodromic solution.

The consistent strain and stress relations that connect one equilibrium state to another used to find out the loxodromic solution is discussed in sub-chapter 2.4.3.

2.4.3 Strain and stress relations

The Green strain tensor in the local Cartesian coordinate system is used to describe the strain field. Insignificant second order effects are neglected. Hooke's material law for isotropic elastic material is assumed. Detailed governing equations refer to [2], kinematic restraint in Eq.(2.16) is applied.

The stress relations are obtained by applying the Principle of Virtual Displacements (PVD). Virtual displacement is an assumed infinitesimal change of system coordinates occurring while time is held constant. It is called virtual rather than real since no actual displacement can take place without the passage of time. This principle computes fictions work down by forces and stresses on a set of kinematical admissible

displacements and strains. The differential equation in this case is fulfilled on an average form rather than point wise.

The error is eliminated on an average form. This is down by equal the error introduced from assumed weight function of external work and the error from internal work. By applying virtual work principle for an arbitrary equilibrium state which excluding volume forces, we get:

$$\int_V \boldsymbol{\sigma}: \delta\boldsymbol{\varepsilon}\sqrt{G}dX^1dX^2dX^3 - \int_S \boldsymbol{t}\cdot\delta\boldsymbol{u}dS = 0 \tag{2.45}$$

This is the basic principle to get stress relations. Details refer to [2].

For large deformation problems of solid mechanics in finite element analysis, incremental form of PVD should be used. Usually, two alternative methods are used: Total Lagrangian(TL) and the Updated Lagrangian(UL) formulation. In TL formulation, all variables are referred to the initial (C^0)configuration. While in UL, formulations are referred to the last obtained equilibrium position, i.e., the current(C^n) configuration. UL formulation is used to describe the stress relations here.

2.5 Finite element implementation

2.5.1 Introduction

A finite element implementation based on the thin curved analytical model described before is introduced in this sub-chapter. This implementation is used as the basis in the finite element software BFLEX introduced in Chapter3. Only some conclusions are given here. Details refer to reference [2].

2.5.2 Finite element implementation

The basic finite element formulations are introduced here. Two nodes beam element is used. The tendon is assumed to be forced to slide on the supporting surface as described in chapter 2.3.3. This gives in total 4 degrees of freedom (DOFs) per node and 8 DOFs per element, as illustrated in figure below.

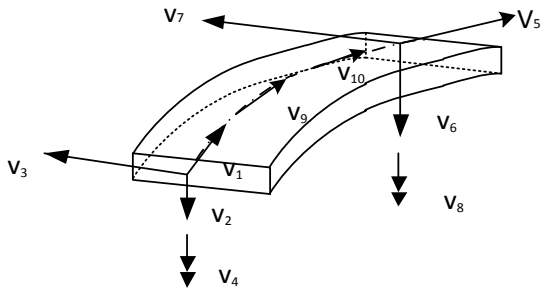

Figure 2-12 Eight (Ten) DOFs curved infinitesimal beam element[2]

Cubic interpolation function of standard beam element is used in the transverse X^3direction as well as in the axial direction. Linear interpolation is used for radial direction. V^9, V^{10} are internal DOFs which can be eliminated by static condensation.

The interaction between helix and core layer is modeled by elasto-plastic (Coulomb friction) springs attached to each node.

Three point Gauss numerical integration procedure is used to carry out the integration of virtual work terms. A reduced integration method with a fifth order polynomial is applied.

The coordinate system, stress and strain relationship together with the finite element implementation will be used in the finite element software BFLEX in chapter 3, but one should notice that in BFLEX, a reversed Z^2 and Z^3 coordinate is used, as in the next figure:

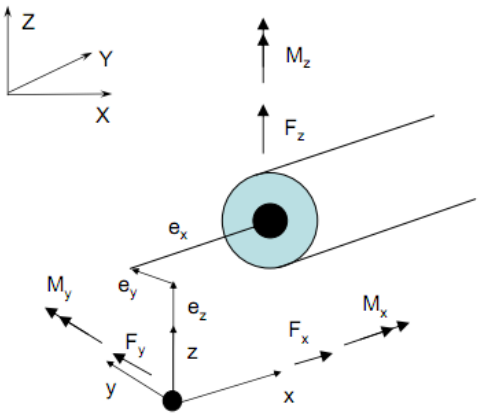

Figure 2-13 Coordinate system in BFLEX 2010[8]

Chapter3 Numerical solutions

3.1 Introduction

Although the global response analysis of flexible pipe could be carried out by a general finite element method(FEM) computer software, however, it is not sufficiently efficient and flexible as needed. Thus, it is required to develop special FEM computer programs that can be used in practical design. BFLEX is hence one of them first developed by SINTEF Civil and Environmental Engineering. In this chapter, a short introduction of BFLEX2010 is introduced. Two BFLEX models with two new types of elements will be built to investigate the transverse slip in this thesis.

3.2 BFLEX2010[8]

BFLEX2010, originally BFLEX, is a computer program used for stress analysis of flexible pipes, typically focus on local stress analysis. The available modulus provided by BFLEX 2010 includes:

- The BFLEX 2010 module.

  Reads and controls the input file, performs global analysis as well as the tensile armour analysis. The result is available in the output .raf file which contains all the data of analysis.

- The BFLEX 2010 POST module

  The result from post processing base to ASCII files can be plotted by the plotting program Matrixplot in this module.

  The following sub-modules are provided to analyze different parts of the cross section:

  1. The PFLEX module. Carry our pressure spiral bending stress analysis.
  2. The BOUNDARY module. Carry out transverse cross-sectional stress analysis.
  3. The BPOST module. Carry out post processing of local results data stored in the .raf file.
  4. The LIFETIME module. Carry out fatigue analysis.
  5. The XPOST 3D graphical user interface for model visualization presentation.

3.3 Finite element models in BFLEX2010

3.3.1 Finite element model

Two models are used in this thesis: a simplified model with one core and one single tendon, which is the same as the analytical model described in Chapter2; another one contains two tensile armour layers with 16 tendons in each, which can be used to study the interaction between layers. Some modeling properties for the two models are given in the table below.

1.Layers

Table 3-1 Finite element modeling properties for the simplified model

Layer name	**Element type**	**Explaination**
core	pipe31	core element group
tenslayer1	hshear353	tensile armour layer
tenscontact1	hcont453	contact layer between the core and tensile layer

The simplified model contains 400 elements in each layer and 8 pitches.

The model is showed in the following figure.

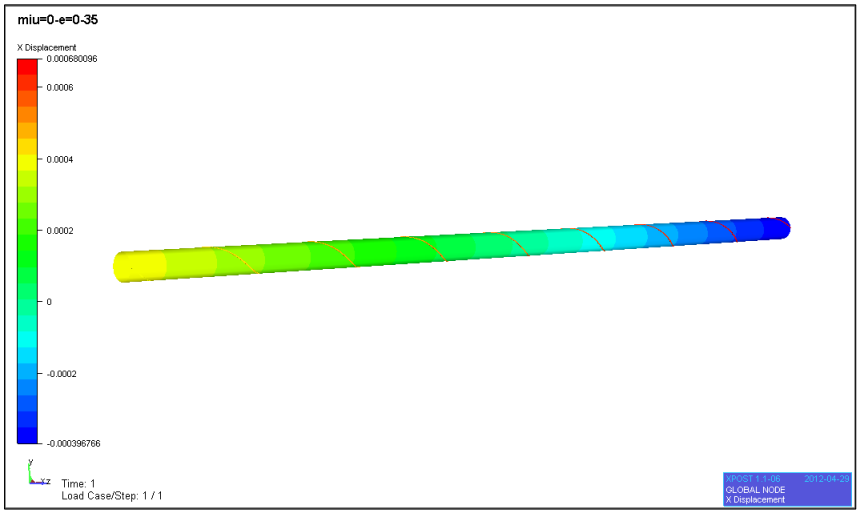

Figure 3-1 Simplified BFLEX model, single tendon

Table 3-2 Finite element modeling properties for the model with two armour layers

Layer	Element type	Explaination
core	pipe31	core element group
tenslayer1	hshear353	inner tensile armour layer
tenslayer2	hshear353	outer tensile armour layer
tenscontact1	hcont453	contact the supporting structure and inner tesile armour layer
tenscontact1-2	hcont453	contact layer between two tensile armour layers
layer2_outward	spring137	contact layer between the second tensile armour layer and the outer structure layer

The complex model contains 100 elements in each tendon. The inner layer contains 4 pitches and the outer layer contains 5. The model is shown in the following figure.

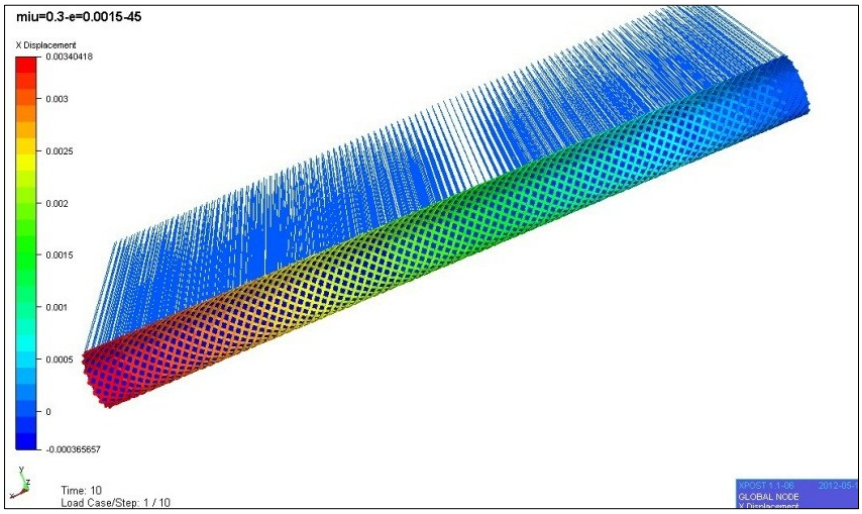

Figure 3-2 Complex BFLEX model, double tensile armour layers

2. Boundary condition

The rotation about x-axis is fixed for all layers, referring to the coordinate system in figure2-13.The core is fixed in translation in x, y and z direction. Other boundary conditions are applied for different cases as needed.

3. Material properties

The core is plastic and the tendon is elastic.

4. Other parameters

The following parameters are used: A global curvature $0.1\mathrm{m}^{-1}$ when exposed to bending; a core with radius 0.1m; a rectangular tensile armour wire cross section 9×3 mm.

3.3.2 Finite element formulations for hshear353 and hcont453

In previous BFLEX finite element program system, the relative displacement in transverse direction was neglected and the loxodromic path assumption was used. The reason[9] is that the transverse slip has been demonstrated to be small and has no significant influence on the fatigue analysis regarding to the calculating the stress ranges from local wire bending.

The main difference in this master thesis is that a new type of beam element hshear353 used to simulate tensile armour layer, together with a new type of contact layer element hcont453 has been used. Thus, transverse slip regime is activated and can be investigated. The aim of including transverse DOF is to study the wire buckling together with end fitting effects and so on.

The models in this thesis are used as examples to demonstrate whether the developed finite element formulation for the beam element hshear353 and the contact element hcont453 can give adequate description of slip behaviour or not. This is done by comparing the BFLEX result with the analytical solution on some simple cases.

- Beam element – hshear353[10]

hshear353 element is a two nodes beam element with 26 DOFs: 12 associated to the standard beam DOFs at the pipe center line used to describe the global strain quantities; 14 DOFs of the tensile layer which describe the local displacements of the wire relative to the core. Cubic interpolation in all directions is applied which leads to the membrane locking phenomena due to curvature coupling terms. A figure illustrates the DOFs is give blow:

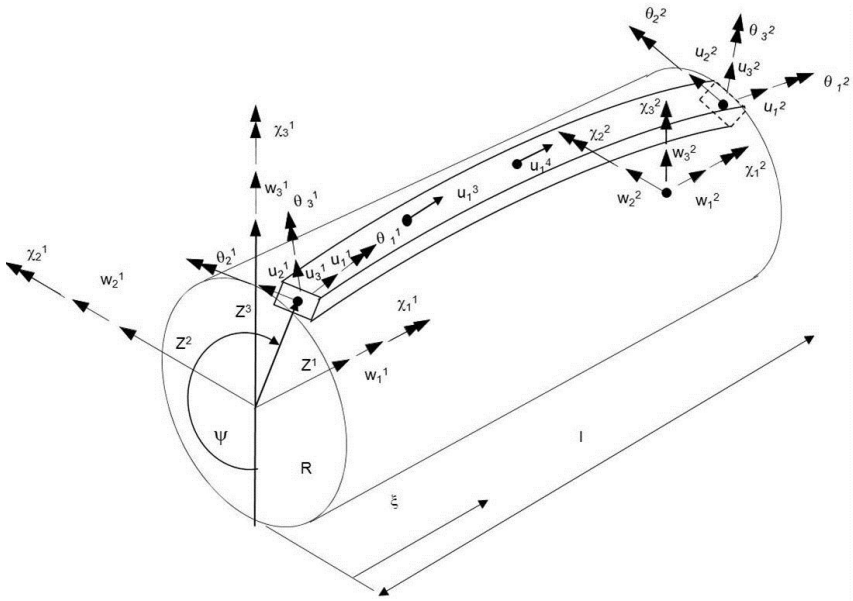

Figure 3-3 coordinate system for hshear353[10]

It should be noted that surface coordinate $'\psi'$ in the above figure is the same as $'v'$ as defined before. Definition $'v'$ will still be used in the following.

The internal virtual work contribution for this element is[10]:

$$W_i = \int_0^l [EA(\beta_{1,1} + u_{1p,1})\delta\beta_{,1} + GI_1(\omega_1 + \omega_{1p})\delta\omega_1 + GI_2(\omega_2 + \omega_{2p})\delta\omega_2 + GI_3(\omega_3 + \omega_{3p})\delta\omega_3 + \beta \cdot k \cdot c \cdot \delta\beta]dX^1 \quad (3.1)$$

Where $\omega_1, \omega_2, \omega_3$ are torsion and curvature quantities obtained from curved beam theory[11] as a result of relative sliding from the reference loxodromic curve. These include coupling terms between current torsion and curvature and the displacements and rotation of centerline[10].

ω_{ip} represents the prescribed torsion and curvature quantities that would result if plane surfaces remain plane and the wire strain, torsion and curvature being described by the loxodromic curve quantities. Quantity β represents the bi-directional relative displacement between tendon and core along the helical path where the sandwich beam theory is applied. c is a two-dimensional shear stiffness tensor determined by the stick-slip condition between layers, reducing to zero in the slip domain.

If we assume small strains and the kinematic restraint in (2.16), the prescribed quantities can be obtained as:

$$u_{1p,1} = Rcos^2\alpha cosvw_{3,11} - Rcos^2\alpha sin^2 vw_{2,11} + cos^2\alpha w_{1,1} + Rcos\alpha sin\alpha\chi_{1,1} \quad (3.2)$$

$$\omega_{1p} = sin\alpha cos^3\alpha\left(-cosvw_{3,11} + sinvw_{2,11}\right) + \frac{sin^3\alpha cos\alpha}{R}w_{1,1} + cos^4\alpha\chi_{1,1} \quad (3.3)$$

$$\omega_{2p} = cos^4\alpha\left(cosvw_{3,11} - sinvw_{2,11}\right) - \frac{cos^2\alpha sin^2\alpha}{R}w_{1,1} + (2\sin\alpha cos^3\alpha + sin^3\alpha cos\alpha)\chi_{1,1} \quad (3.4)$$

$$\omega_{3p} = (1 + sin^2\alpha)cos\alpha(-sinvw_{3,11} - cosvw_{2,11}) \quad (3.5)$$

It should be noted the transverse curvature $\kappa_t = \frac{cos^2\alpha}{R}$ is used here. It is because the prescribed quantities are applied before bending and hence no contribution is given by κ_c.

Where w_i are the transverse displacement components at the center of cross section, χ_i represents the prescribed rotation quantities at the pipe centerline.

- Contact element –hcont453[10]

The interlayer contact forces and the friction with regard to the relative displacement are described by the contact element hcont453 in the new version of BFLEX2010. hcont453 contains 24 DOFs as illustrated in the figure below:

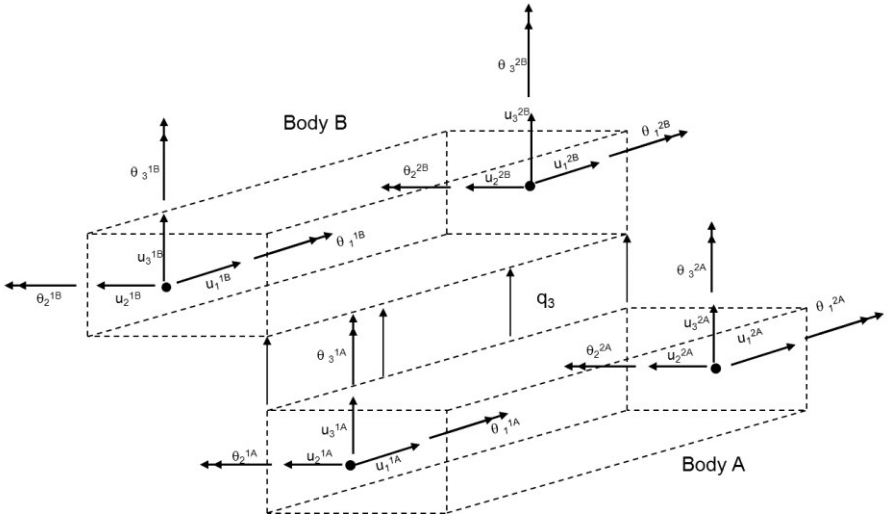

Figure 3-4 New contact element hcont453[9]

This element is based on a Hybrid Mixed formulation described in [11]-[12]. The basis of the concept is the incremental potential formulated as:

$$\Delta\pi = -\int_{S_c}(q_3+\Delta q_3)\cdot u_3 ds - \frac{1}{2c_n}\int_{S_c}\Delta q_3^2 ds - \int_{S_c} q_t\cdot\Delta\beta ds - \frac{1}{2}\int_{S_c}\Delta q_t\cdot\Delta\beta ds \tag{3.6}$$

Where q_3 is the distributed normal reaction, q_t is the distributed tangential reaction assuming a bi-directional friction model and c_n is a penalty stiffness parameter.

The finite element includes the following key features[10]:

1.Describing contact between layers of crossing tensile wires

2.Enabling easy description of the resistance against wire rotation from other layers by including torsion coupling terms

Chapter4 Numerical studies

4.1 Introduction

One of the main purposes of this chapter is to study how the numerical solution can be influenced by different parameters, e.g., friction coefficient, global curvature, cyclic bending effect and so on. In addition, the numerical and analytical results are compared for both axisymmetric loading case and bending. The aim of the comparisons is to verify that the numerical model can give adequate description of the tendon's stress and slip behaviour.

First of all, a verification of the numerical model on axisymmetric behaviour is carried out. The numerical solution for axisymmetric loading is compared with the analytical result. Two analytical solutions, one by Sævik[2], one by Witz & Tan[13] are compared with BFLEX result.

Also, an investigation on the maximum local curvilinear displacements in terms of friction coefficient, global curvature and strain under bending is carried out. The aim is to find out how the local curvilinear displacements can vary as a function of the three variables.

Moreover, the numerical model is compared with the analytical solution stated in Chapter2.4 where the pipe exposed to constant curvature. The aim of this is to verify that the numerical model can give successful description of the tendon's kinematic when subjected to bending.

Finally, the influence from cyclic bending effect on local curvilinear displacements is carried out. Both simplified model and the model with double tensile layers are used.

Beam element hshear353 and contact element hcont453 are used throughout this chapter. The control parameter for hcont453 is set to zero which means the friction force acting between layers is dependent on each other, i.e., the interaction of friction forces between layers is included.

4.2 Comparison on numerical and analytical solutions- axisymmetric loading

4.2.1 Description of the problem

This example case compares two analytical solutions with the numerical result from BFLEX2010 regarding axisymmetric loading, i.e., tension, torque and internal/external pressure. On the one hand, this case is used to find out that which analytical solution can better predict the motion of tendon, i.e., give closer result when comparing to numerical solution. On the other hand, it can also be used to prove that the developed numerical model can give adequate description of the tendon kinematic.

The simplified BFLEX model described in Chapter3 is used. Additional boundary condition is that the tensile armour layer is fixed on axial and transverse displacements at both ends.

4.2.2 Two analytical descriptions

Two existing analytical solutions are studied:

- From Sævik[2] :

The analytical description by Sævik is introduced in Chapter2.3. Eqs.(2.34)- (2.35) regarding twist and normal curvature increment are used to represent the tendon's kinematic behaviour and hence compared with other solutions. This is because the curvature increments have a linear relationship with local moment stress.

- From Witz & Tan[13] :

Witz & Tan suggest another method to describe axisymmetric loading; stated in [13].The difference for their solution comparing to Sævik's is that the center line straining of the tendon is excluded by them. Their results are directly obtained by input accumulated torsion and curvature which is expressed by updated lay angle and layer radius into Eqs.(2.7)-(2.8). The formulas obtained from their reference are given in Eqs. (4.1) - (4.2).

$$\Delta\kappa_1 = -\frac{1}{4R}\sin(4\alpha)\,\varepsilon_z + cos^2\alpha\cos(2\alpha)\theta_{,z} + \frac{2}{R}\cos\alpha sin^3\alpha\frac{u_2}{R} \tag{4.1}$$

$$\Delta\kappa_3 = -\frac{2}{R}sin^2\alpha cos^2\alpha\varepsilon_z + 2sin\alpha cos^3\alpha\theta_{,z} + \frac{1}{R}cos\alpha sin^2\alpha\frac{u_2}{R} \tag{4.2}$$

4.2.3 Comparison with numerical solution

In BFLEX2010, the Green strain theory and the Principle of virtual displacements discussed in Chapter2 are used to calculate stress relations. The simplified model discussed in Chapter3 is used.

Axial strain, torsion and radial displacements are applied to the model respectively. Comparison on twist and normal curvature increments by using the above three methods are carried out and discussed. Lay angles varying from 25°to 55°are studied. Initial principal curvature for a constant pipe is subtracted and only the curvature increment is shown in the plot.

- Axial strain

Axial strain (ε_z), which represents tension, is applied from 0 to 0.01 within one hundred load steps in BFLEX2010.

Curvature increments are plotted as a function of axial strain in the figures below.

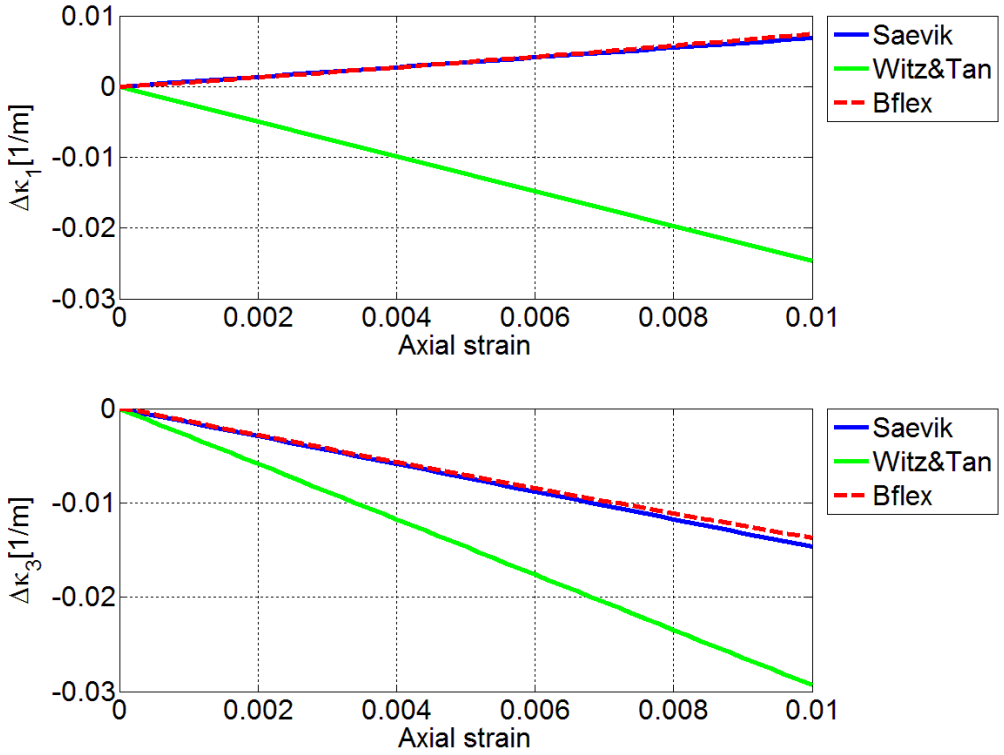

Figure 4-1 Curvature increments as a function of axial strain- 25°lay angle

It is observed in the above figure that the difference between Sævik's and BFLEX solution is smaller than the difference between Witz&Tan's and BFLEX solution. In all solutions, curvature increase linearly to axial strain.

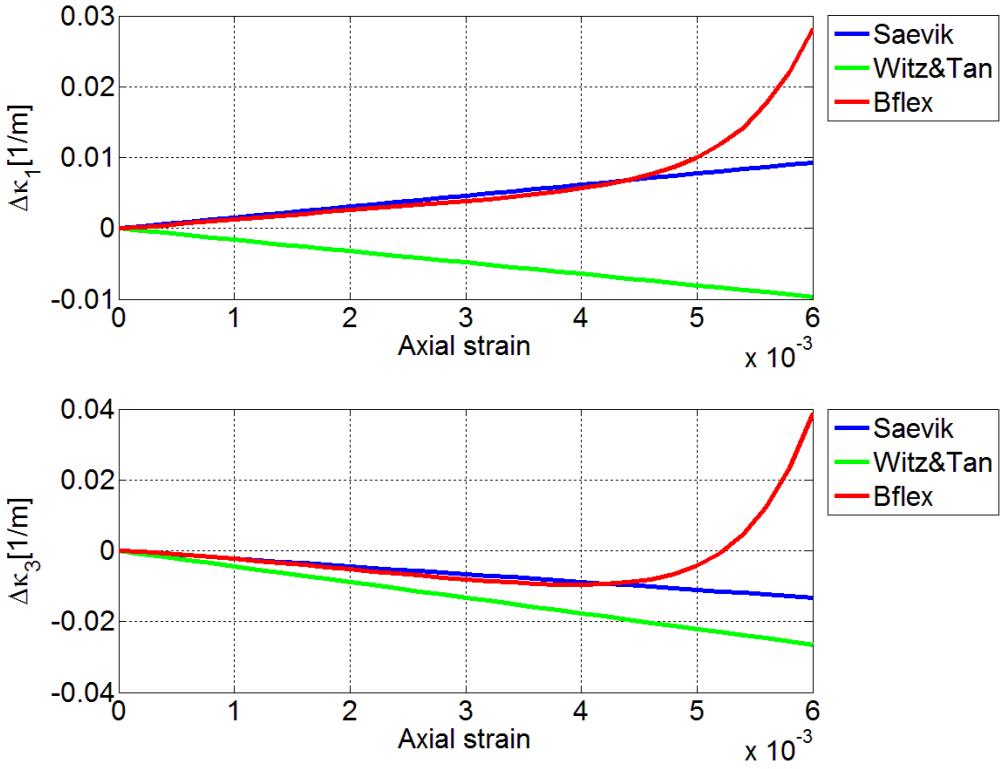

Figure 4-2 Curvature increments as a function of axial strain-35°lay angle

For 35°lay angle, it is found that the BFLEX solution increases rapidly when axial strain exceeds 0.0045. It is because nonlinear effects become significant in the model as the axial strain increases. For the region axial strain is smaller than 0.0045, linear relationship between axial strain and curvature increment is found, and Sævik's results have smaller deviation to BFLEX results comparing to Witz&Tan's.

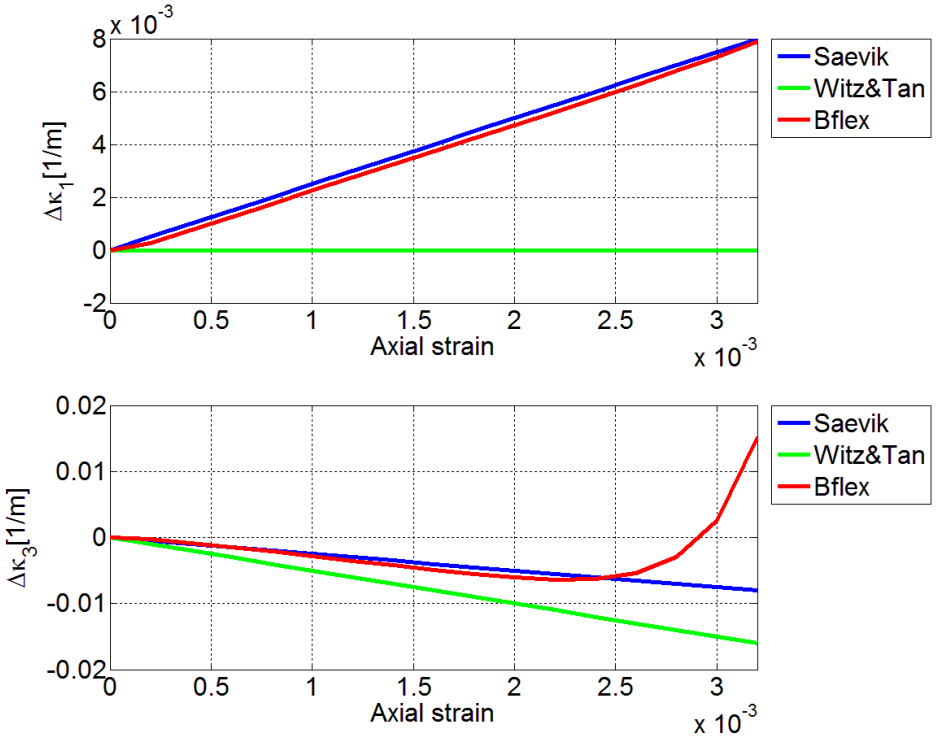

Figure 4-3 Curvature increments as a function of axial strain-45°lay angle

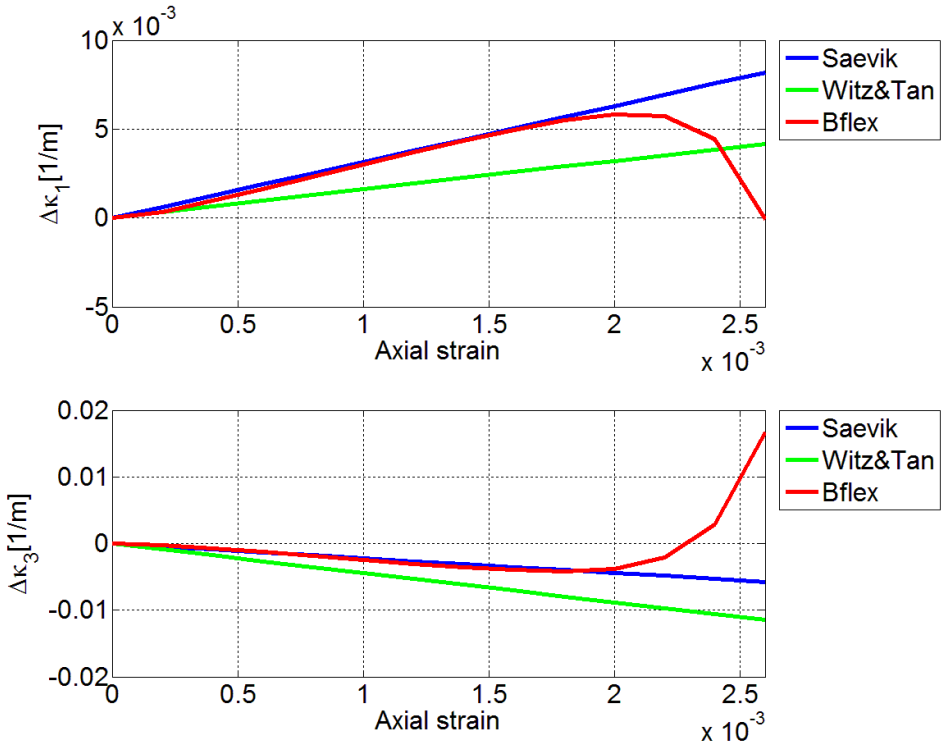

Figure 4-4 Curvature increments as a function of axial strain-55°lay angle

For 45 and 55° lay angle, similar results are found as for 35° lay angle: When the axial strain exceeds a certain value, the curvature increment is governed by non-linear effect and thus none of the two analytical solutions can give adequate prediction. In the linear region, Sævik's solution gives closer results with numerical solution.

- Torsion

This thesis tests the region of global torsion($\theta_{,z}$) from 0 to 0.01(m^{-1}), results are shown in the figures below.

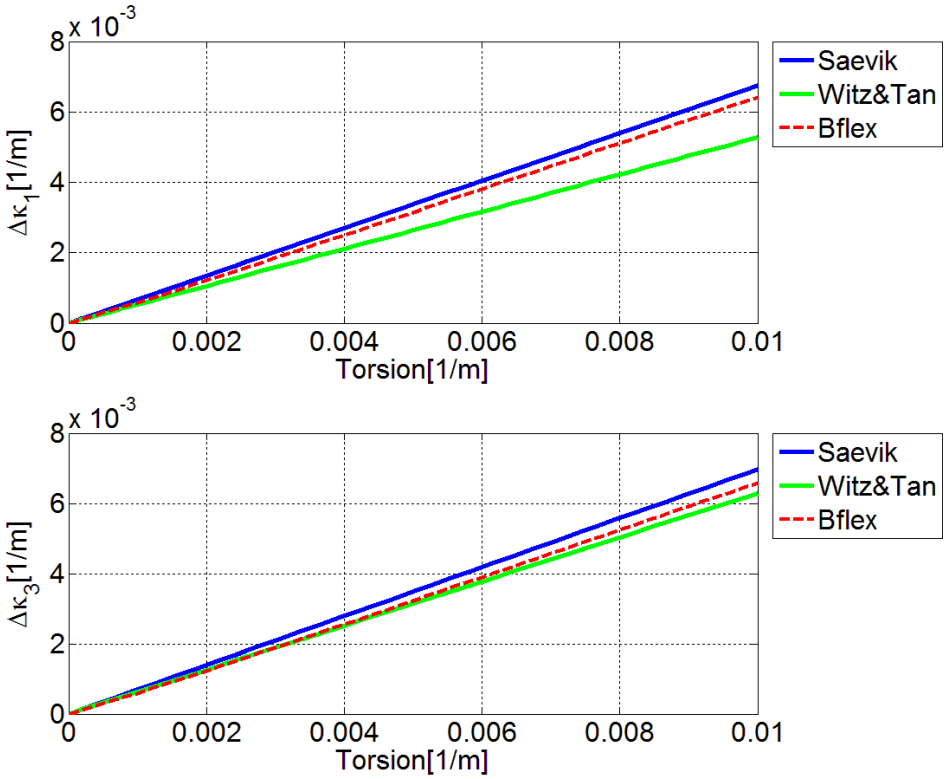

Figure 4-5 Curvature increments as a function of torsion-25°lay angle

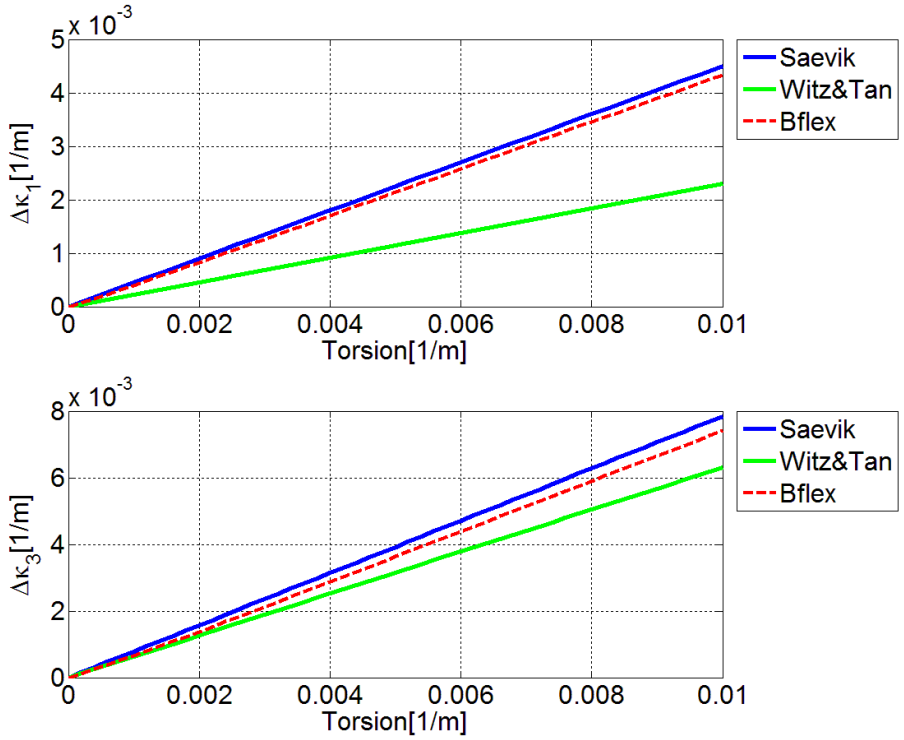

Figure 4-6 Curvature increments as a function of torsion-35°lay angle

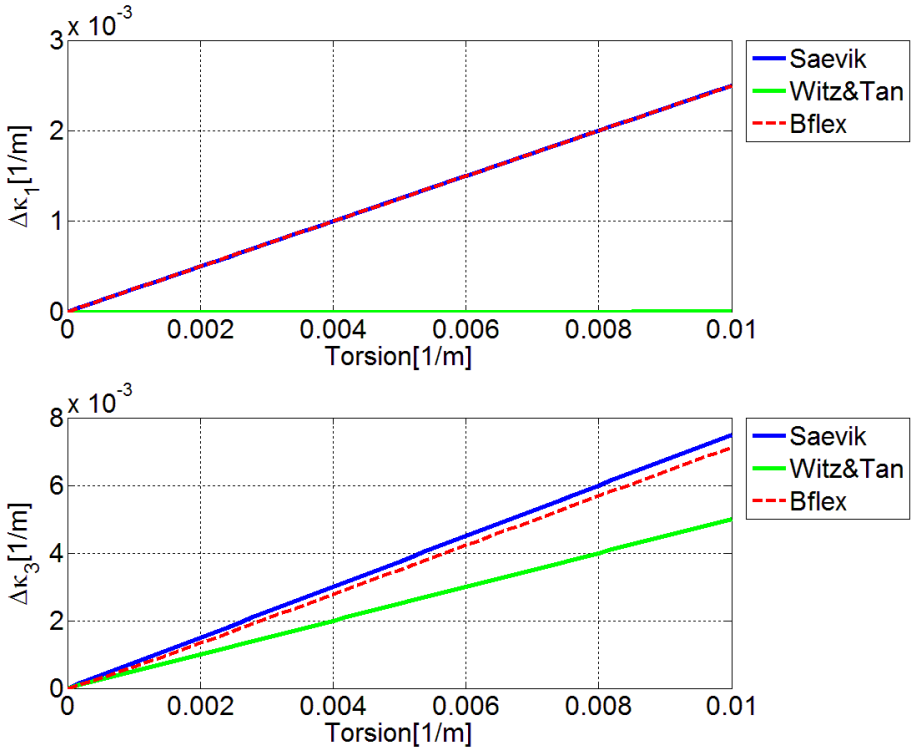

Figure 4-7 Curvature increments as a function of torsion-45°lay angle

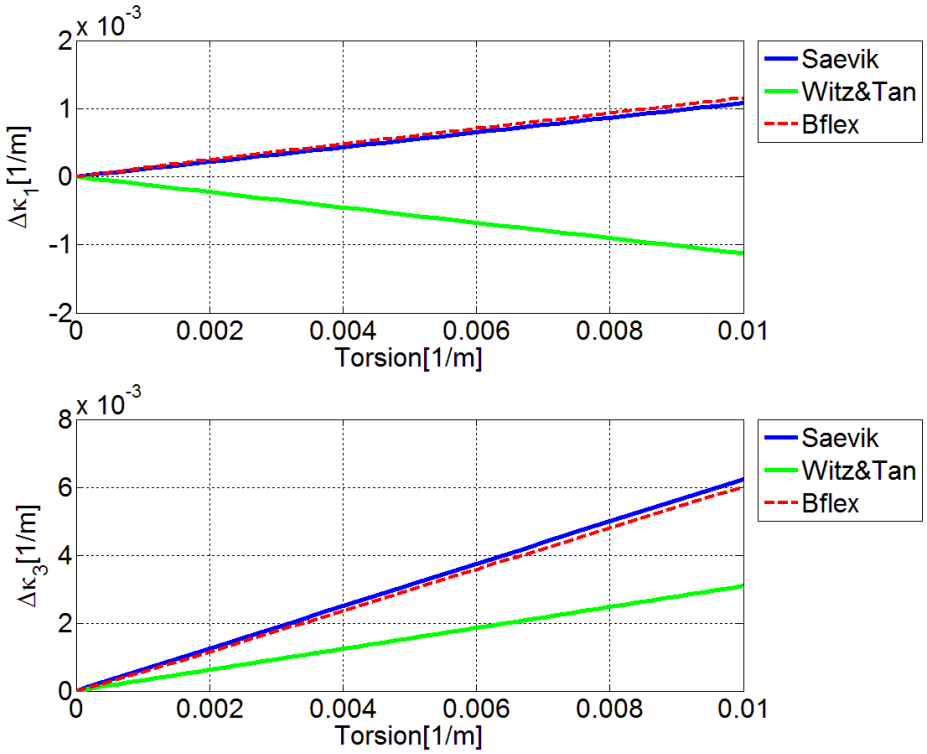

Figure 4-8 Curvature increments as a function of torsion-55°lay angle

It is found that both twist and normal curvatures increase linearly as the global torsion $\boldsymbol{\theta}_{,z}$ increases. Sævik's solution gives very good prediction of the BFLEX results where the blue solid line is almost overlapped with the red dash line. However, Witz&Tan's results show larger deviations.

- Radial displacement

Radial displacement u_2, which represents for internal/external pressure is applied from 0 to 0.001(m).

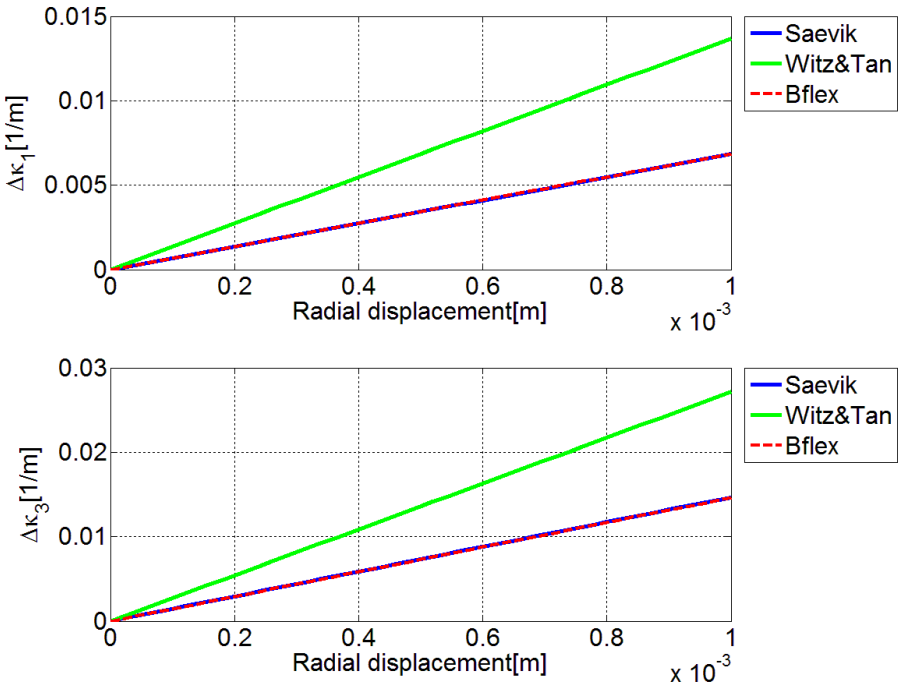

Figure 4-9 Curvature increments as a function of radial displacement-25°lay angle

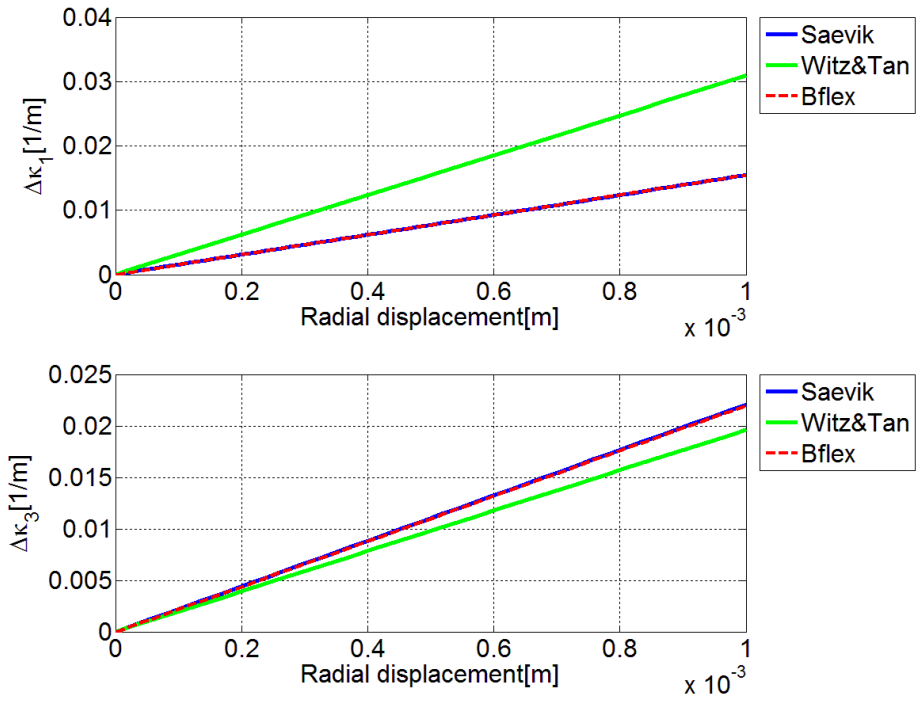

Figure 4-10 Curvature increments as a function of radial displacement-35°lay angle

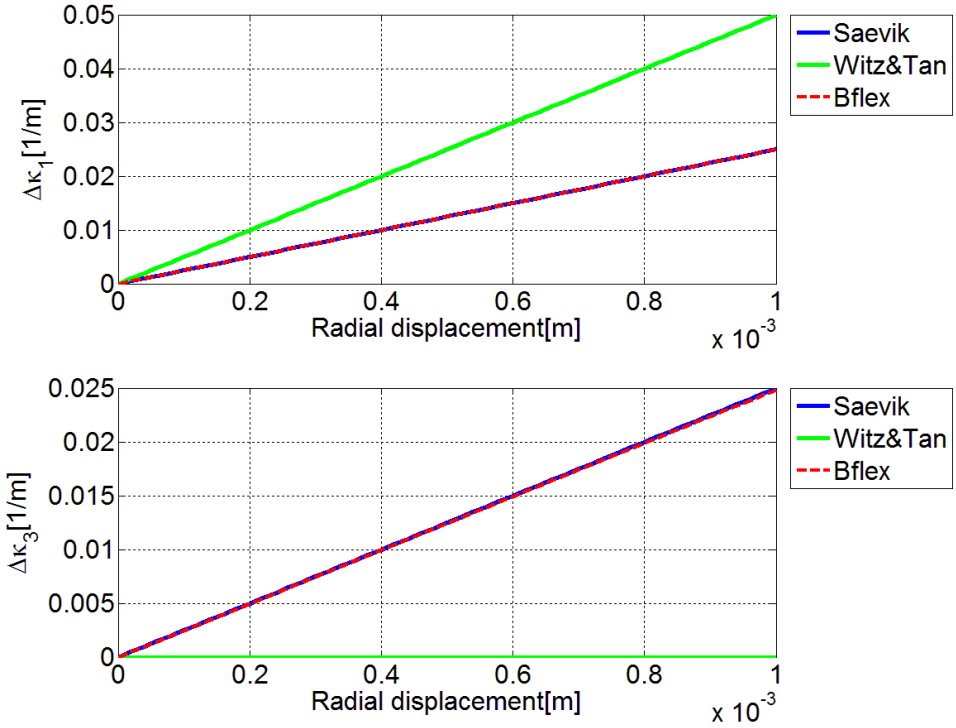

Figure 4-11 Curvature increments as a function of radial displacement-45°lay angle

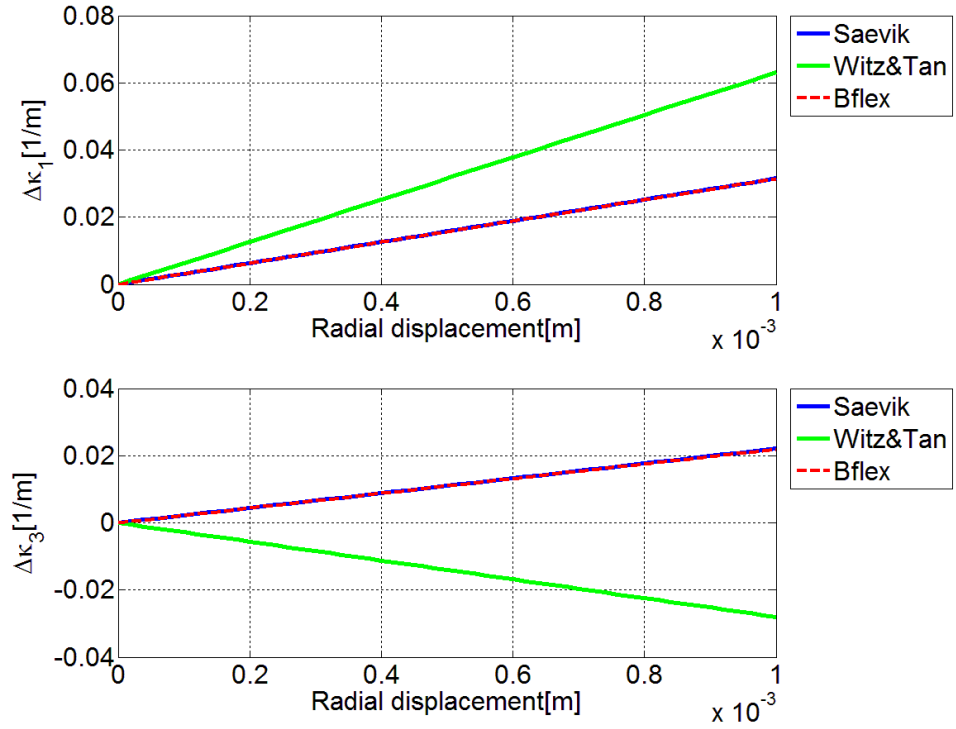

Figure 4-12 Curvature increments as a function of radial displacement-55°lay angle

Sævik's formulas give very close result to numerical result from BFLEX2010, while Witz &Tan's shows relative larger deviation.

All in all, the curvature increments obtained by Witz&Tan have larger deviations with numerical solutions comparing to Sævik's. It is because they express the accumulated torsion and curvature by using the updated lay angle and layer radius. They insert the accumulated quantities directly into Eq. (2.7)-(2.8) without taking the central line straining into account.

4.3 Parameter study on local displacements under bending

4.3.1 Description of the problem

This example studies how the maximum displacement/curvature increments can be influenced by certain pipe parameters, i.e., global curvature/friction coefficient/axial strain when exposed to bending. The simplified BFLEX model with single tendon and 35°lay angle is studied as an example here.

In this case, the tensile layer in BFLEX model is fixed in x and y direction at one end and have prescribed axial displacement, which is introduced by axial strain ε_z at the other end in order to simulate tension in the pipe and avoid buckling. The axial strain is applied before bending and the influence of this is further subtracted.

The aim of this sub-chapter is to find out that at which level of global curvature/friction coefficient/axial strain, the maximum displacement/curvature increments become stable. Those values are chosen when comparing BFLEX results with loxodromic solution in chapter4.4.

4.3.2 Global curvature's influence

In this case, friction coefficient and axial strain are assumed as given quantities, equals 0.05 and 0.0015 respectively. Maximum displacements/curvature increments are studied regarding different global pipe curvatures: 0, 0.01, 0.0125, 0.02, 0.025, 0.05, 0.1(m^{-1}), Initial principal curvature for a straight pipe and increments induced by axial strain are subtracted.

The results are given below:

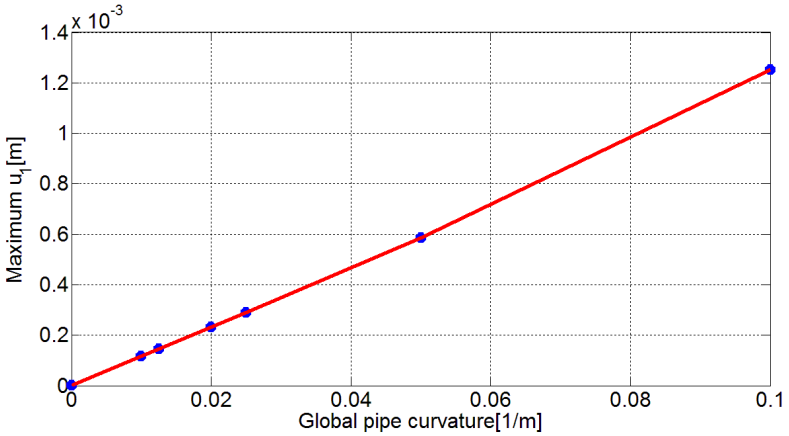

Figure 4-13 Maximum longitudinal displacement as a function of global pipe curvature

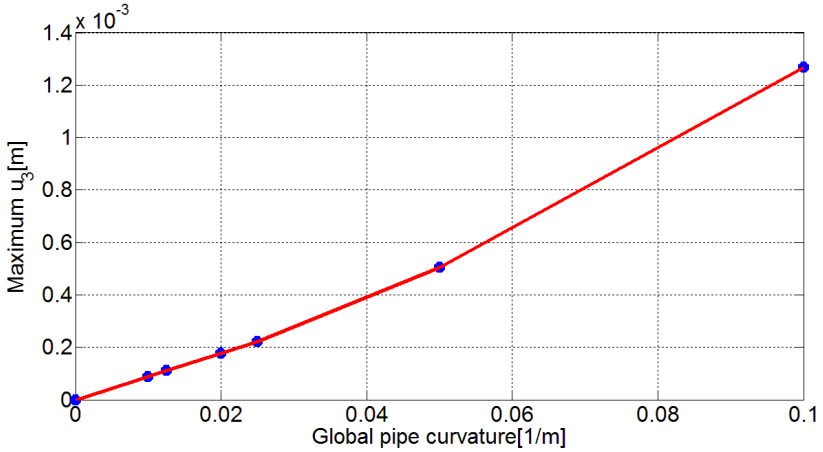

Figure 4-14 Maximum transverse displacement as a function of global pipe curvature

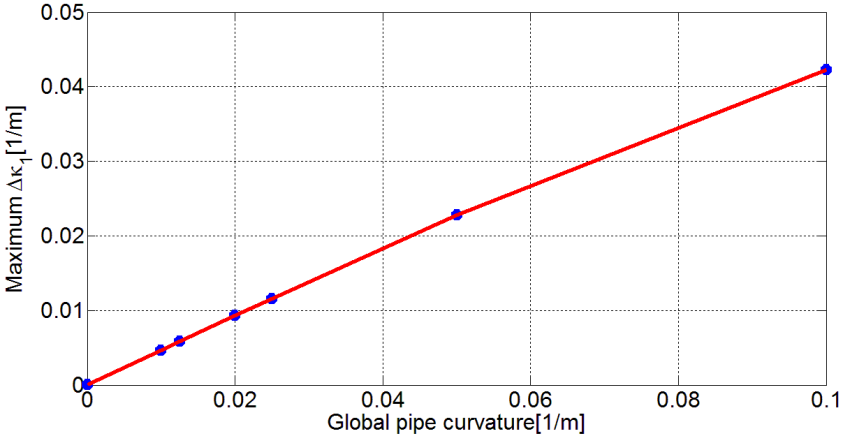

Figure 4-15 Maximum twist curvature increment as a function of global pipe curvature

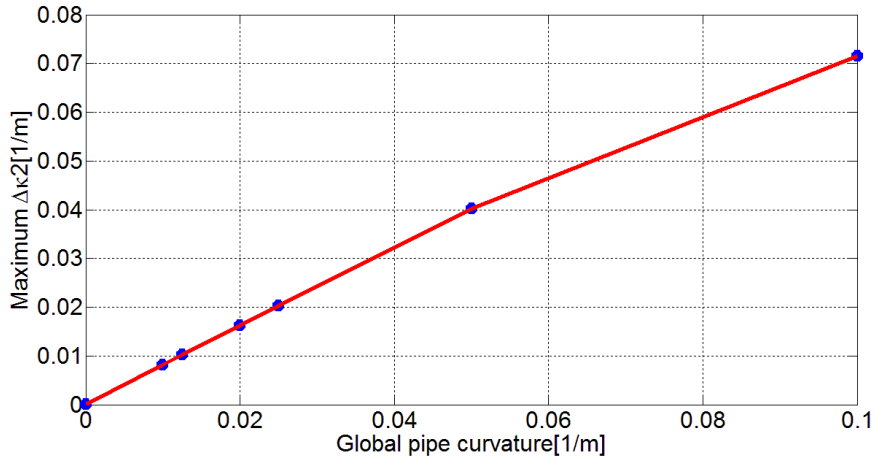

Figure 4-16 Maximum transverse curvature increment as a function of global pipe curvature

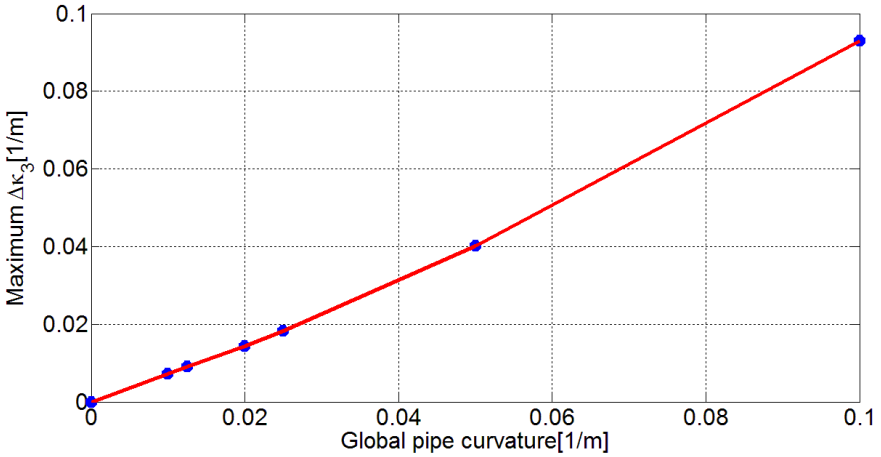

Figure 4-17 Maximum normal curvature increment as a function of global pipe curvature

The results show that displacements/curvatures increase linearly as global pipe curvature increases. In the thesis, a 0.1 m^{-1} global curvature for later tests is used. This is in order to make sure that the slip behaviour is governed by the bending process instead of axial stiffness.

4.3.3 Friction coefficient's influence

Now the maximum displacements/curvature increments are tested with varying friction coefficient: 0, 0.05, 0.1, 0.2, 0.3, 0.4, 0.5. Axial strain 0.0015, global curvature 0.1 $m^{-1}$are applied. Increments induced by axial strain are subtracted.

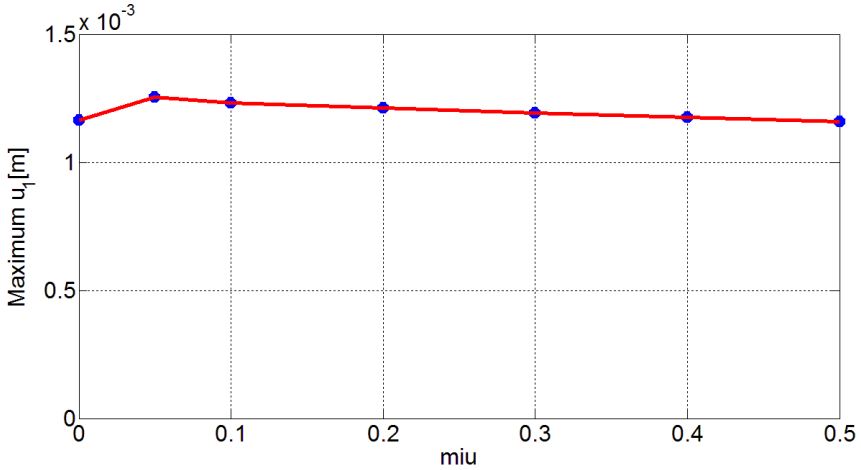

Figure 4-18 Maximum longitudinal displacement as a function of friction coefficient

The x-axis label 'miu' in the figure above represents for friction coefficient. It is stated in Chapter2 that the longitudinal slip depends on the axial strain from the compressive side to the tensile side and thus not much influenced by friction coefficient, which Figure 4-18 shows consistent result.

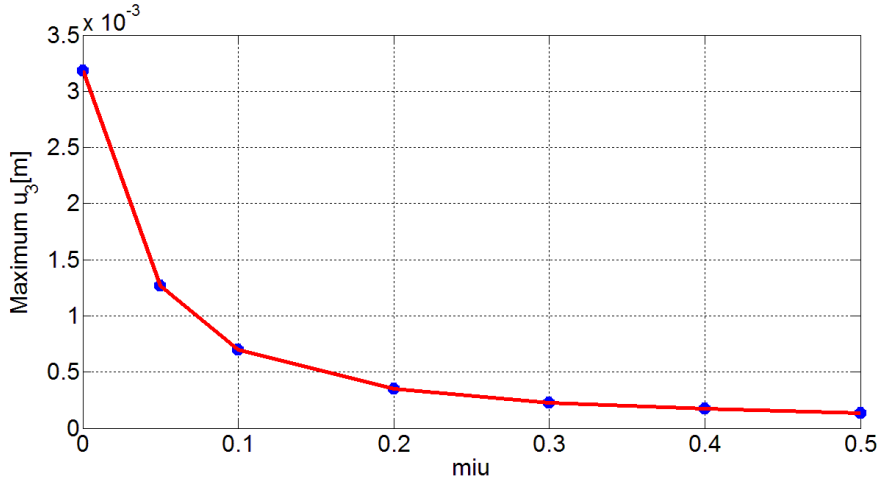

Figure 4-19 Maximum transverse displacement as a function of friction coefficient

The analytical solution stating that transverse displacement will be prohibited by friction is approved by numerical result showed in figure 4-19: the transverse slip is reduced rapidly as friction coefficient increases and soon become a negligible value.

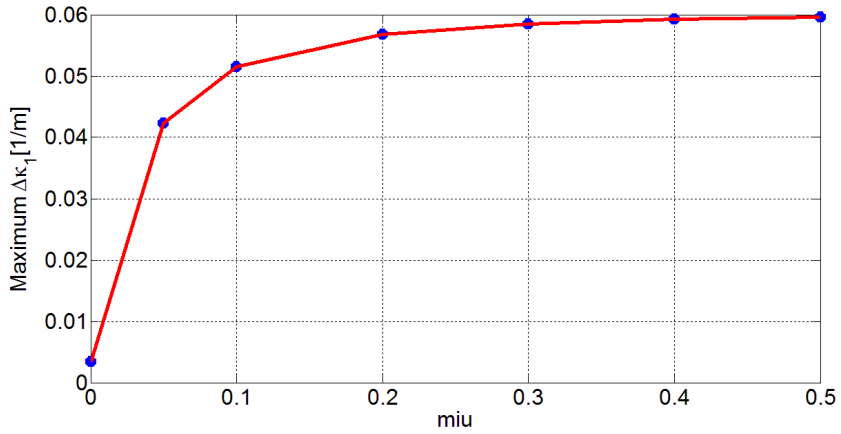

Figure 4-20 Maximum twist curvature increment as a function of friction coefficient

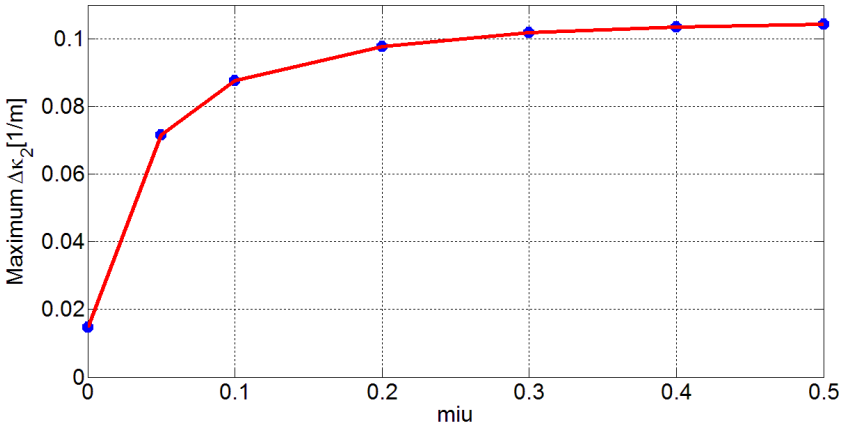

Figure 4-21 Maximum transverse curvature increment as a function of friction coefficient

At the meantime, transverse curvature is eliminated by transverse slip when the friction coefficient is small as described in figure 4-21.

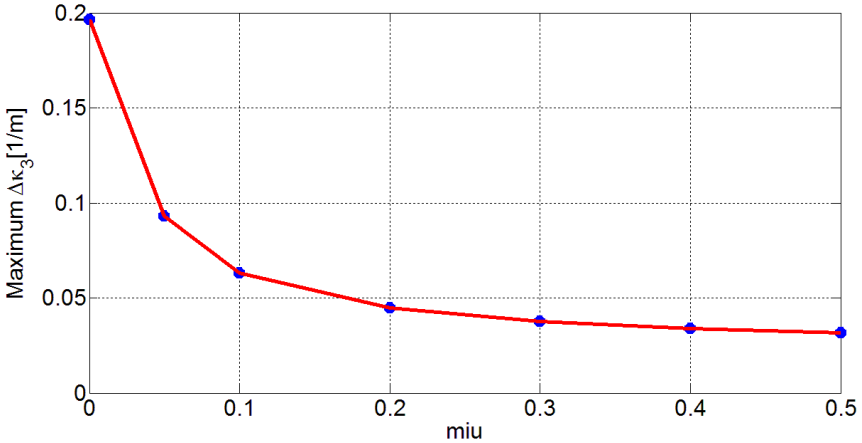

Figure 4-22 Maximum normal curvature increment as a function of friction coefficient

The transverse displacement and other curvature increments tend to become constant when friction coefficient becomes larger than 0.3. Thus, when comparing the numerical and loxodromic solution in Chapter4.4, the BFLEX result with friction coefficient 0.3 is used.

4.3.4 Axial strain's influence

Axial strain is applied in order to make sure the tendon is subjected to tension and such avoid buckling. In this part, maximum displacements/curvature increments with different global pipe axial strains: 0.001, 0.0015, 0.002, 0.003, 0.004, 0.005 are studied. Friction coefficient 0.05 and global pipe curvature $0.1\mathrm{m}^{-1}$ is applied. 35°lay angle is used as an example here.

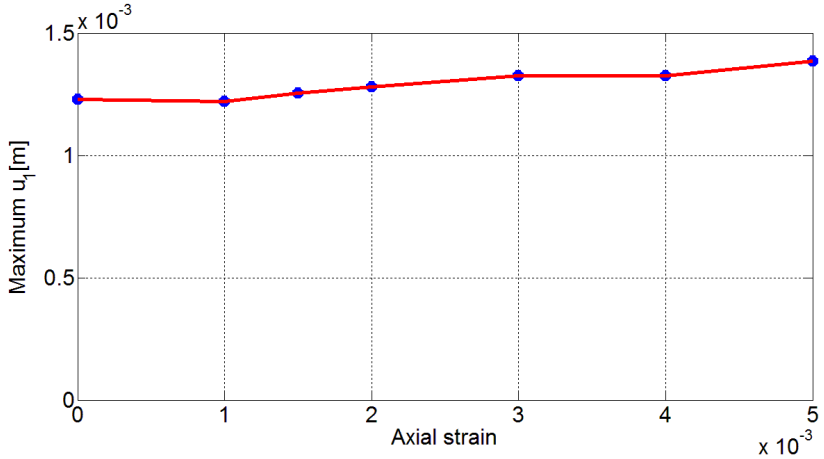

Figure 4-23 Maximum longitudinal displacement as a function of axial strain

It is observed from the above figure that the longitudinal displacement is not much influenced by axial strain when the axial strain changes from 0 to 0.005. It could be explained by that this effect is governed by axial force along the tendon which developed from the compression side to the tensile side, but not global tension.

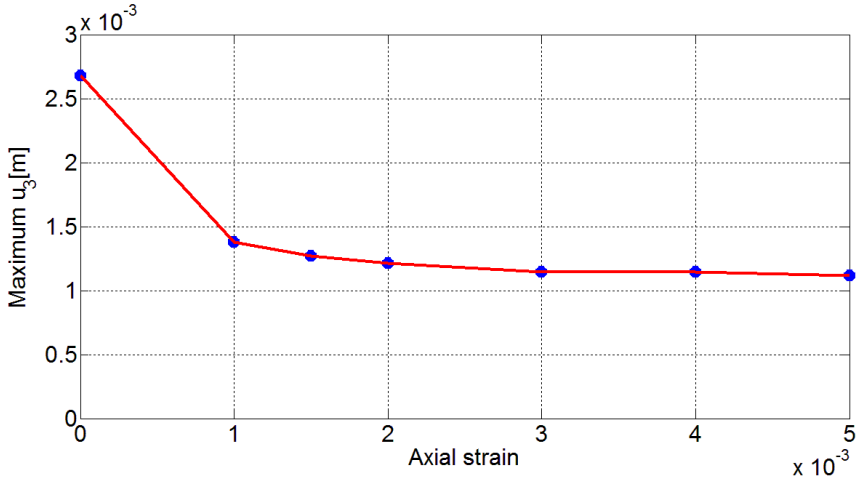

Figure 4-24 Maximum transverse displacement as a function of axial strain

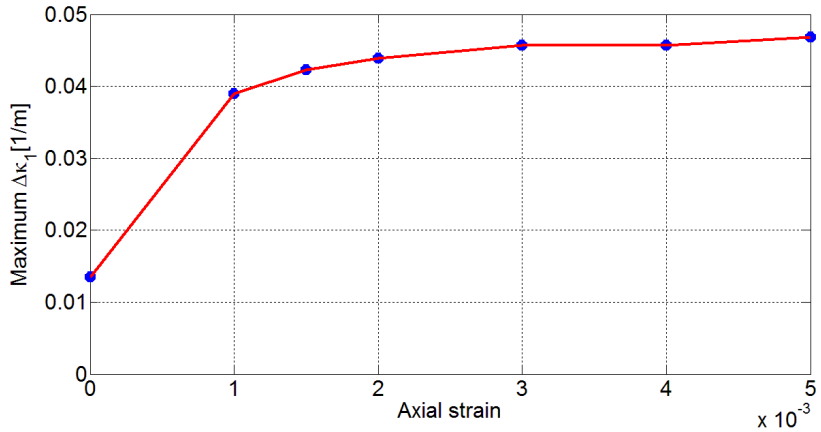

Figure 4-25 Maximum twist curvature increment as a function of axial strain

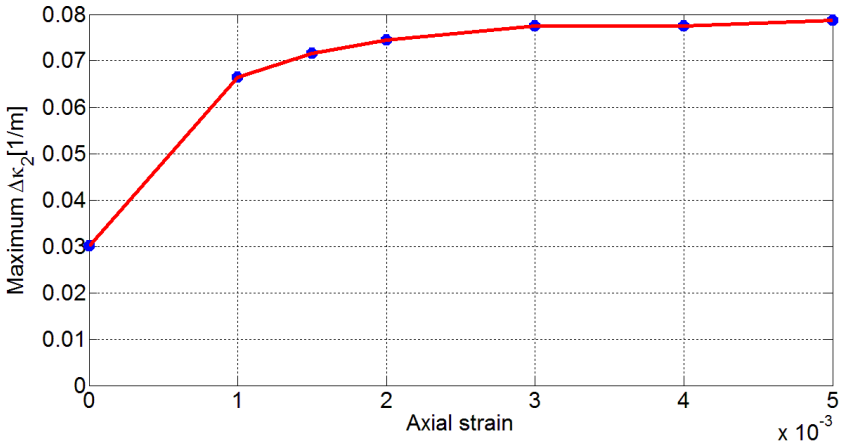

Figure 4-26 Maximum transverse curvature increment as a function of axial strain

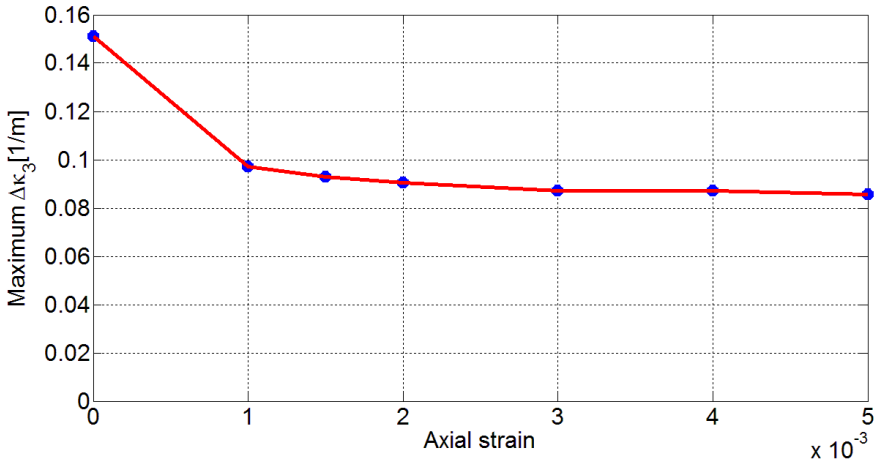

Figure 4-27 Maximum normal curvature increment as a function of axial strain

All the displacements/curvature increments are not varying too much when axial strain is larger than 0.001. Thus, axial strain 0.0015 is used in the numerical model in

Chapter4.4 and compared with the analytical solution. Other reasons to use axial strain 0.0015 are that it provides reasonable axial stress as used in real life and the numerical model converges faster within this value.

4.4 Comparison on numerical and analytical solutions-bending

4.4.1 Description of the problem

The aim of this sub-chapter is to verify that whether the numerical model can provide adequate description of the pipe bending behaviour or not. Comparison between BFLEX numerical simulations and analytical results with the help of the model described in Chapter2.4 is carried out.

Both simplified and complex BFLEX models are used and the pipe is bent step by step from straight to a constant global curvature $0.1(m^{-1})$. It should be noted that the complex model has only half-length of the simplified model. The inner layer of the complex model has the same lay-angle as the simplified model with 4 pitches while the simplified model has 8.

Two groups of comparison are carried out, namely:

1. The geodesic solution: referring to Eqs. (2.38)-(2.41), is compared with the BFLEX solution with 0 friction and 0.0015 axial strain;
2. The loxodromic solution: referring to Eqs. (2.42)-(2.44), is compared with the BFLEX result where friction coefficient equals 0.3 with 0.0015 axial strain.

The friction coefficient, axial strain and global curvature used here are chosen based on experiments in Chapter4.3. Local displacements and curvature increments induced by bending are studied. Axial strain is applied before bending and the influence is subtracted when plotting the figures in this sub-chapter. Initial principal curvature for a constant pipe is further deducted and only the curvature increments are studied.

4.4.2 Discussion of the results

The slip/curvature increments during bending are studied for different lay angles from 25°to 55°as showed below, where ‘miu’ in the figure represents friction coefficient used in BFLEX simulation. For the complex model, the results are taken out from the inner tendon. The figures marked with “16 tendons” are results from the inner layer of the complex model.

- **Longitudinal slip**

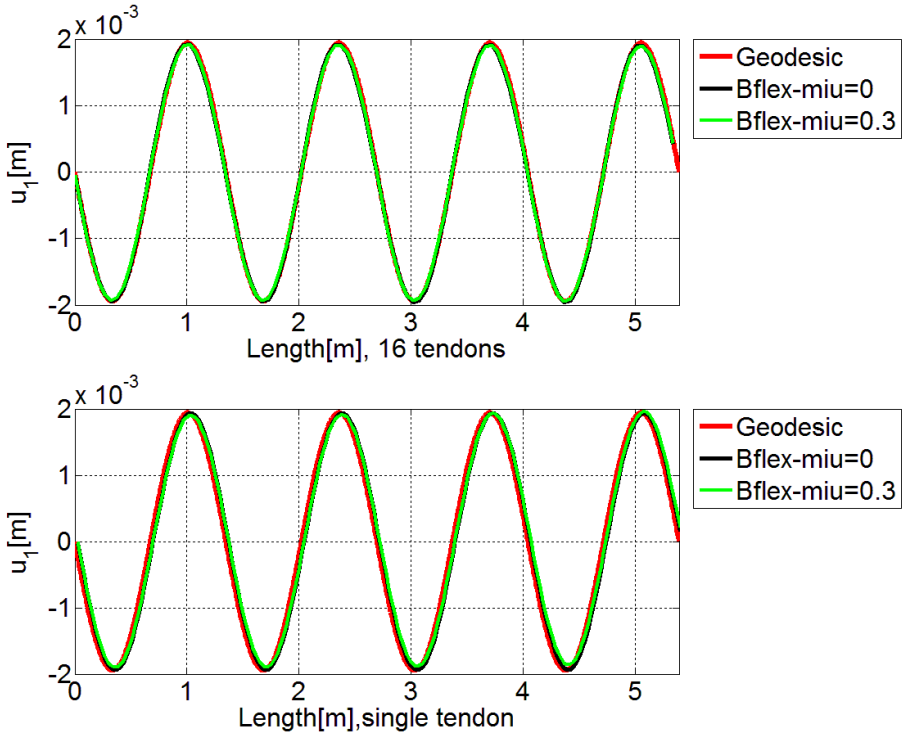

Figure 4-28 Longitudinal slip- 25°lay angle

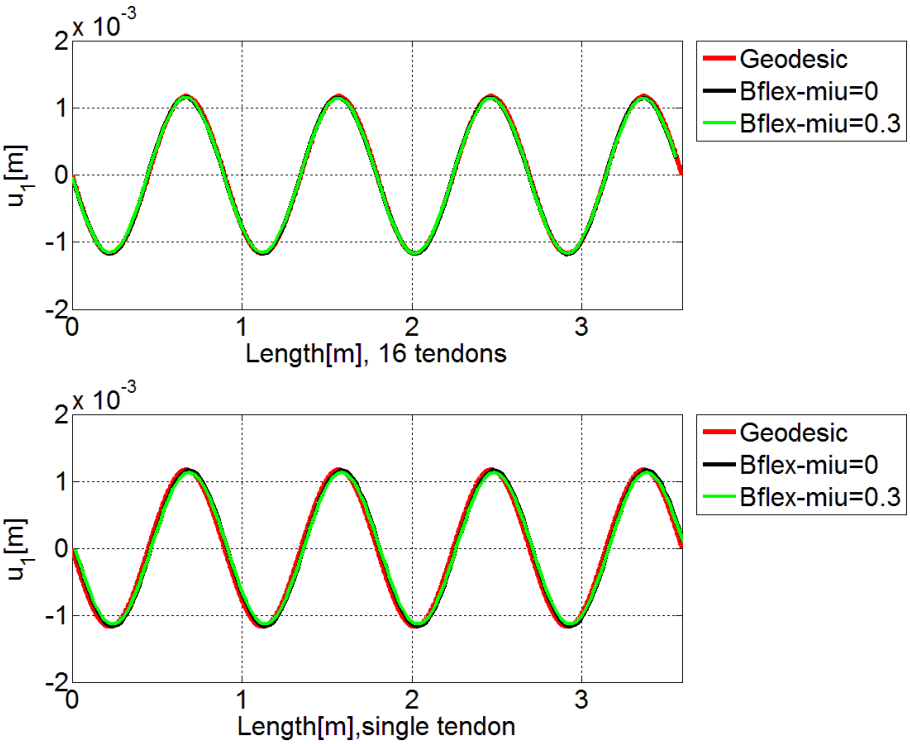

Figure 4-29 Longitudinal slip- 35°lay angle

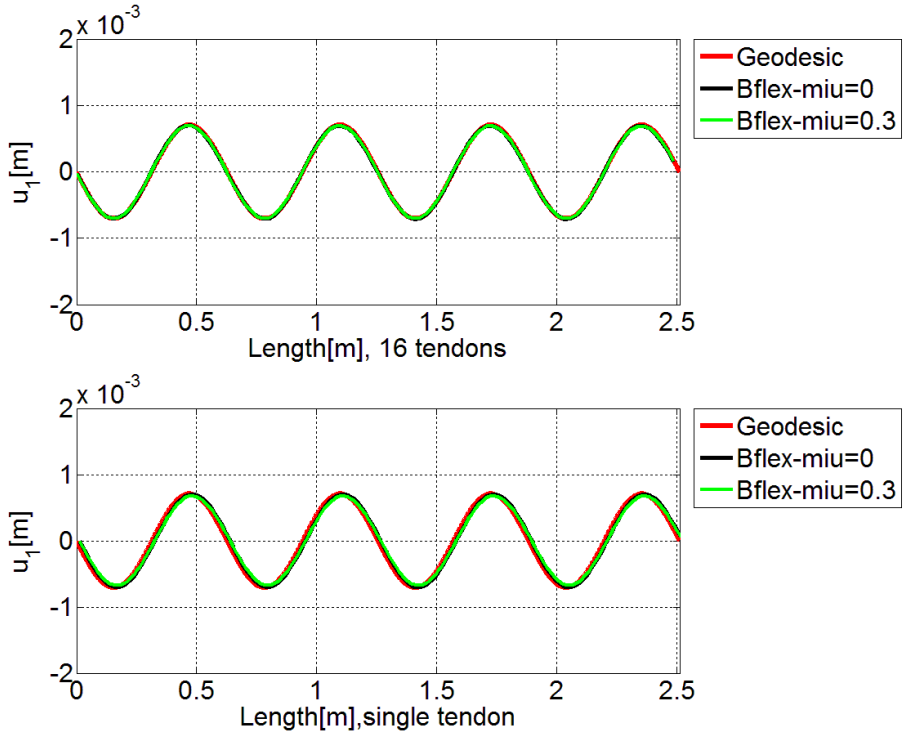

Figure 4-30 Longitudinal slip- 45°lay angle

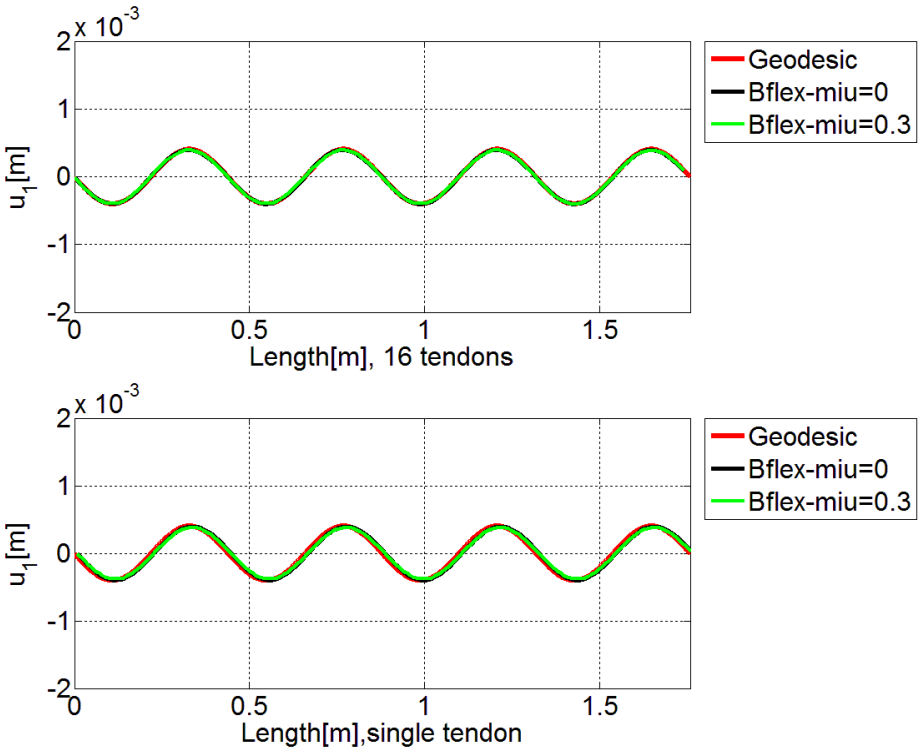

Figure 4-31 Longitudinal slip- 55°lay angle

From Figure4-28 to Figure4-31, it is observed that the longitudinal slip is independent on friction force. This gives agreement with the statement in Chapter2: the longitudinal slip is governed by the axial strain developed in the tendon from compression side to tension side induced by bending but not friction force.

It is further found that the longitudinal slip is not influenced by the outer tensile armour layer as the longitudinal displacements are same for both models and all lay angles.

The maximum longitudinal slip reduces as the lay angle increases as illustrated by the following figure:

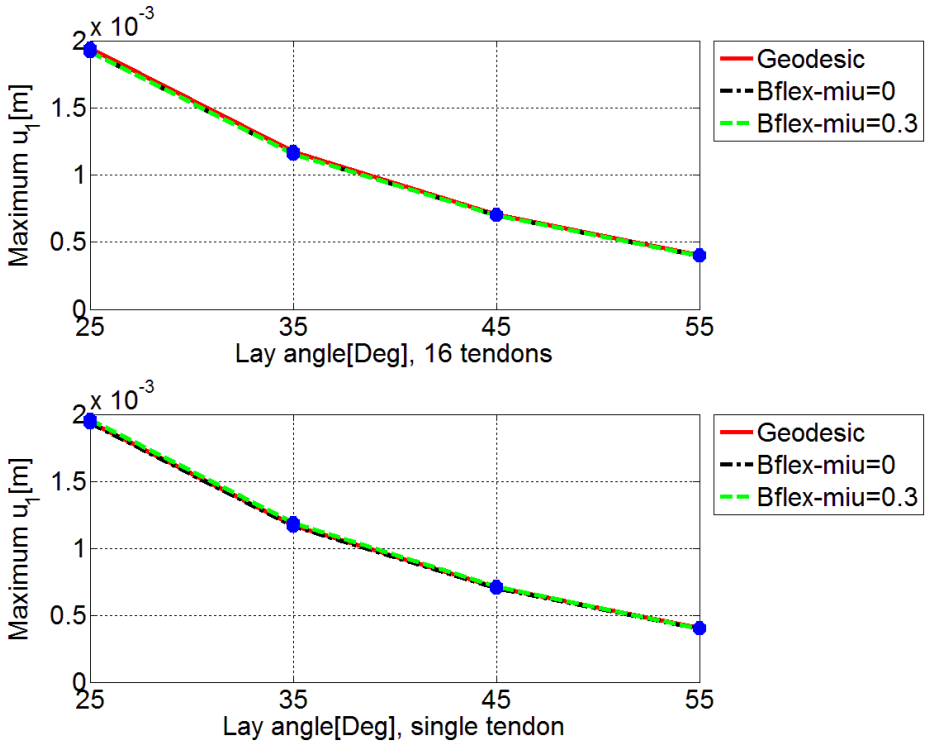

Figure 4-32 Maximum longitudinal slip as a function of lay angle

- **Transverse slip**

Transverse slips along the tendon are plotted for different lay angles:

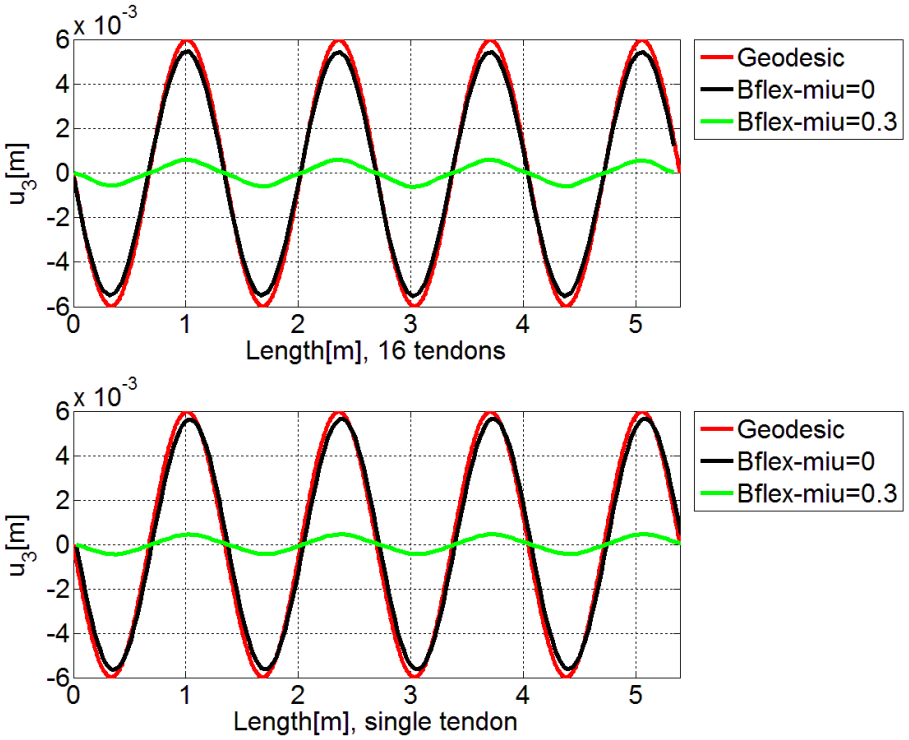

Figure 4-33 Transverse slip- 25°lay angle

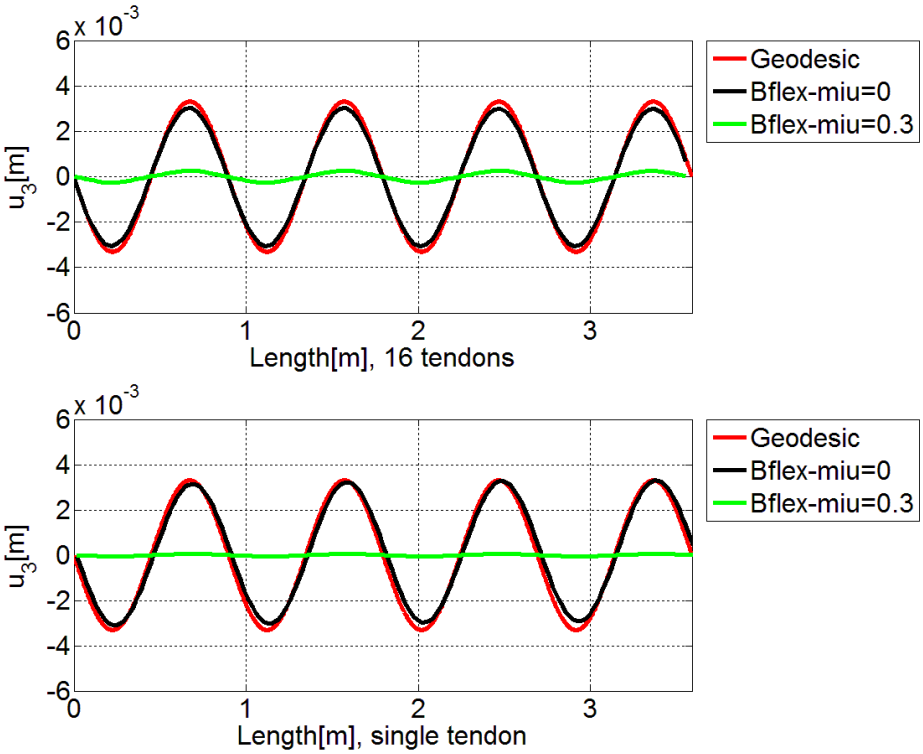

Figure 4-34 Transverse slip- 35°lay angle

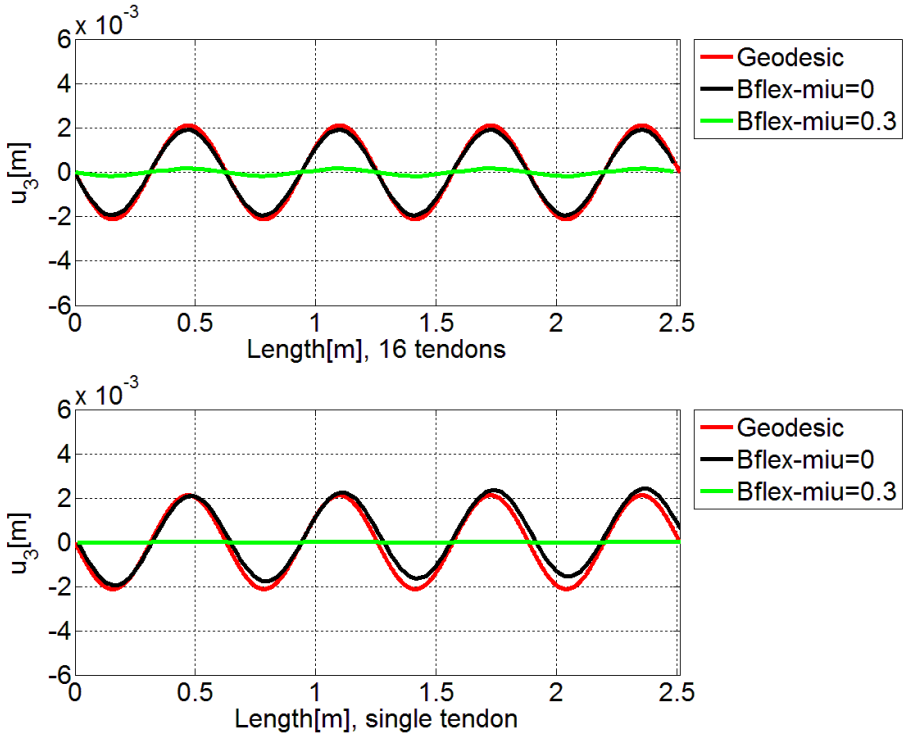

Figure 4-35 Transverse slip- 45°lay angle

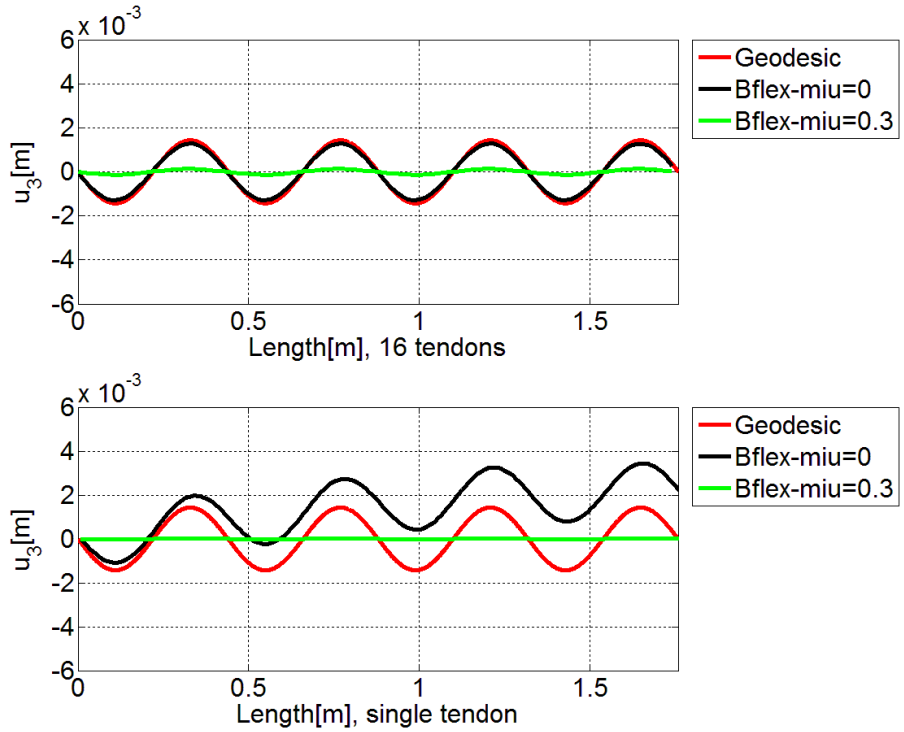

Figure 4-36 Transverse slip- 55°lay angle

As described in Chapter2.4, transverse curvature will occur under loxodromic assumption when the pipe is subjected to bending. A transverse slip will start if zero friction condition is assumed. Tendon will in this way follows the geodesic assumption. When the friction is large enough, transverse slip will be restraint and the tendon will follow the loxodromic path.

The BFLEX results with zero friction give harmonic solutions which are consistence with the geodesic solution stated in Eq. (2.39). The transverse slip amplitude simulated by BFLEX matches well with the geodesic solution. However, a difference in mean value is observed for large lay angles for the simplified model. This is introduced by the prescribed displacements.

It is observed the transverse slip is very small for friction coefficient 0.3 in BFLEX. The results match the loxodromic assumption: transverse slip is prohibited by friction force.

It is observed that the out armour layer does not influence the transverse slip significantly.

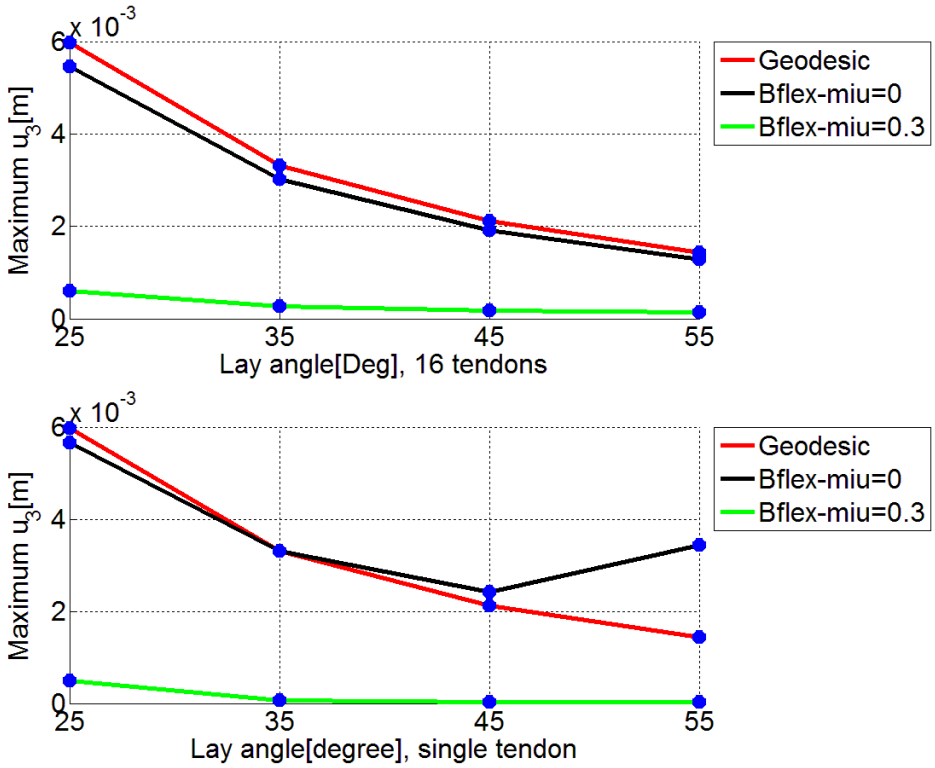

Figure 4-37 Maximum transverse slip as a function of lay angle

Refer to figure 4-37, the amplitude of transverse slip reduces as the lay angle increases when friction coefficient is set to zero. While the transverse slip reduces to almost zero for all lay angle with large friction. The increase in maximum transverse slip for the

simplified model with zero friction at **55°**lay angle is because the increase in mean value as stated in figure 4-36.

- **Twist curvature increment**

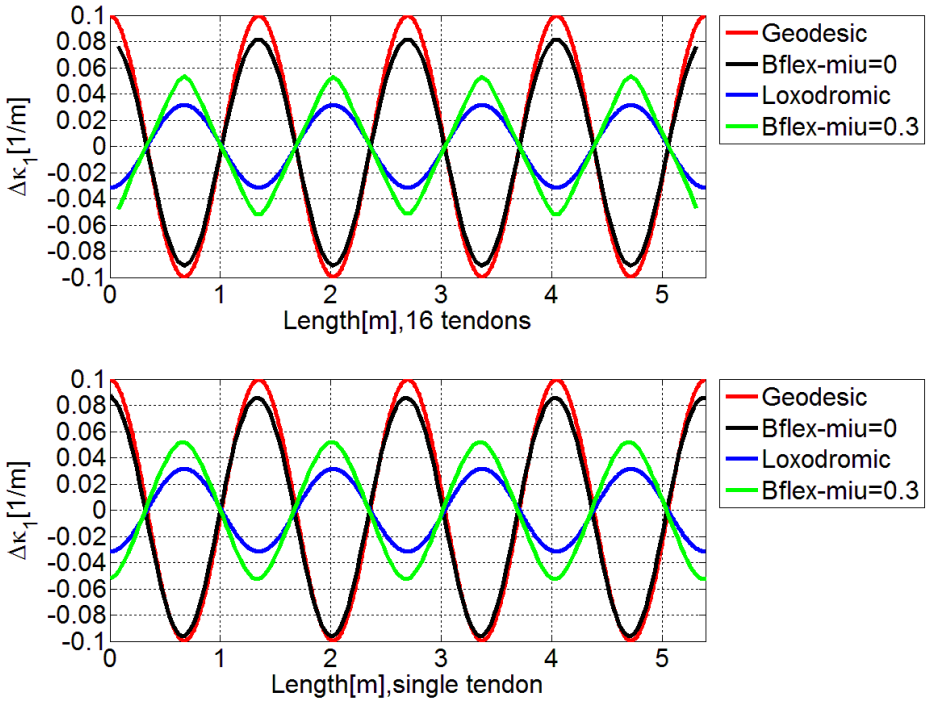

Figure 4-38 Twist curvature increment- 25°lay angle

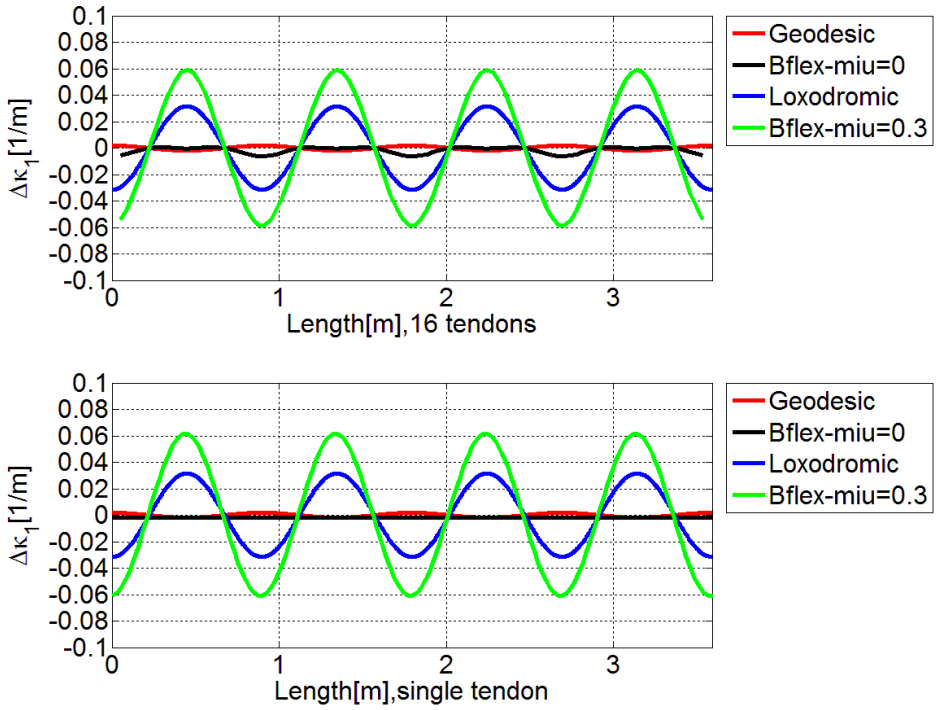

Figure 4-39 Twist curvature increment- 35°lay angle

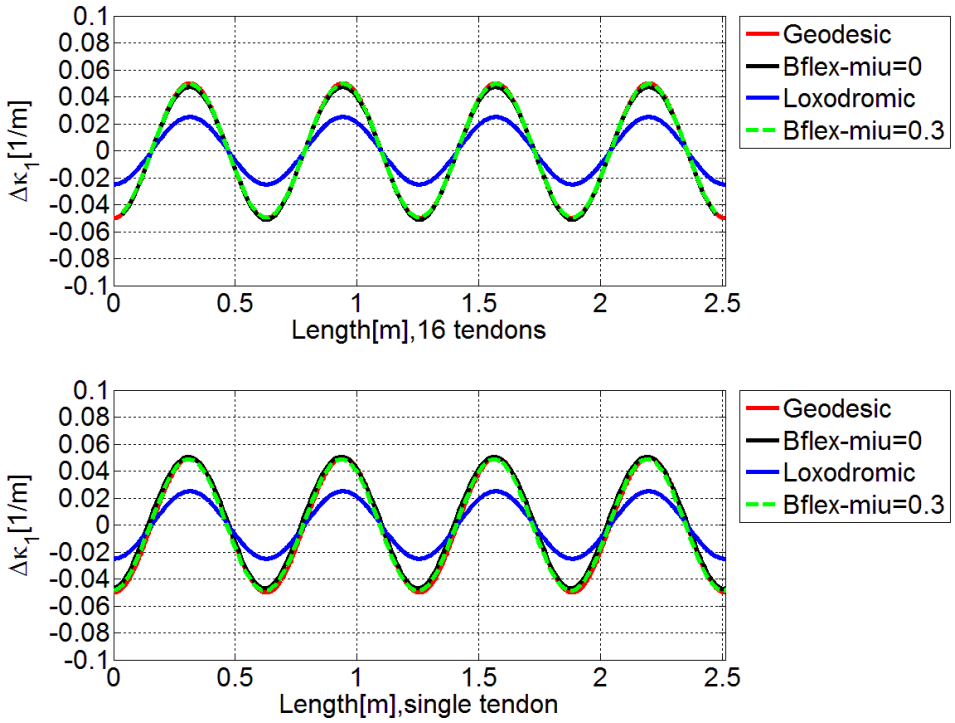

Figure 4-40 Twist curvature increment- 45°lay angle

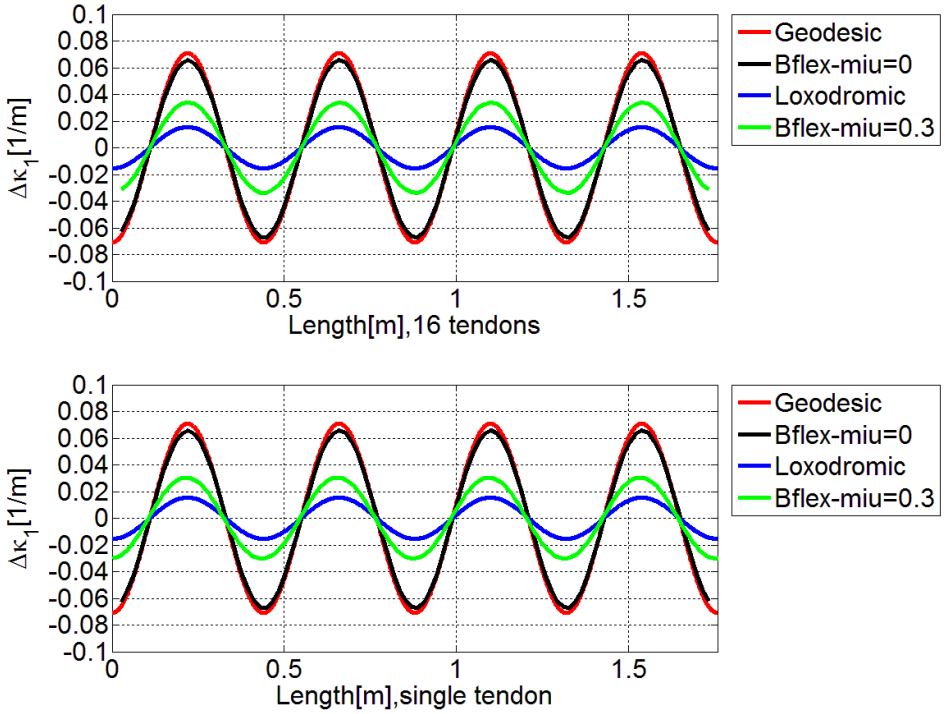

Figure 4-41 Twist curvature increment- 55°lay angle

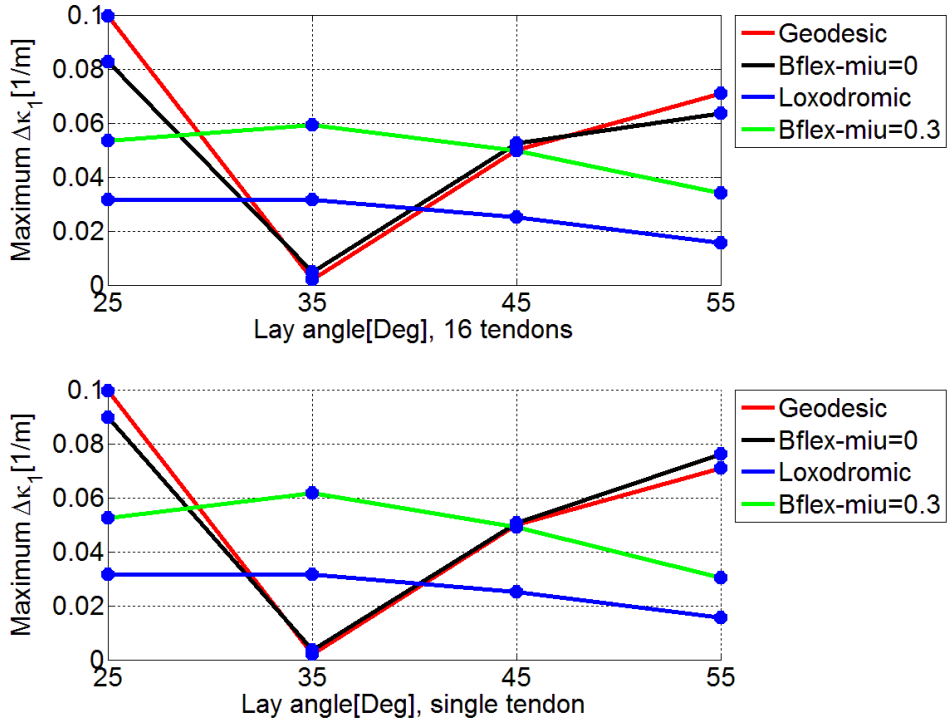

Figure 4-42 Maximum twist curvature increment as a function of lay angle

It is concluded from the above figures that the BFLEX solution matches well with geodesic solution when friction coefficient is set to zero. A sign change around 35°lay angle in both solutions is observed. For the geodesic solution, this is introduced by $\left(\frac{1}{sin^2\alpha} - 3\right)$term in Eq.(2.40). The BFLEX results reflect this change of sign and thus approve geodesic solution.

However, the BFLEX result with 0.3 friction coefficient is larger than the loxodromic solution for all lay angles. This is explained by the following.

The loxodromic curvature increments (2.42) and (2.44) are deduced on the basis that no slip occurs during bending. However, a longitudinal slip (2.38) will always be introduced in order to eliminate longitudinal strain. In BFLEX result with 0.3 friction coefficient, the curvature increment is calculated after this longitudinal slip. Thus, in order to include the influence from longitudinal slip and compare with BFLEX result, equation (2.42) which represents for curvature increment without any slip, should be added an extra term which including longitudinal slip in [2].

According to [2], by using kinematic restraint Eq.(2.16) and assume 2D effect, the twist curvature increments induced by longitudinal slip using loxodromic curve as reference:

$$\Delta\kappa_1 = \kappa_1 u_{1,1} \tag{4.3}$$

By including the influence induced by longitudinal slip, i.e., adding Eq.(4.3) to the loxodromic solution (2.42), the twist curvature change along the pipe is shown in the figure below:

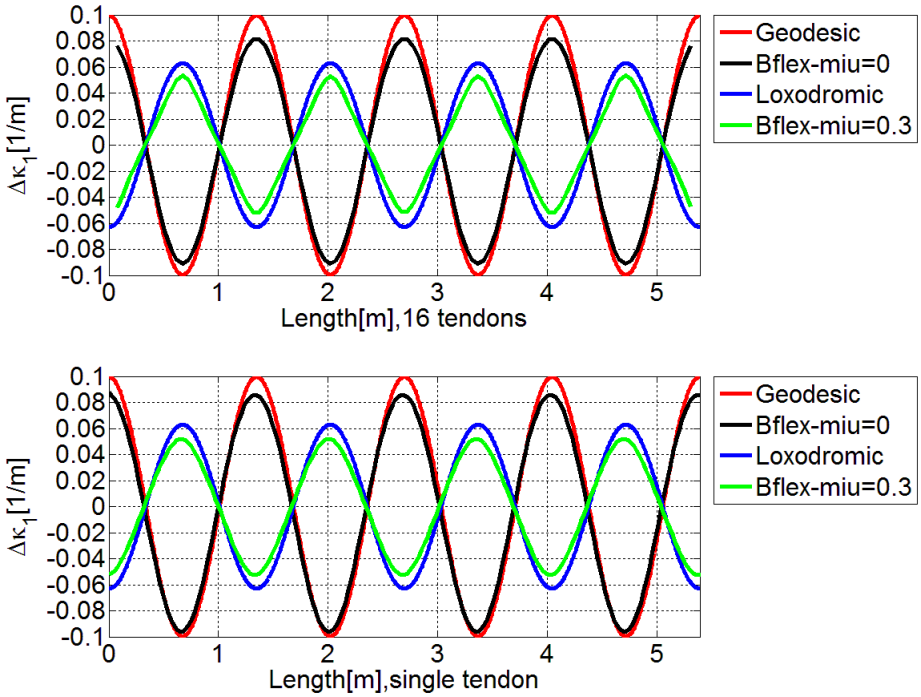

Figure 4-43 Modified twist curvature increment-25°lay angle

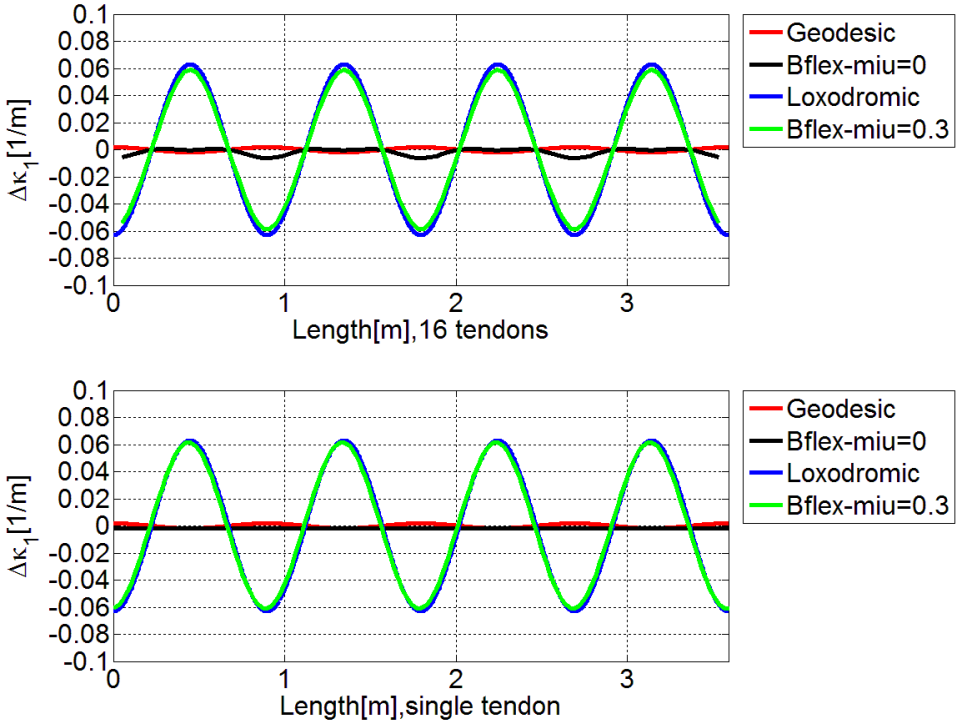

Figure 4-44 Modified twist curvature increment- 35°lay angle

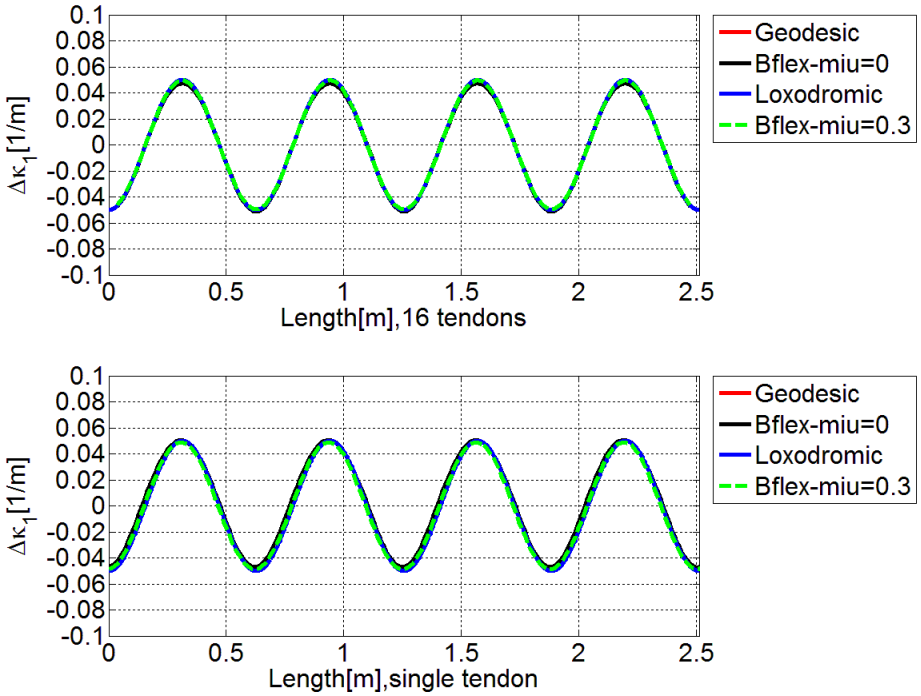

Figure 4-45 Modified twist curvature increment- 45°lay angle

Geodesic, loxodromic and BFLEX results are overlapped for 45°lay angle.

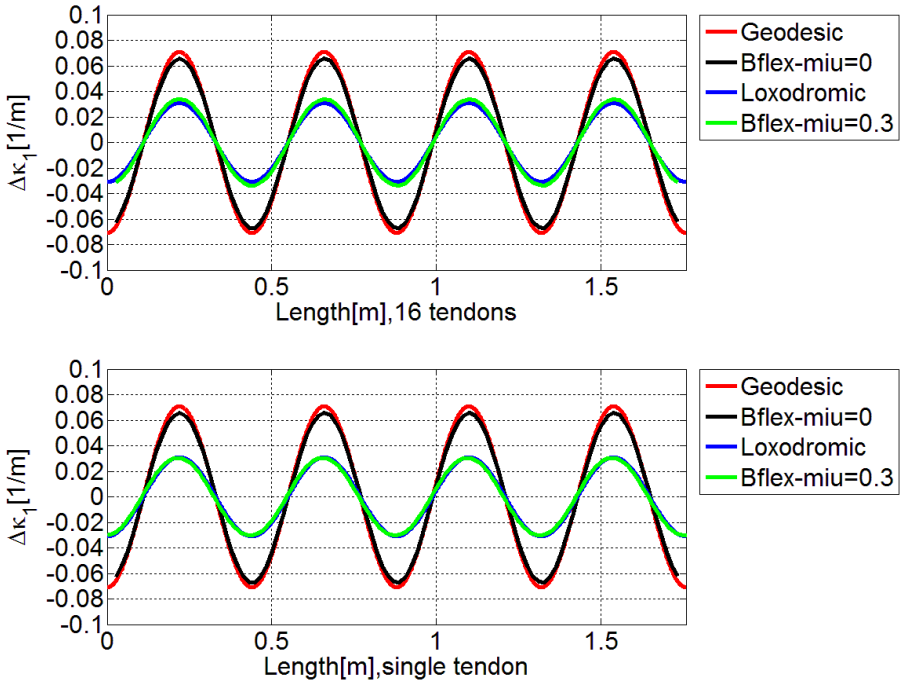

Figure 4-46 Modified twist curvature increment- 55°lay angle

Maximum curvature changes hence become:

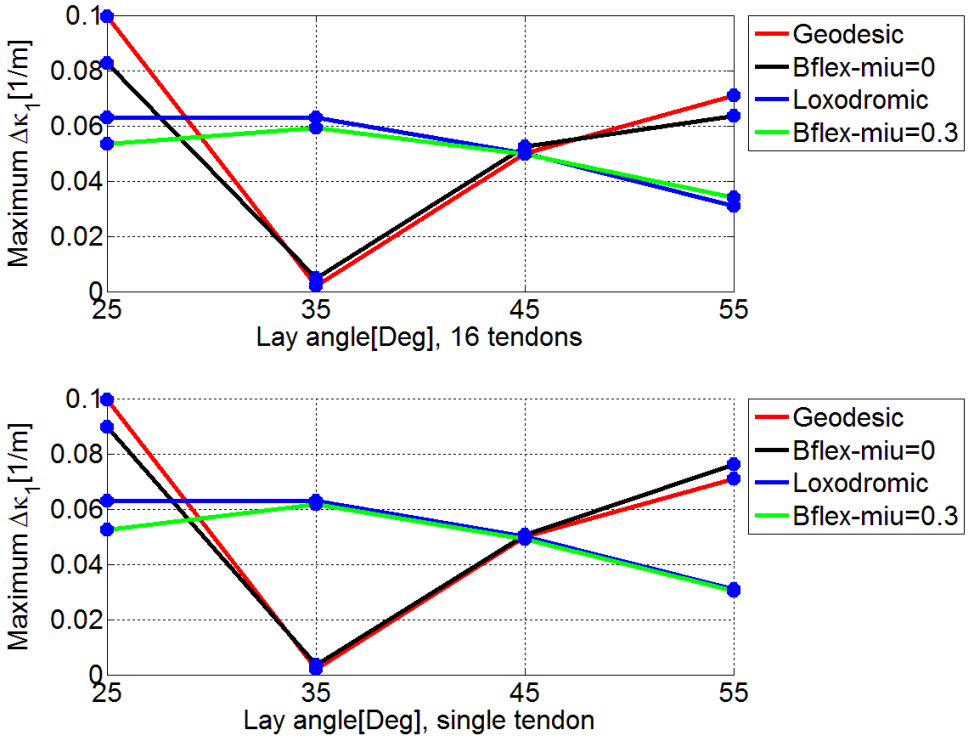

Figure 4-47 Maximum twist curvature change with longitudinal slip, modified

Here we can conclude that the twist curvature for BFLEX with friction agrees with loxodromic solution which including the additional influence from longitudinal slip.

- **Transverse curvature increment**

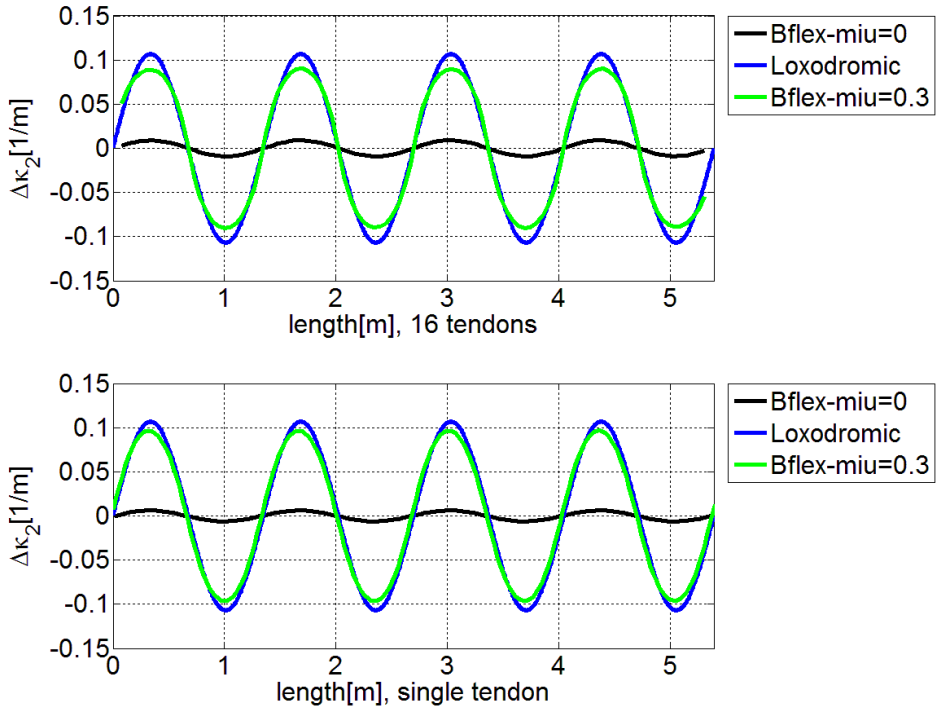

Figure 4-48 Transverse curvature increment- 25°lay angle

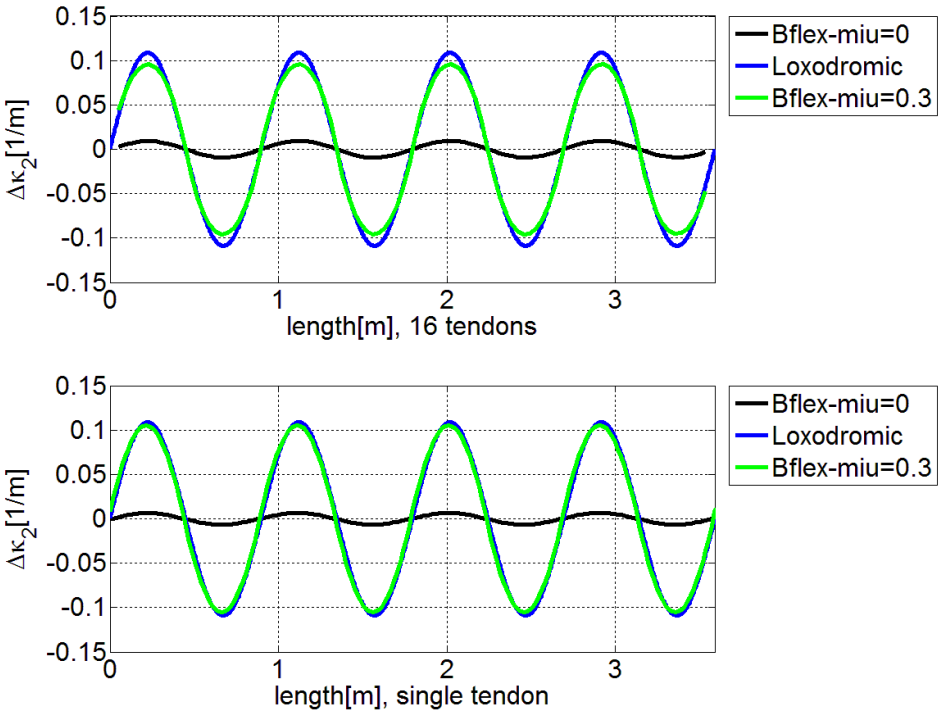

Figure 4-49 Transverse curvature increment- 35°lay angle

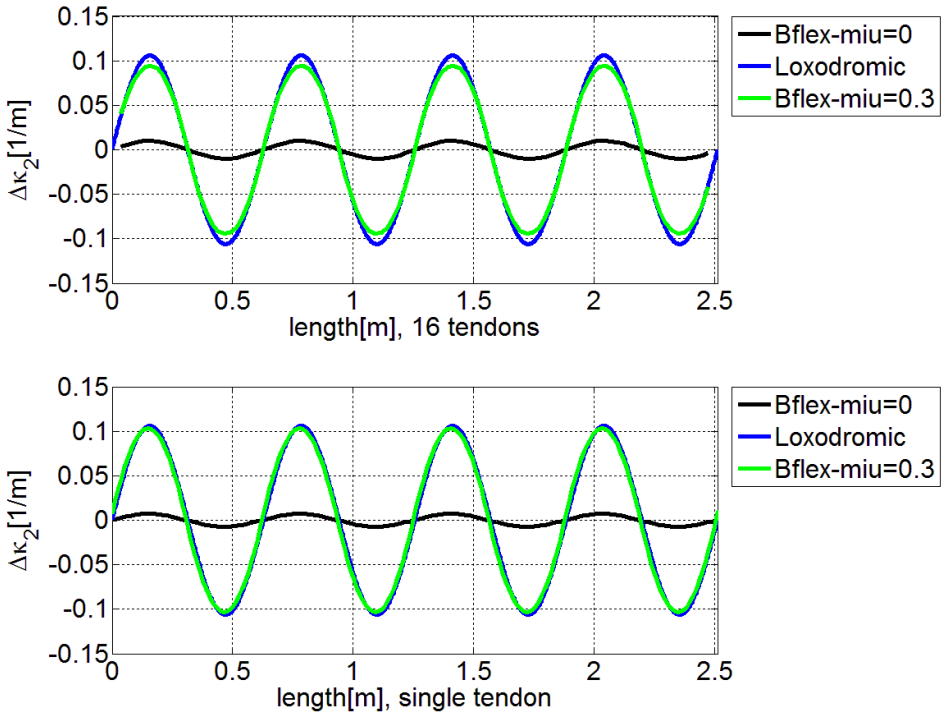

Figure 4-50 Transverse curvature increment- 45°lay angle

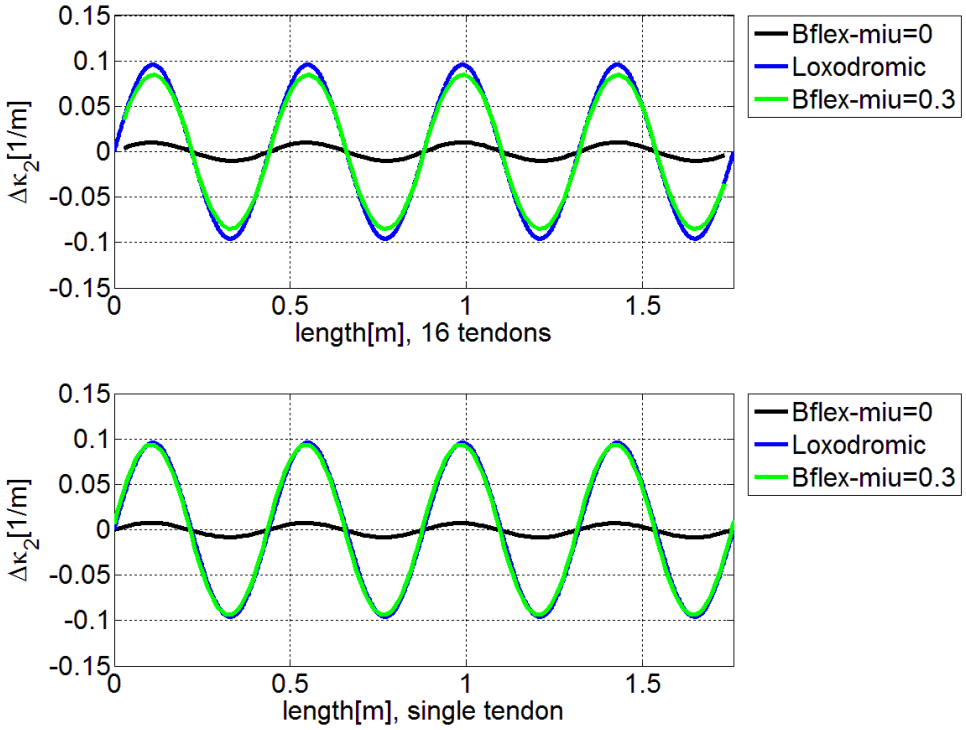

Figure 4-51 Transverse curvature increment- 55°lay angle

From Figure4-48 to Figure4-51, the loxodromic solutions agree well with the BFLEX solutions when miu=0.3. A small transverse curvature is observed for BFLEX solution where friction is assumed to be zero. Such a small curvature could be neglected and can be concluded that the BFLEX solution matches the geodesic solution very well.

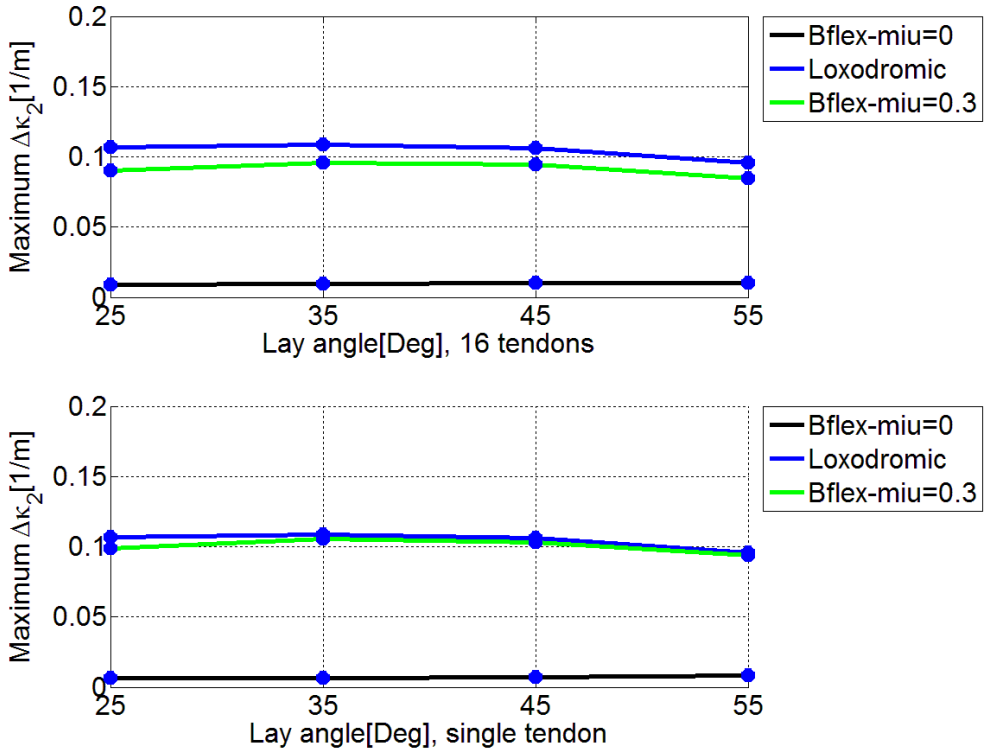

Figure 4-52 Maximum transverse curvature increment as a function of lay angle

It is found from above figure; transverse curvature increment is not influenced by lay angle.

- **Normal curvature increment**

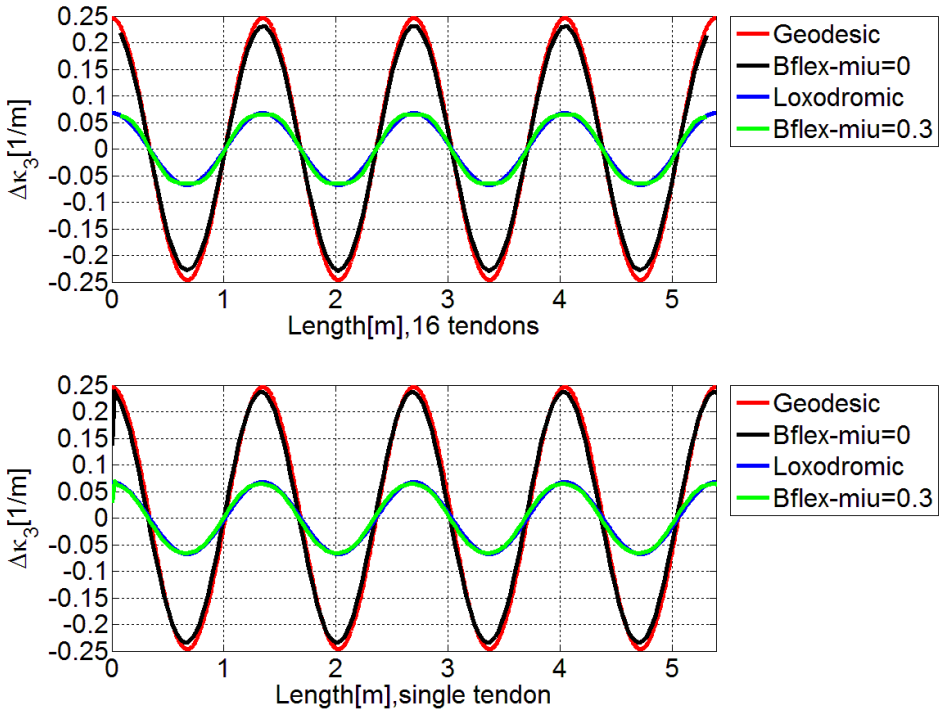

Figure 4-53 Normal curvature increment- 25°lay angle

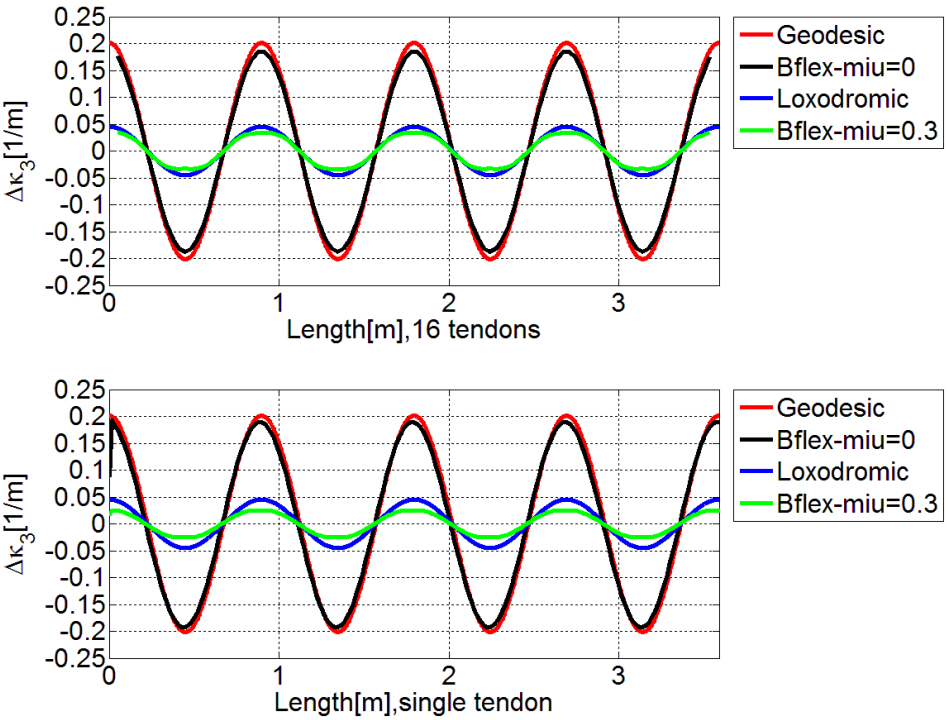

Figure 4-54 Normal curvature increment- 35°lay angle

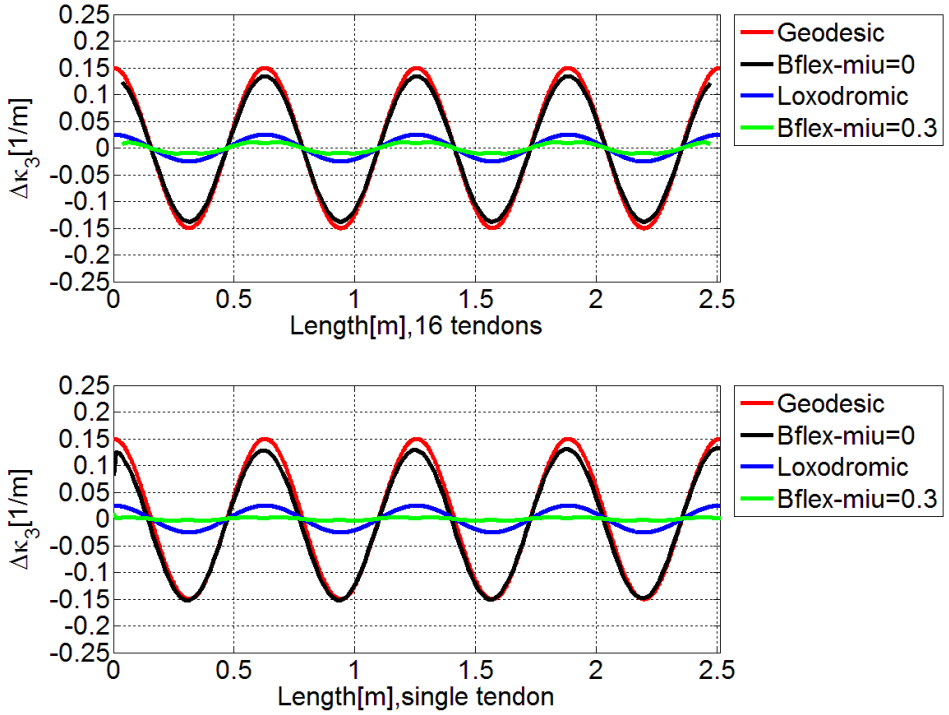

Figure 4-55 Normal curvature increment- 45°lay angle

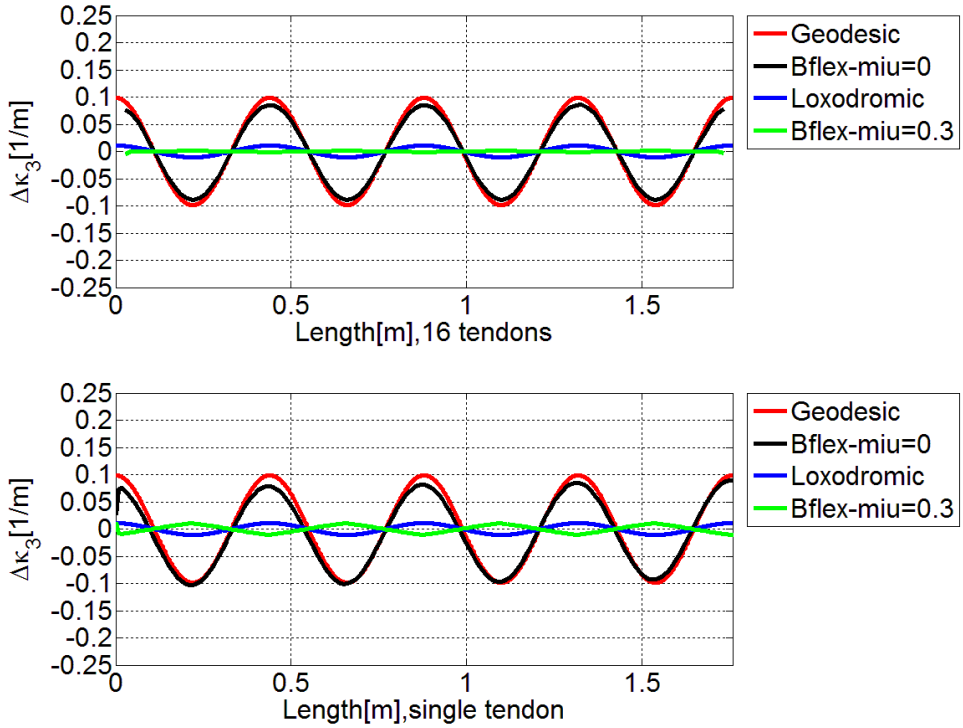

Figure 4-56 Normal curvature increment- 55°lay angle

The geodesic solutions and BFLEX solutions give good agreement with each other as observed in Figure 4-53 to Figure 4-56.

However, the difference between loxodromic solution and numerical simulation increases as the lay angle increases. Even an opposite sign is observed between loxodromic and BFLEX result for 55°lay angle. This could be explained in the same way for the twist curvature: the difference is introduced by the longitudinal slip which is not included in the loxodromic solution Eq.(2.44). By including the longitudinal slip's influence on normal curvature, an additional term should be added to Eq.(2.44)[2]:

$$\Delta\kappa_3 = \kappa_3 u_{1,1} \tag{4.4}$$

The new loxodromic solution by including Eq.(4.4) in is plotted in the figure below:

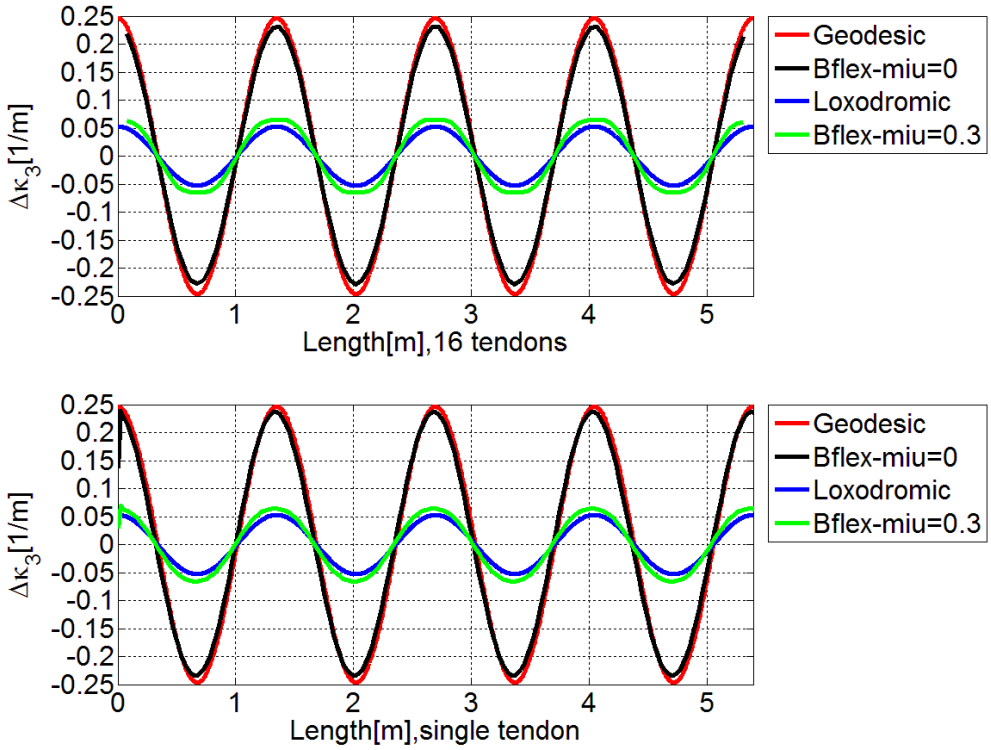

Figure 4-57 Modified normal increment- 25°lay angle

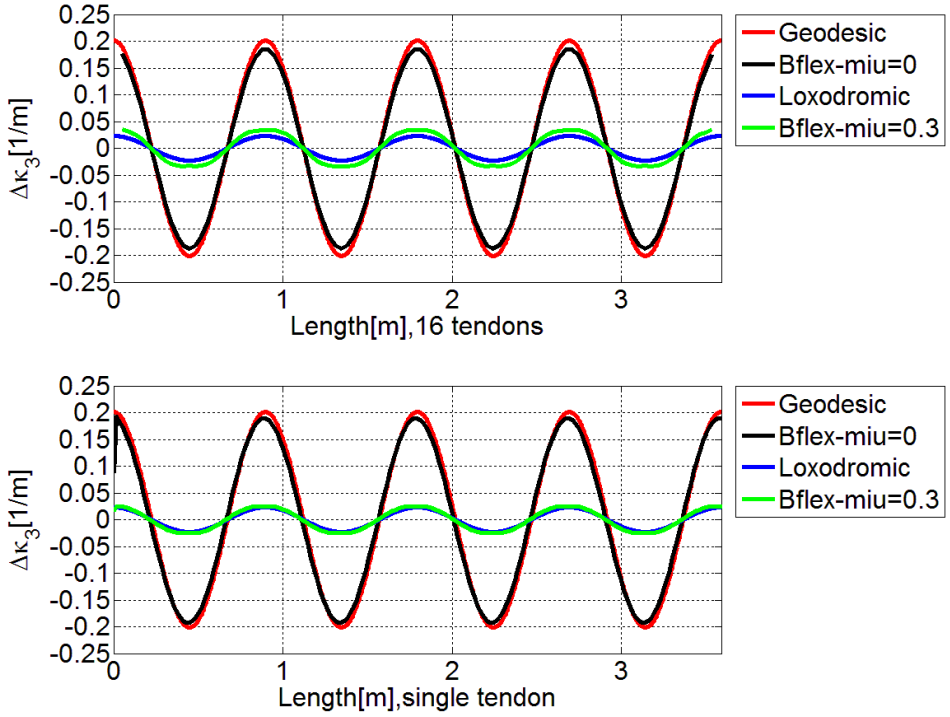

Figure 4-58 Modified normal increment- 35°lay angle

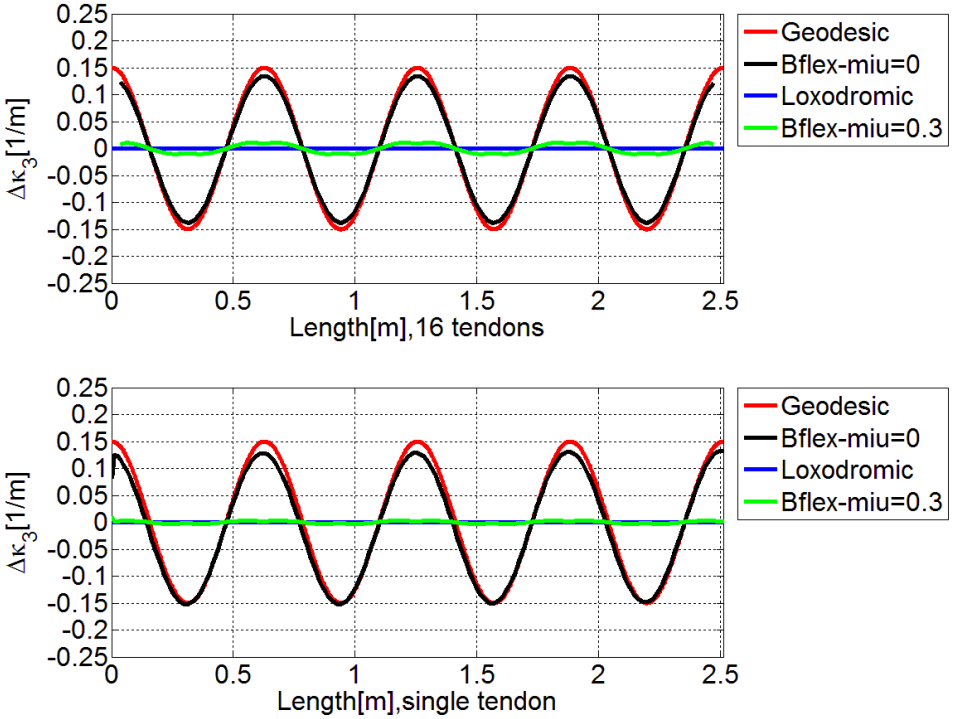

Figure 4-59 Modified normal curvature increment- 45°lay angle

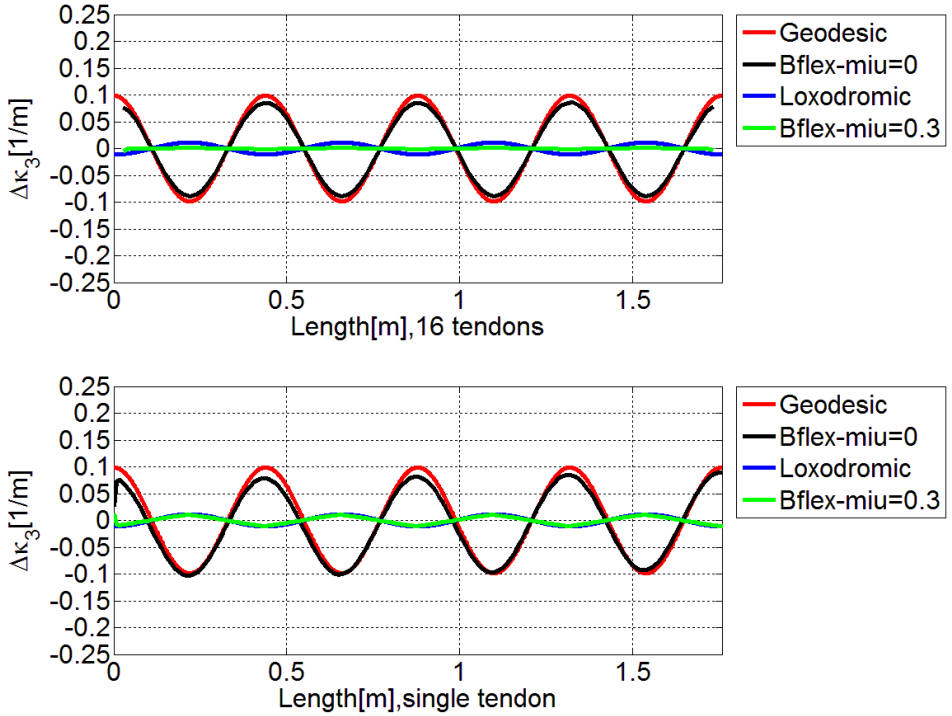

Figure 4-60 Modified normal curvature increment- 55°lay angle

From the above four figures, it is found the BFLEX results match the loxodromic solution very well by including the influence due to longitudinal slip. No significant influence from the outer armour layer in the complex model is observed.

The normal curvatures decrease as the increase of lay angles, maximum normal curvature increments for different lay angles are plotted in the figure below:

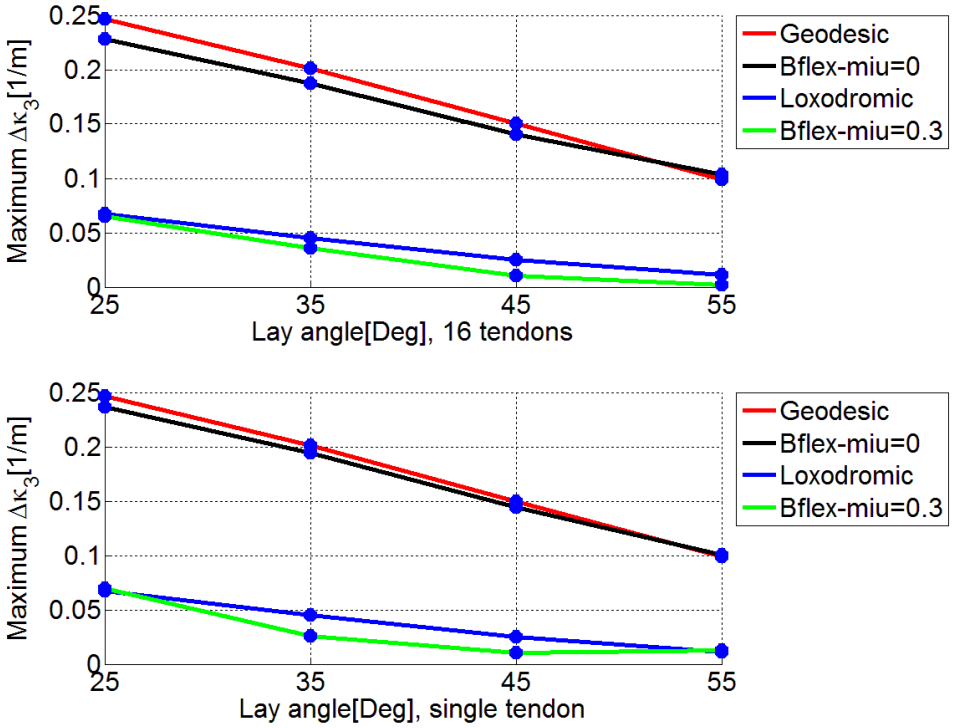

Figure 4-61 Maximum normal curvature increment as a function of lay angle, modified

4.4.3 Conclusion for this sub-chapter

From this chapter, it is found that the outer armour layer does not have significant influence on local displacements/curvature increments for the single bending problem. Moreover, the numerical simulation matches the analytical solution very well and it can be concluded the developed finite element formulation can provide adequate description of the tendon's kinematic in bending.

4.5 Study on cyclic bending problem

4.5.1 Description of the problem

In real operation, flexible risers are always exposed to oscillating loads which may cause fatigue in the tensile armour layer. Since fatigue analysis can be performed based on different assumptions of slip behaviour, the slip behaviour under cyclic bending is of interest. The aim of this part is to study the influence of cyclic bending on slip behaviour by using BFLEX models. The non-zero static curvature assumption is used. Both models stated in Chapter3 are used.

4.5.2 Discussion on the results from the simplified model

The simplified model with only a core and a single tendon is studied here. The pipe is forced to be bent from straight to a constant global curvature $0.1(m^{-1})$ and then back to straight. This procedure is repeated for several times. The influencing parameters that will be studied are axial strain and friction coefficient.

- Axial strain's influence

First, the influence from axial strain on cyclic bending is studied. 45°lay angle and friction coefficient 0.15 are used in the simplified BFLEX model. Initial axial strain is applied at first ten seconds, and then the pipe is bent with a period 40 seconds per cycle. The twist and normal curvatures at the tension side in the middle of the pipe are studied.

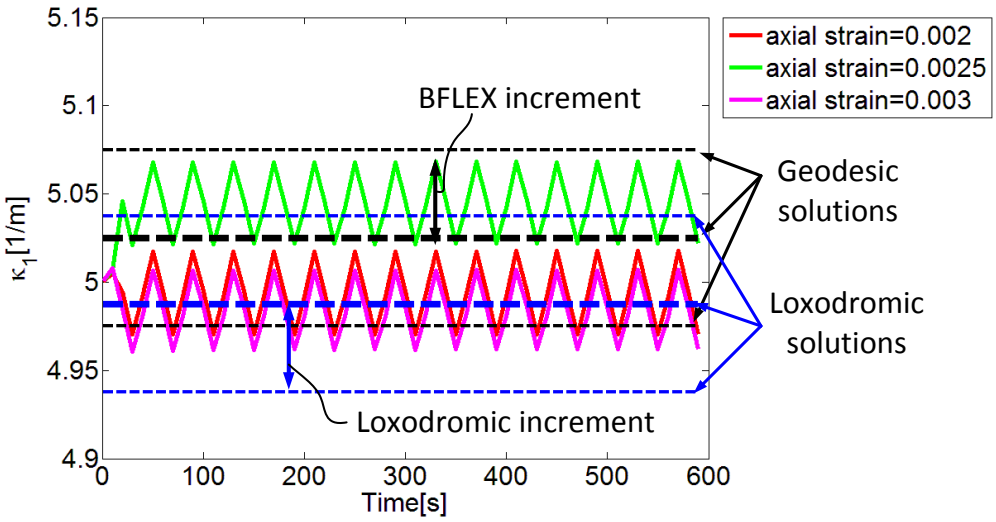

Figure 4-62 Twist curvature as a function of time, axial strain's influence

In figure 4-62, the three black lines represent for the Geodesic solutions. The thick one in the middle represents geodesic solution (Eq. (2.40))with half global pipe curvature, i.e., curvature $0.05(m^{-1})$, plus the principal curvature for a straight pipe(Eq.(2.7)). The other two thinner ones represent for the plus and minus geodesic increments with curvature $0.1(m^{-1})$ in addition to the thick black line.

The three blue lines represent for the Loxodromic solutions. Similarly, the thick blue line in the middle represents for loxodromic solution (Eq.(2.42)) with half global curvature plus the principal curvature valid for a straight pipe. The other two blue lines represent for the plus and minus loxodromic increment with curvature $0.1(m^{-1})$ in addition to the thick blue line.

In figure 4-62, it is observed that twist curvature increment does not vary from cycle to cycle and agrees with the loxodromic assumption as indicated by the arrows.

The mean twist curvature does not change along time series and can be explained by that the tendon is still in elastic range in this direction.

However, it is abnormal that the mean twist curvature for axial strain 0.0025 is larger than the other two.

The normal curvature as a function of time series is given in the figure blow:

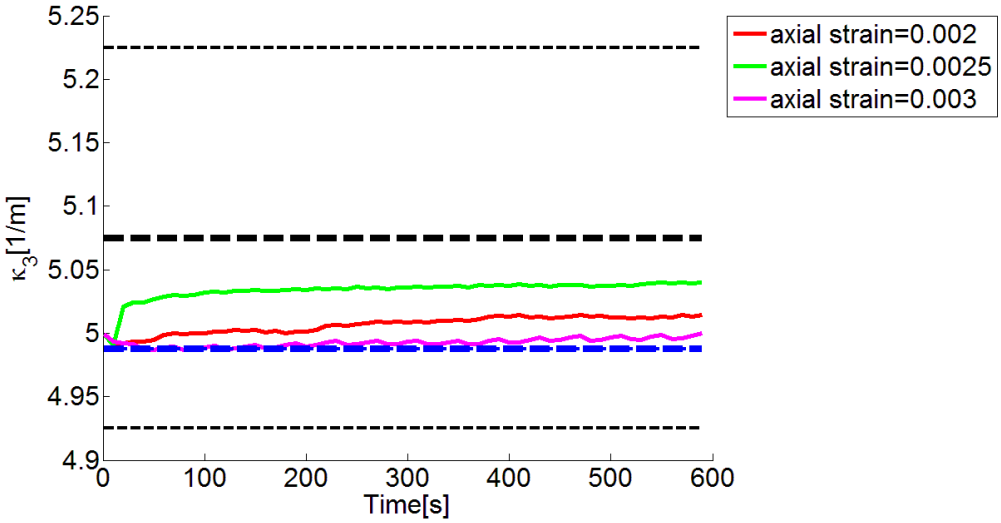

Figure 4-63 Normal curvature as a function of time, axial strain's influence

The black and blue lines represent the geodesic/loxodromic normal curvature increments plus the principal normal curvature respectively as described before.

It should be noted that the loxodromic normal curvature increment including the longitudinal slip effect is very small for 45° lay angle(stated in figure 4-59) as the blue lines are almost overlapped with each other. This explains why the normal curvature does not have the cycle to cycle increments as for the twist curvature.

The mean normal curvatures for different axial strains increase slowly with a trend to reach the geodesic solution valid for half curvature(thick black line), however, more cycles are needed here. The largest mean value occurs for axial strain 0.0025.

The curvature deviation of axial strain equals 0.0025 may be due to that only the first order of κ_c, i.e., the principal curvature in longitudinal direction of the surface, is taken into account in current BFLEX2010(refer to Eq.(2.17)). A new BFLEX version is made in order to include the second order of κ_c.

Where κ_c with second order terms is give in Eq.(4.5).

$$\kappa_c = -\frac{1}{\rho - Rcosv} cosv \tag{4.4}$$

The new results by using the new version of BFLEX are plotted below:

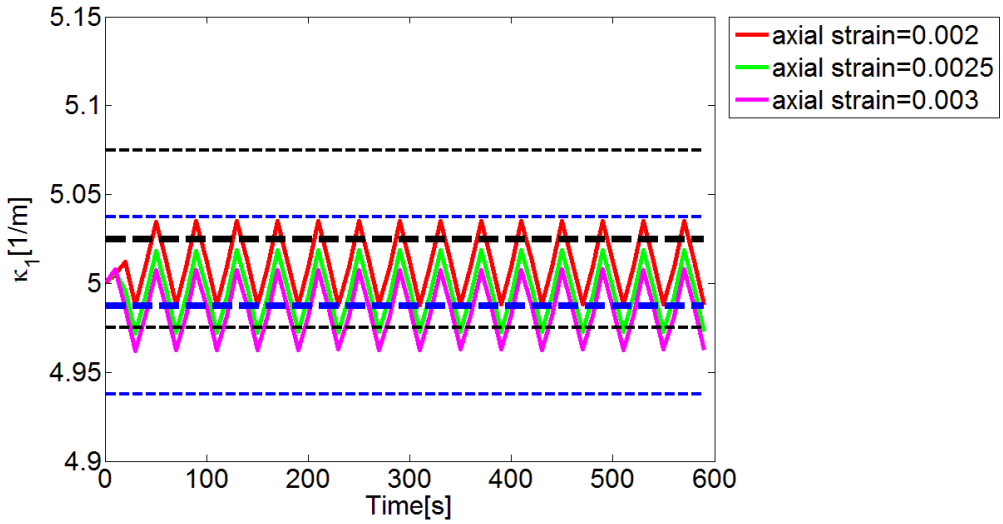

Figure 4-64 Twist curvature as a function of time, axial strain's influence, modified

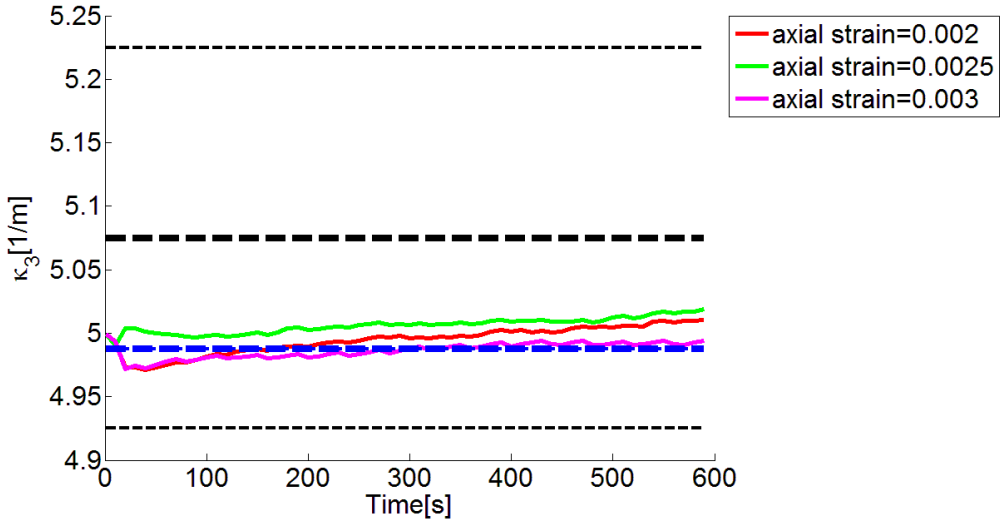

Figure 4-65 Normal curvature as a function of time, axial strain's influence, modified

It is observed from the above figures that the mean twist curvature for axial strain 0.0025 is now between the two for axial strain 0.002 and 0.003. This means the twist curvature become more reasonable by including the second order terms in κ_c. Moreover, the differences for normal curvature among the three axial strains are smaller. However, the mean normal curvature for axial strain 0.0025 is still larger than the other two.

In this part, only a simple case with 45° lay angle and friction coefficient 0.15 has been studied. This is because those values are corresponding to real flexible pipe operation. What's more, convergence problem is found for current BFLEX input file for some other lay angles.

- Friction's influence

(1) 35°lay angle

A model with 35°lay angle and axial strain 0.0025 is first used. Axial strain is applied during the first 10 seconds and cyclic bending with period 40 seconds is applied afterwards. The twist and normal curvatures at the tension side in the middle of the pipe are plotted below.

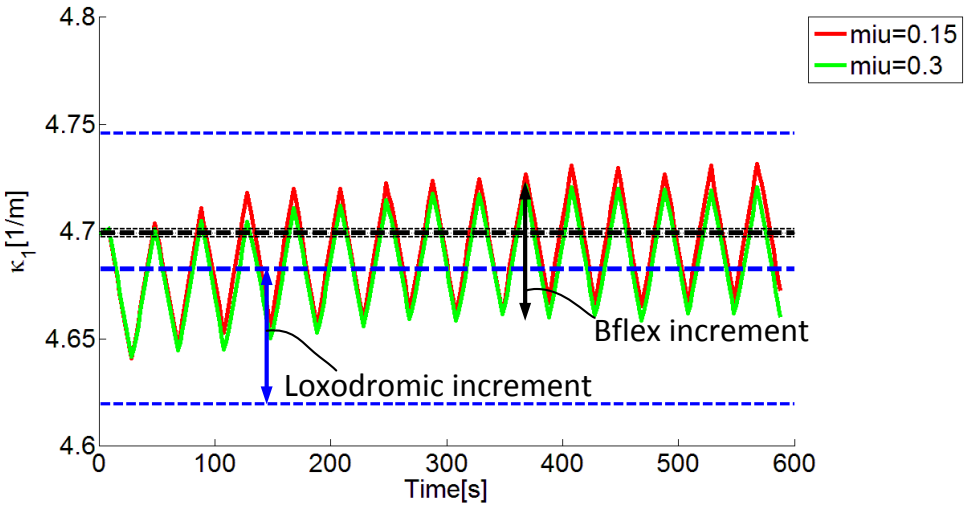

Figure 4-66 Twist curvature as a function of time, friction's influence

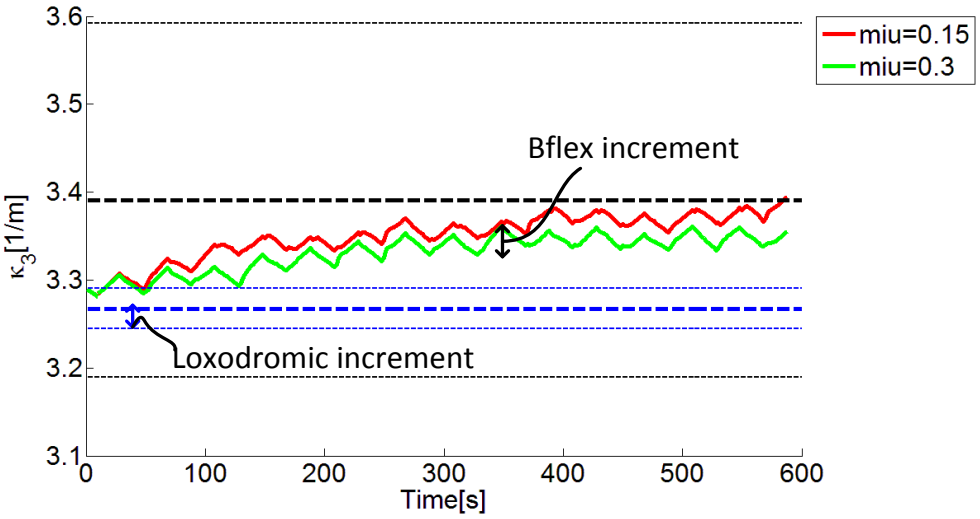

Figure 4-67 Normal curvature as a function of time, friction's influence

In figure 4-66 and 4-67, the blue lines and black lines represents the same meaning as described before. One should note that the geodesic solution for twist curvature

increment is very small for 35° lay angle (figure 4-44), so the three black lines become very close to each other in figure 4-66.

It can be concluded that the cyclic curvature increments follows the loxodromic assumption as indicated by the arrows.

In addition, it is observed that the friction coefficient does not have significant influence on cycle to cycle curvature increments in this case. However, an influence on mean curvatures is observed: the mean curvature quantities are a bit larger for friction coefficient 0.15 than for 0.3.

It is also found that the mean twist and normal curvatures increase along time axis. The increments show a tendency to reach the thick black line, i.e., the geodesic solution valid for half curvature plus the principal curvature. This is reasonable as the pipe is bent from straight to a certain curvature and then back to straight. In figure 4-67, the mean normal curvature increases slowly and does not reach a stable value at the end of time series. It shows that more than ten cycles are needed to reach stable for both curvatures.

(2) 45°lay angle

In addition, a study for 45° lay angle is carried out. Friction coefficient 0.1 and 0.2 are chosen based on convergence requirement in BFLEX. Results are given in figures below:

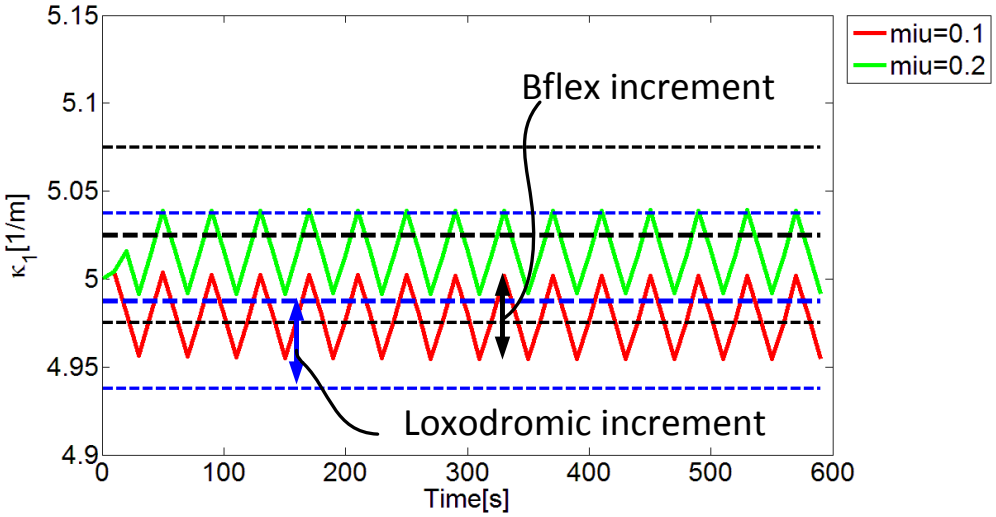

Figure 4-68 Twist curvature as a function of time, friction's influence

It can be concluded from the above figure that the mean twist curvature for 45° lay angle does not vary with time. This is consistent with result from figure 4-62 and can be explained by that the pipe is still in elastic range here. The cyclic increment of twist

curvature simulated by BFLEX gives agreement with the loxodromic solution, as indicated by the arrows.

Again, friction coefficient does not have any influence on cycle to cycle increment but has influence on mean curvature.

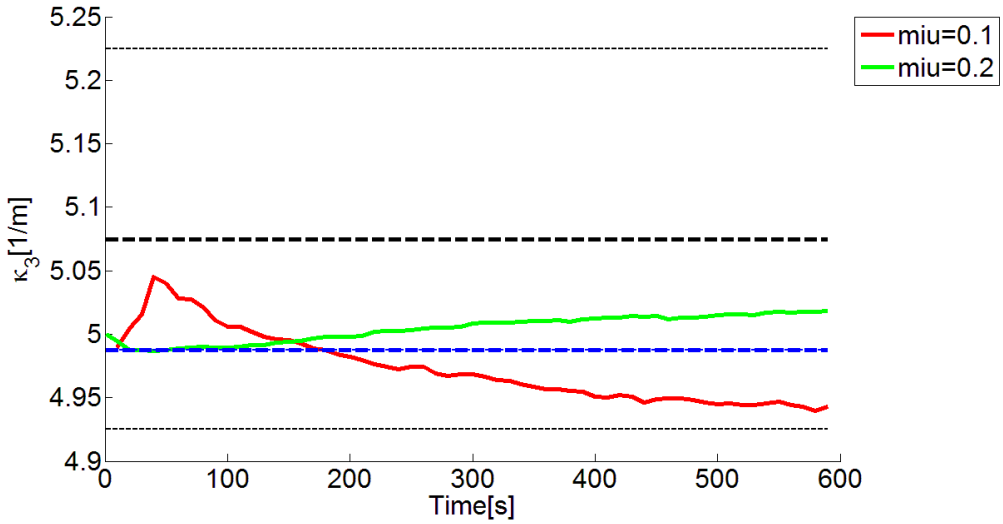

Figure 4-69 Normal curvature as a function of time, friction's influence

For normal curvature, an increase in mean value for miu=0.2 is observed. However, the mean value for miu=0.1 decreases during cyclic bending. The cyclic increment is consistent with the loxodromic assumption as it is very small for 45° lay angle.

This case with 45° lay angle is further tested by using the new version of BFLEX by including the second order term for κ_c, the results are given below.

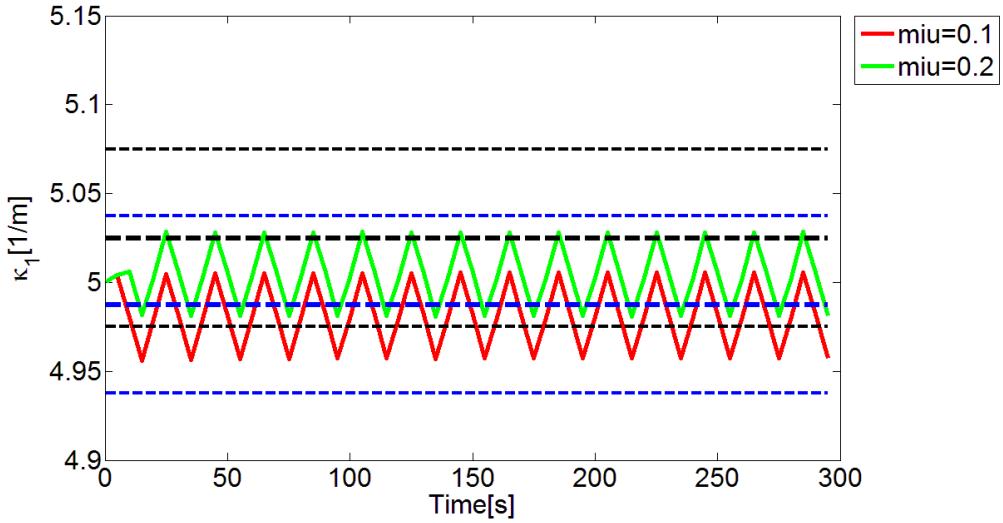

Figure 4-70 Twist curvature as a function of time, friction's influence, modified

A decrease in mean twist curvature for friction coefficient 0.2 is observed under the influence of the second order term of κ_c.

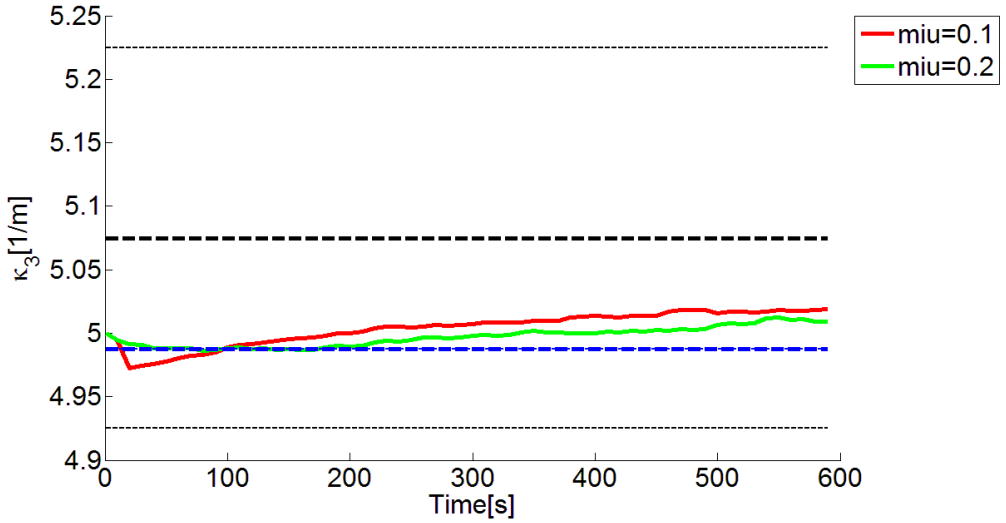

Figure 4-71 Normal curvature as a function of time, friction's influence, modified

It can be concluded from figure 4-70 and 4-71 that the second order term of κ_c has significant influence on twist and normal curvatures.

4.5.2 Discussion on the results from the complex model

The complex model with two tensile armour layers is used in this case. For the complex model, the inner layer contains 4 pitches and has lay angle 35°, the outer layer contains 5 pitches and has lay angle 42°. Initial axial strain is applied at first ten seconds, cyclic bending with period 20 seconds is applied afterwards. Cyclic bending effects on inner and outer layer are studied respectively.

First, the curvature quantities for the inner layer are studied. The curvature increments are taken out at the middle of the tensile side, i.e., where the maximum increments occur.

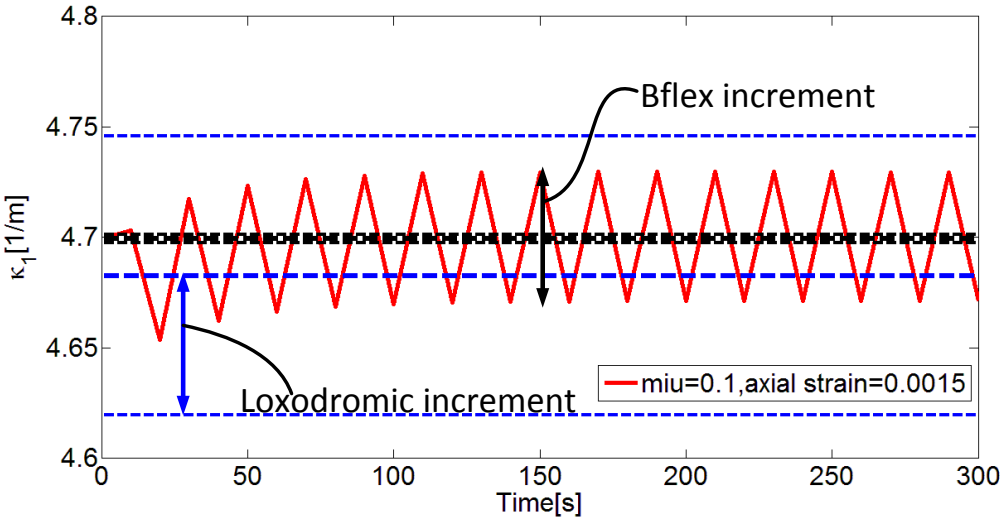

Figure 4-72 Twist curvature as a function of time, inner layer

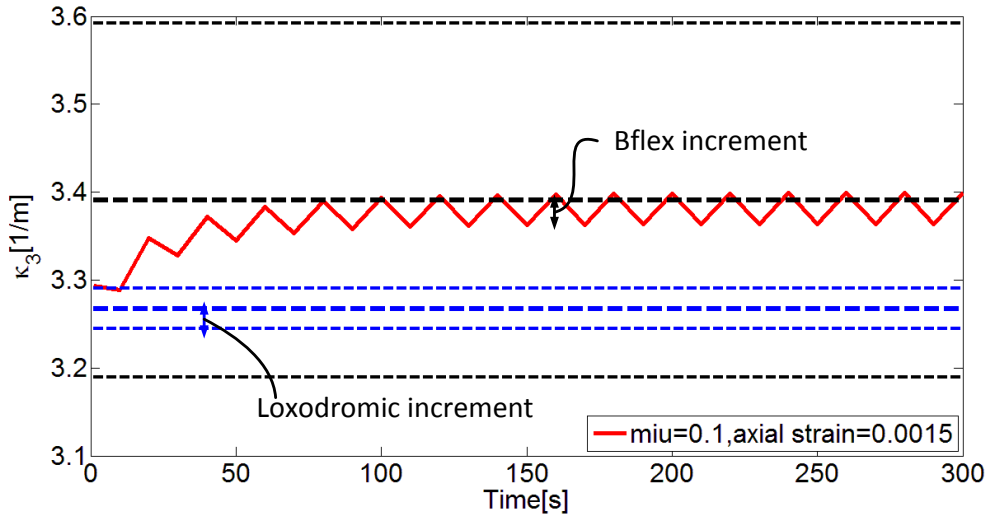

Figure 4-73 Normal curvature as a function of time, inner layer

The black and blue lines represent the geodesic and loxodromic solutions with different global curvature as indicated previously.

It is observed that both mean twist and normal curvatures increase as a function of time and tend to reach the geodesic solution (thick black line) valid for half global curvature plus principal curvature after a few cycles. Fewer cycles are needed to reach the stable mean value comparing to the simplified model.

It is also found that the curvature increments from cycle to cycle calculated by loxodromic assumption are consistent with the BFLEX's increment as indicated by the arrows.

For the outer layer, results are taken from the middle of the pipe at the tensile side, as given below:

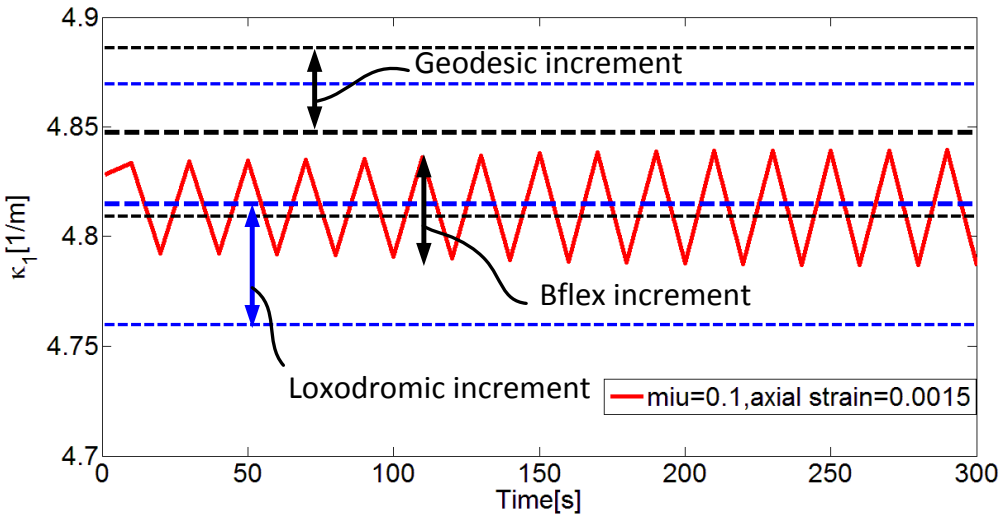

Figure 4-74 Twist curvature as a function of time, outer layer

It is observed that the twist curvature increment for the outer layer follows the geodesic solution at beginning. The increment increases from cycle to cycle and approximately reaches the loxodromic solution after many cycles. The curvature increment does not reach its stable value and more cycles are suggested to be included.

In addition, the mean twist curvature does not change from cycle to cycle for the outer layer.

The normal curvature increment as a function of time is given below:

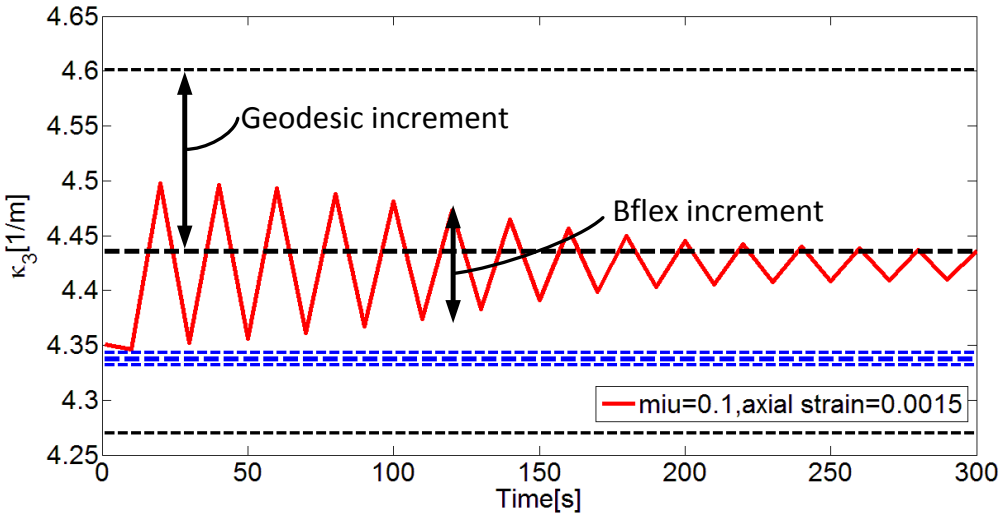

Figure 4-75 Normal curvature as a function of time, outer layer

Similar to twist curvature increment, the normal curvature increment follows the geodesic solution at beginning. The increment decreases and tends to reach the loxodromic solution after many cycles. However, many cycles are needed in order to reach a stable normal curvature. Again, the mean normal curvature does not vary with time.

Chapter 5 Summery

5.1 Conclusions

The main purpose of this thesis is to study the stress and slip behaviour for non-bonded flexible pipes. Numerical studies are carried out both to verify the model by comparing the numerical results with analytical results and to study various physical effects. The main advantage of this thesis is the application of two new element types in BFLEX2010, namely hshear353 and hcont453 which include the transverse degrees of freedom of the tendon.

For flexible pipes exposed to axisymmetric loading, two analytical methods, one obtained from the reference by Witz&Tan[13], one from Sævik[2], are compared with the numerical result from BFLEX. It has been concluded that Sævik's method gives better agreement with BFLEX result comparing to Witz&Tan's.

For flexible pipes exposed to bending, important parameters that can significantly affect the slip behaviour (e.g., global pipe curvature, friction coefficient and axial strain) have been studied. The simplified BFLEX model with single tendon is used. When studying one of these parameters, the other two are fixed to a certain value.

The result shows that the tendon's local displacements and curvature increments have linear relationship with global curvature. When friction coefficient is within the range from 0 to 0.3 or axial strain from 0 to 0.001, local displacements and curvature increments are significantly influenced (either increased or decreased). For larger friction coefficient or axial strain, local displacements and curvature increments tend to be constant.

Furthermore, comparison between numerical simulation and analytical solution for bending has been performed. For a single bending process, i.e., from straight to a constant curvature, it has been concluded that the numerical solutions match well with analytical solutions for either a simplified BFLEX model with single tendon or a complex model with double tensile layers. It has been demonstrated that the slip/curvature increments in the inner layer are not influenced by the outer tensile layer during a simple bending procedure.

At last, cyclic bending effects on local curvature increments have been studied with different BFLEX models.

For the simplified model with only one tendon, it has been found that cyclic twist/normal curvature increments obtained from numerical simulation have good agreement with the loxodromic assumption for 35° and 45° lay angles. The mean twist and normal curvatures for 35° lay angle and the mean normal curvature for 45° lay angle increase as a function of time and show a tendency to reach the geodesic

solution valid for half curvature after many cycles. It should be noted the twist curvature for 45° lay angle does not have this increment since it is in the elastic range.

It has been found the friction coefficient does not have significant influence on cycle to cycle curvature increments in this case. However, influence on mean curvatures is observed. In addition, it has been noted that the second order effect of the surface principal curvature in longitudinal direction has important influence on the mean curvature.

For the test of the complex model with double tensile armour layers, the one with 35° inner layer lay angle and 42° outer layer lay angle has been used. The pipe parameters are chosen based on a convergence requirement from BFLEX. Convergence difficulties are found for some pipe parameters.

For the inner layer, it has been observed that the mean curvatures increase as a function of time. The mean curvatures for this case increase faster than for the simplified model. It has been observed that approximately only five cycles are needed to reach the stable mean curvatures. At the same time, the loxodromic solutions have good agreement with BFLEX results for cycle to cycle curvature increments.

For the outer layer, the mean curvatures do not vary as a function of time. The cyclic curvature increments have started from geodesic solution and tended to reach the loxodromic solution after many cycles.

5.2 Suggestions for future work

The cyclic bending effects have only been studied for some simple cases because convergence problems have been found for some friction coefficients and axial strain values. It is suggested that the model should be further improved and, as long as the convergence problem has been solved, studies on cyclic bending regarding the influence from different friction coefficients, axial strains, and lay angles can be carried out and compared.

Further, for the model contains two tensile armour layers, the influence from the outer layer on several things can be carried out: the influence on curvature increment of the tendon, the influence on the relative displacement of the contact element, the influence on local bending stress and so on.

Reference

[1] Berge,S., Engseth,A., Fylling,I., Larsen,C,M., Leira,B,J. and Olufsen,A.,1992. "Handbook on design and operation of flexible pipes". *FPS2000*, 1992.

[2] Sævik,S.,1992. "On stresses and fatigue in flexible pipes". PhD thesis, NTH Trondheim, Norway.

[3] B,Yong.,B,Qiang. *SUBSEA PIPELINES AND RISERS.* Elsevier, London, 1st edition, 2005.

[4] API. Ansi/api recommended practice 17b, 2008. Technical Report 4. Edition, ANSI/API.

[5] Efficient Fatigue analysis of helix elements in umbilicals and flexible risers.

[6] Eisenhart, L.P.: "A Treatise on the differential Geometry of Curves and Surfaces", Dover Publ. Inc., 1960

[7] Feret, J.J, Bournazel, C.L.: "Calculation of Stresses and Slip in Structural Layers of Unbounded Flexible Pipes", Proc. of the Offshore Mechanics and Arctic Engineering Conference, OMAE, 1986.

[8] Sævik,S. BFLEX2010- theory manual. *MARINTEK*, 2010.

[9] Sævik,S., J.Thosrsen,Mats. DRAFT: "Techniques for predicting tensile armour buckling and fatigue in deep water flexible risers." To be published, Proc. of the Offshore Mechanics and Arctic Engineering Conference, OMAE, 2012.

[10] Sødahl,N.,1990. "Methods for design and analysis of flexible risers". PhD thesis, Norwegian University of Science and Technology, Trondheim, Norway.

[11] Shyu, S. C., Chang, T. Y., and Saleeb, A. F., 1987. "Finite element solutions of two-dimensional contact problems based on a consistent mixed formulation". *Computers and Structures, **27***(4), pp. 455-466.

[12] Shyu, S. C., Chang, T. Y., and Saleeb, A. F., 1988. "Friction-contact analysis using a mixed finite element method". *Computers and Structures, **27***(4), pp. 223-242.

[13] Witz, J.A. and Tan, Z,. "On the axial-torsional structural behaviour of flexible pipes, umbilicals and marine cables", *Marine Structures*, vol5, pp205-227, 1992.

[14] Sævik,S., " Theoretical and experimental studies of stresses in flexible pipes". *Computers and Structures*, 89 (2011) 2273-2291.

[15] API. Ansi/api recommended practice 17j, 2008. Technical Report 3. Edition, ANSI/API.

[16] Sævik,S. BFLEX2010- user manual. *MARINTEK*, 2010.

Appendix A

BFLEX2010 input file for the simplified model:

```
#
HEAD #Text
#-------------------------------------------------------------------------
# Control data
#
#               maxit    ndim    isolvr npoint ipri    conr    gacc        iproc
CONTROL        100        3        2            16        11    1.e-5      0.0        stressfree
#CONTROL        100        3        1            16        11    1.e-5      9.81        restart 70
DYNCONT 1 0.0 0.09 -0.05
#                    t          dt        dtvi    dtdy      dt0        type              hla?
#TIMECO           1.0      1.0      1.0      100.0    STATIC             auto              go-on        disp        50
5           1e-5
TIMECO           100.0          1.0      10.0        100.0    static           auto              go-on        disp        20
5           1e-5
#TIMECO           100.0        0.10      2.0        100.0    dynamic           auto              go-on        disp        20
5           1e-5

#
#-------------------------------------------------------------------------
# Nocoor input
#
#                              no             x         y         z
Nocoor Coordinates
                     1             0.0             0.0       0.0
                   401             #len        0.0       0.0
#
#           no           x0       y0      z0      b1      b2      b3            R node        xcor    theta
Nocoor Polar    0.0      0.0    0.0    0.0    0.0    0.0    0.100
1001   0.00      3.1416
1401   #len     53.4071
#
#
#           no           x0       y0      z0      b1      b2      b3            R node        xcor    theta
Nocoor Polar    0.0      0.0    0.0    0.0    0.0    0.0    0.100
20001 0.00    3.1416
20401 #len     53.4071
#
Visres Integration 1 Sigma-xx-ax Sigma-xx-my Sigma-xx-mz
#
#
#-------------------------------------------------------------------------
# Elcon    input
#
#
# The core
#
#           group             elty            material    no    n1          n2    n3      n4
Elcon    core             pipe31          plastic    1      1           2
#             n      elinc    nodinc
Repeat 400      1              1
#
```

```
# Tensile Layer 1
#          group              elty     flexcrossname        no     n1       n2       n3       n4
Elcon    tenslayer1 hshear353     tendon       20001     1          2       20001     20002
#           n      elinc    nodinc
Repeat 400      1              1
#
# Contact tensile Layer 1
#          group              elty     flexcrossname        no     n1       n2       n3       n4
Elcon    tenscontact1 hcont453       contmat1       50001     1001          1002       20001     20002
#           n      elinc    nodinc
Repeat 400      1              1
#
#-------------------------------------------------------------------------
# Orient input
#
# The core
#                                  no        x    y       z
Elorient Coordinates       1          0    1e3       0
                                    400       0    1e3       0
#
#                                  no        x    y       z
# Tensile Layer 1
#                                  no        x    y       z
Elorient Coordinates    20001        0    1e3       0
                                  20400        0    1e3       0
elorient eulerangle 50001 0.0 0.0 0.0
                                 50400 0.0 0.0 0.0
#
#
#             groupn             mname     sname          is1       isn        istx          isty        istz    gt1
gt2
#                                                                                                                    1
means that friction is independent (tape between layers) else (isotropic model)
CONTINT tenscontact1     core       tenslayer1 1          3          10       10       0        60       1
#-------------------------------------------------------------------------------
#
#---------------------------------------------------------------
#
# Element property input
#
#          name    type       rad    th    CDr    Cdt    CMr    CMt              wd             ws       ODp    ODw
rks
ELPROP core       pipe    0.0985    0.001       1.0    0.1    2.0    0.2 500.00 0.00    0.197    0.197 0.5
#                                                                    b          t          md      ms      scale    thims thimd
iop    iop=1 turn off axisymmetric shear inetraction =2 turn off bending shear interaction
ELPROP tenslayer1       shearhelix rectangle 0.009    0.003       1.4    0.0    1.0      200      100       0
#                                                gap0 tunetime AUTOMNPC
ELPROP tenscontact1    layercontact d d    d 0
#                 name      type              shearm
# Boundary condition data
#          Loc       node    dir
BONCON GLOBAL 1           1
BONCON GLOBAL 1           2
BONCON GLOBAL 1           3
BONCON GLOBAL 1           4    repeat 401 1
BONCON GLOBAL 401         2
```

```
BONCON GLOBAL 401         3


# fix the relative disp at ends
BONCON gLObAL 20001          1
BONCON gLObAL 20001          2
BONCON gLObAL 20001          4 repeat 401 1
#
BONCON gLObAL 1001           1 repeat 401 1
BONCON gLObAL 1001           2 repeat 401 1
BONCON gLObAL 1001           3 repeat 401 1
BONCON gLObAL 1001           4 repeat 401 1
BONCON gLObAL 1001           5 repeat 401 1
BONCON gLObAL 1001           6 repeat 401 1
#---------------------------------------
#-----------------------------------------------
#
# Constraint input
CONSTR PDISP GLOBAL       20401    1      #len*#as*#ca      300
CONSTR PDISP GLOBAL       20401    2      #len*#as*#sa      300
#
#-----------------------------------------------
# Cload input
#
#         hist    dir    no1 r1    no2 r2                n m
#
#CLOAD    300       1    51    270000.00
#piload 300 1 3e6 50 3e6
inistr 400          5          1    #strain 400 #strain
#-----------------------------------------------
#PELOAD 200 100
#-------------------------------------------------------------
# History data
# force
  THIST 100    0                 0.0
                 1                 0.00
                10                 0.00
  THIST 200    0                 0.0
                 1                 0.00
                10                 0.00
  THIST 300    0                 0.0
               10                 1.00
               100                1.00
  THIST 400 0                    0.00
                10                 0.00
                100                1.00

# prescribed displacement
    THIST_R 400    0.0                0.0 rampcos 0.0
                       0.0                0.0 rampcos    1.0
#                      11.0               20.0 rampcos 0.0
thist 450 0.0 0.0
              11.0 0.0
              20.0 0.0
#
#-------------------------------------------------------------------------------
```

```
#    Material data
#
#             name         type       poiss       ro            talfa    tecond    heatc beta      em      gm       em2
#
#             name       type                poiss ro          talfa       tecond    heatc    eps sigma
#             name          type          poiss talfa         tecond    heatc    beta ea       eiy         eiz          git
em         gm         den
MATERIAL plastic     linear       0.4     11.7e-6     50         800     0       1.02e8    3.210e8    3.210e8
3.210e8      2.1e11    8e10        1000E-9 2.1e11
MATERIAL tendon        elastic      0.3      7850 11.7e-6      50         800      2e11 8.0e10 2e11
#             name         type                alfa poiss ro          talfa       tecond    heatc eps sigma
MATERIAL nl_steel elastoplastic    1        0.3    7850       1.17e-5      50         800    0                0
                                                                                                                1.691E-03
3.50E+02
                                                                                                                0.005
450
                                                                                                                0.0998
835
#             name                type         alfa      eps       sigma (asphalt 0.1-0.3) (1 MPa for pp)
MATERIAL shearmat    epcurve              1      0.0         0.00
                                                 0.2         0.9
                                                 1.0         1.0
                                              1000.0         2.0
#
#            Contact coil-swift:
#
#             name                type         rmyx    rmyz    xmat       ymat          zmat
MATERIAL contmat1 isocontact    #miu       bellx       bellz
#             name          type         alfa      eps          sig
MATERIAL bellx         epcurve    1          0            0
                                              0.00001        1.00
                                              1000        10.00
#
MATERIAL bellz         hycurve             -1000      -1.4e12
                                              1000        1.4e12
```

Appendix B

BFLEX2010 input file for the complex model:

```
#
HEAD BFLEX2010 - Buckling          2011-12-11. strong tape, mu=0.001, cyclic curvature
#-------------------------------------------------------------------------
# Control data
#
#                maxit    ndim    isolvr npoint ipri    conr    gacc        iproc
CONTROL         20       3       2           16       11    1.e-5      0.0        stressfree
#CONTROL        100       3       1           16       11    1.e-5      9.81       restart 70
DYNCONT 1 0.0 0.09 -0.05
#                    t          dt       dtvi    dtdy      dt0       type              hla?
#TIMECO      1.0    1.0      1.0    100.0    STATIC      auto      go-on    disp    50      5          1e-5
TIMECO      10.0    1.0      10.0    100.0    static      auto      go-on    disp     100    5          1e-4
TIMECO     300.0    0.1      10.0    100.0    static      auto      none     disp     100     5          1e-5
#
# Nocoor input
#                              no            x         y         z
Nocoor Coordinates
                      1            0.0            0.0       0.0
                    101            7.1787/2       0.0       0.0
# supporting first layer
#          no          x0       y0      z0      b1      b2      b3          R node       xcor    theta
Nocoor Polar    0.0      0.0    0.0    0.0    0.0    0.0    0.100
100010.00     3.1416
101017.1787/2 6.28*8/2+3.1416
repeat 16 101 0.0 0.3926
# outer coating
#          no          x0       y0      z0      b1      b2      b3          R node       xcor    theta
Nocoor Polar    0.0      0.0    0.0    0.0    0.0    0.0    0.103
200010.00     3.1416
201017.1787/2 -6.28*8/2+3.1416
repeat 16 101 0.0 0.3926
# 1st structural layer
#          no          x0       y0      z0      b1      b2      b3          R node       xcor    theta
Nocoor Polar    0.0      0.0    0.0    0.0    0.0    0.0    0.100
300010.00     3.1416
301017.1787/2 6.28*8/2+3.1416
repeat 16 101 0.0 0.3926
# 2nd structural layer
#          no          x0       y0      z0      b1      b2      b3          R node       xcor    theta
Nocoor Polar    0.0      0.0    0.0    0.0    0.0    0.0    0.103
400010.00   3.1416
401017.1787/2 -6.28*8/2+3.1416
repeat 16 101 0.0 0.3926
#
Visres Integration 1 Sigma-xx-ax Sigma-xx-my Sigma-xx-mz Vconfor-z
#-------------------------------------------------------------------------
# Elcon    input
```

```
# The core
#          group           elty          material   no   n1       n2   n3     n4
Elcon    core            pipe31        plastic    1    1        2
#          n     elinc    nodinc
Repeat 100     1             1
#
# Tensile Layer 1
#          group           elty     flexcrossname       no     n1       n2       n3       n4
Elcon    tenslayer1      hshear353     tendon       30001     1        2       30001     30002
                                                    30016     1        2       31516     31517
                                                                repeat 100 16 1
# Tensile Layer 2
#          group           elty     flexcrossname       no     n1       n2       n3       n4
Elcon    tenslayer2      hshear353     tendon       40001     1        2       40001     40002
                                                    40016     1        2       41516     41517
                                                                repeat 100 16 1
# Contact tensile Layer 1
#          group           elty     flexcrossname       no     n1       n2       n3       n4
Elcon    tenscontact1 hcont453       contmat1       50001     10001         10002       30001
30002
                                                    50016     11516         11517       31516
31517
#          n     elinc    nodinc
Repeat 100     16            1
# Contact tensile Layer 1-Layer2
#          group           elty     flexcrossname       no     n1       n2       n3       n4
Elcon    tenscontact1-2 hcont453       contmat1_2       70001     30001         30002       40001
40002
                                                    70016     31516         31517       41516
41517
#          n     elinc    nodinc
Repeat 100     16            1
# Contact tensile Layer 2-outwards
#          group           elty     flexcrossname       no     n1       n2       n3       n4
Elcon    layer2_outward_mid spring137       springmat1       60017     20002       40002
                                                    60032     21517       41517
#          n     elinc    nodinc
Repeat 99      16            1
#
# Contact tensile Layer 2-outwards, ends
#          group           elty     flexcrossname       no     n1       n2       n3       n4
Elcon    layer2_outward_ends spring137       springmat2       60001     20001     40001
                                                    60016     21516     41516
#          n     elinc    nodinc
Repeat 2         1600          100

#
#-------------------------------------------------------------------------
# Orient input
#
# The core
```

```
#                                   no          x    y       z
Elorient Coordinates        1           0    1e3       0
                                    100        0    1e3       0
#
#                                   no          x    y       z
# Tensile Layers
#                                   no          x    y       z
Elorient Coordinates    30001         0    1e3       0
                                  31600         0    1e3       0
Elorient Coordinates    40001         0    1e3       0
                                  41600         0    1e3       0
# contact
elorient eulerangle 50001 0.0 0.0 0.0
                                  51600 0.0 0.0 0.0
elorient eulerangle 70001 0.0 0.0 0.0
                                  71600 0.0 0.0 0.0
elorient eulerangle 60001 0.0 0.0 0.0
                                  61616 0.0 0.0 0.0

#
#
#             groupn              mname      sname          is1       isn        istx          isty         istz
gt1      gt2
#
1 means that friction is independent (tape between layers) else (isotropic model)
CONTINT tenscontact1      core        tenslayer1 1            3           10.1          10.1          0
60        0
CONTINT tenscontact1-2      tenslayer1        tenslayer2 1           3           10.1          10.1
0         60        0
#CONTINT layer2_outward_mid      tenslayer1        core 1           3           1           5000          1
60        1
#CONTINT layer2_outward_ends      tenslayer1        core 1           3           1           5000
1         60        1
#-------------------------------------------------------------------------------
#
#---------------------------------------------------------------
#
# Element property input
#
#           name    type          rad        th          CDr    Cdt    CMr    CMt    wd         ws        ODp
ODw        rks
ELPROP core        pipe    0.0985    0.001        1.0    0.1    2.0    0.2 500.00 0.00    0.197    0.197
0.5
#                                                                   b          t          md       ms       scale
thims thimd    iop    iop=1 turn off axisymmetric shear inetraction =2 turn off bending shear
interaction
ELPROP tenslayer1      shearhelix rectangle 0.009    0.003    1.4    0.0    4.0      200      100       0
ELPROP tenslayer2      shearhelix rectangle 0.009    0.003    1.4    0.0    4.0      200      100       0
#                                                 gap0 tunetime AUTOMNPC autosearch
ELPROP tenscontact1    layercontact D D    D 0
ELPROP tenscontact1-2    layercontact D D    D 1
```

```
#                                                                turnofftransformation
isotropic hardening (requires coulomb in material card)
ELPROP layer2_outward_mid    genspring    10.1      10.1      10.1      10.1      10.1      10.1 1
1
ELPROP layer2_outward_ends    genspring    10.1      10.1      10.1      10.1      10.1      10.1 1
1
#                name      type              shearm
# Boundary condition data
#          Loc        node    dir
BONCON GLOBAL 1          1
BONCON GLOBAL 1          2
BONCON GLOBAL 1          3
BONCON GLOBAL 1          4
repeat 101 1
BONCON GLOBAL 101          2
BONCON GLOBAL 101          3
#
#
# fix the relative disp at ends
BONCON gLObAL 30001          1 repeat 16 101
BONCON gLObAL 30001          2 repeat 16 101
BONCON gLObAL 30001          4 repeat 1616 1
BONCON gLObAL 30101          1 repeat 16 101
BONCON gLObAL 30101          2 repeat 16 101
#
BONCON gLObAL 40001          1 repeat 16 101
BONCON gLObAL 40001          2 repeat 16 101
BONCON gLObAL 40001          4 repeat 1616 1
BONCON gLObAL 40101          1 repeat 16 101
BONCON gLObAL 40101          2 repeat 16 101
#
BONCON gLObAL 10001          1 repeat 1616 1
BONCON gLObAL 10001          2 repeat 1616 1
BONCON gLObAL 10001          3 repeat 1616 1
BONCON gLObAL 10001          4 repeat 1616 1
BONCON gLObAL 10001          5 repeat 1616 1
BONCON gLObAL 10001          6 repeat 1616 1
#
BONCON gLObAL 20001          1 repeat 1616 1
BONCON gLObAL 20001          2 repeat 1616 1
BONCON gLObAL 20001          3 repeat 1616 1
BONCON gLObAL 20001          4 repeat 1616 1
BONCON gLObAL 20001          5 repeat 1616 1
BONCON gLObAL 20001          6 repeat 1616 1
#---------------------------------------------
#
# Constraint input
Constr coneq global 30002 3 0.0 30001 3 1.0 repeat 1615 1 0
Constr coneq global 40002 3 0.0 30001 3 1.0 repeat 1615 1 0
Constr pdisp global 30101 1 7.1787/2*0.0015*0.8192 300 repeat 16 101
Constr pdisp global 40101 1 7.1787/2*0.0015*0.8192 300 repeat 16 101
```

```
Constr pdisp global 30101 2 7.1787/2*0.0015*0.5726 300 repeat 16 101
Constr pdisp global 40101 2 -7.1787/2*0.0015*0.5726 300 repeat 16 101
#
#-------------------------------------------------------------------------
#    Material data
#
#              name         type       poiss       ro            talfa    tecond    heatc beta      em      gm
em2
#
#              name       type                 poiss ro          talfa       tecond    heatc    eps sigma
#              name          type          poiss talfa         tecond    heatc    beta ea       eiy         eiz
git          em          gm          den
MATERIAL plastic     linear       0.4     11.7e-6     50         800     0       1.02e11    3.210e8
3.210e8 3.210e8     2.1e11    8e10        1000E-9 2.1e11
MATERIAL tendon       elastic     0.3      7850 11.7e-6      50         800      2e11 8.0e10 2e11
#              name         type                 alfa poiss ro          talfa       tecond    heatc eps sigma
MATERIAL nl_steel elastoplastic    1        0.3    7850        1.17e-5      50          800    0
0

1.691E-03      3.50E+02

0.005            450

0.0998           835
#              name                 type         alfa      eps        sigma (asphalt 0.1-0.3) (1 MPa for pp)
MATERIAL shearmat    epcurve               1      0.0         0.00
                                                  0.2         0.9
                                                  1.0         1.0
                                               1000.0         2.0
#
#            Contact coil-swift:
#
#              name                 type         rmyx    rmyz    xmat        ymat         zmat
MATERIAL contmat1 isocontact    0.10      bellx       bellz
MATERIAL contmat1_2 isocontact    0.10      bellx       bellz_1
MATERIAL springmat1 genspring      bellx      bellx       bellz2       zero       zero       zero
coulomb
MATERIAL springmat2 genspring      bellx      bellx       bellz3       zero       zero       zero
coulomb
#              name          type        alfa      eps         sig
MATERIAL bellx         epcurve    1          0           0
                                             0.0001       0.150
                                             1000         0.250
#
MATERIAL bellz         hycurve             -1000      -1.4e12
                                            1000        1.4e12
#
MATERIAL bellz_1         hycurve             -1000      -1.4e13
                                            1000        1.4e13
#
MATERIAL bellz2        hycurve             -1000      -6.944e3
```

```
                                          0          0
                                      0.001      15.3e3
                                       1000      15.3e3*1e6
#
MATERIAL bellz3       hycurve          -1000     -6.944e3/2
                                          0          0
                                      0.001      15.3e3/2
                                       1000      15.3e3*1e6/2
#
MATERIAL zero         hycurve          -1000      0
                                       1000      0
#

#             name              type        rmyx   rmyz   xmat      ymat       zmat
#MATERIAL contmat    contact   0.30   0.60   bellx     belly      bellz
#-----------------------------------------------
# Cload input
#
#        hist   dir   no1 r1    no2 r2              n m
#
#CLOAD   500      1       1     -9000.00
inistr 400        5        1    0.1 100 0.1
#inistr 400        5        30001    0.1 31600 0.1
#inistr 400        5        40001    0.1 41600 0.1
#inistr 400        5        41    0.05 60 0.05
#inistr 400        5        61    0.05 100 0.01
#inistr 400        5 20001    0.05 20189 0.36
#inistr 400        5 20190    0.36 20210 0.36
#inistr 400        5 20211    0.36 20400 0.05
#
#piload 300 1 50.0e6 100 50.0e6
#-----------------------------------------------
#PELOAD 200 100
#-------------------------------------------------------------
# History data
# force
 THIST 100   0                0.0
                1                0.00
               10                0.00
               20                0.00
THIST 200   0                  0.00
              1                  0.00
              10                 0.00
#THIST 300 0                   0.00
#               10                 1.00
#               100                1.00
THIST_R 300   0                10.0   rampcos 1
#THIST 400 0                   0.00
#               10                 0.00
#               110                1.00
THIST_R 500   0                1.0   rampcos 10
```

```
# THIST 300    0              0.0
#                 1             -0.000010
#                 2             -0.20
#                10             -0.20
#               100             -0.20
#               200             -0.20
#     THIST_R 300    0.0             10.0 rampcos 1
# prescribed displacement
    THIST_R 400    0.0             10.0 rampcos 0.0
                  10.0             20.0 rampcos    1.0
                  20.0             30.0 rampcos 0.0
                  30.0             40.0 rampcos    1.0
                  40.0             50.0 rampcos 0.0
                  50.0             60.0 rampcos    1.0
                  60.0             70.0 rampcos 0.0
                  70.0             80.0 rampcos    1.0
                  80.0             90.0 rampcos 0.0
                  90.0            100.0 rampcos    1.0
                 100.0            110.0 rampcos 0.0
                110.0             120.0 rampcos 1.0
                     120.0              130.0 rampcos 0.0
                                  130.0              140.0 rampcos 1.0
                                  140.0              150.0 rampcos 0.0
                                  150.0              160.0 rampcos 1.0
                                  160.0              170.0 rampcos 0.0
                                  170.0              180.0 rampcos 1.0
                                  180.0              190.0 rampcos 0.0
                                  190.0              200.0 rampcos 1.0
                                  200.0              210.0 rampcos 0.0
                                  210.0              220.0 rampcos 1.0
                                  220.0              230.0 rampcos 0.0
                                  230.0              240.0 rampcos 1.0
                                  240.0              250.0 rampcos 0.0
                                  250.0              260.0 rampcos 1.0
                                  260.0              270.0 rampcos 0.0
                                  270.0              280.0 rampcos 1.0
                                  280.0              290.0 rampcos 0.0
                                  290.0              300.0 rampcos 1.0
```